ATOMISTIC AND CELLULAR ANALYSIS OF START PHOSPHATIDYLINOSITOL TRANSFER PROTEINS IN THE CONTEXT OF THE PHOSPHOLIPID EXTRACTION MECHANISM AND PHOSPHOINOSITIDE SIGNALING IN THE PARASITE *TOXOPLASMA*

Aby Grabon

A dissertation submitted to the faculty of the University of North Carolina at Chapel Hill in partial fulfillment of the requirements for the degree of Doctor of Philosophy in Cell and Developmental Biology, in the Department of Cell Biology and Physiology in the School of Medicine.

Chapel Hill
2016

Approved by:

Vytas Bankaitis

Keith Burridge

Scott Hammond

Ben Major

Ellen Weiss

ABSTRACT

Aby Grabon: Atomistic and Cellular Analysis of START Phosphatidylinositol Transfer Proteins in the Context of the Phospholipid Extraction Mechanism and Phosphoinositide Signaling in the Parasite *Toxoplasma*
(Under the direction of Vytas Bankaitis)

Phosphatidylinositol transfer proteins (PITPs) are essential regulators of the interface between phosphoinositide (PIP) signaling and membrane trafficking in eukaryotic cells. Genetic derangement of PITPs in multicellular organisms results in pathologies such as neurodegeneration, metabolic diseases, and vision and neurosensory defects. How PITPs sense multiple metabolic inputs to specify a membrane signaling event is key to our understanding of these pathologies and of PIP networks in general. To that end, we describe a novel multi-domain PITP of the START structural family: PITP Multidomain Protein (PIMP) is encoded by the eukaryotic parasite *Toxoplasma,* and associated with specialized parasite organelles called dense granules. Dense granules are secretory organelles that traffic *Toxoplasma* proteins during parasite infection of the mammalian host. PIMP links a PITP domain to an oxysterol binding protein (OSBP) domain. PITP and OSBP orthologs in other eukaryotes are expressed as separate proteins known to antagonize each other in specific PIP signaling pathways. We report that PIMP is a *bona fide* PITP *in vivo* and *in vitro*, and its binding and extraction of phosphatidylinositol (PtdIns) from membranes is required for this function. Furthermore, PIMP binds phosphatidylcholine as a counter-ligand to PtdIns, and senses specific higher order PIPs, PtdIns4P and PtdIns(4,5)P_2 through a conserved plekstrin homology (PH) domain. We describe how *Toxoplasma* codes its secretory system with unique PtdIns4P pools,

and define PIMP as a sensor of PIP pools on dense granules. Thus PIMP is a dense granule protein that represents a novel platform for the integration of multiple metabolic inputs with PtdIns4P signaling.

The mechanism by which the PIMP PITP domain, or indeed any START PITP, extracts phospholipids from bilayers is unknown. We performed molecular dynamics simulations using the mammalian PITPα as a START PITP model. We report atomistic detail of the trajectory of phospholipids into the START PITP binding pocket. Overall, this work analyzes START PITP function on the atomistic and cellular levels, and offers possible explanations for how these proteins organize specific PIP signaling events.

Dla Basi i Zygmunta

ACKNOWLEDGEMENTS

PREFACE

Chapter 1 is adapted from a published review:

Grabon, A., Khan, D., & Bankaitis, V. A. (2015). Phosphatidylinositol transfer proteins and instructive regulation of lipid kinase biology. *Biochimica et Biophysica Acta (BBA)-Molecular and Cell Biology of Lipids, 1851*(6), 724-735.

Chapter 2 represents work that will eventually be solicited for publication with an as-of-yet undetermined journal.

Chapter 3 is adapted and modified from a manuscript in revision at *Journal of Lipid Research*, as a co-author work with Adam Orłowski (Department of Physics, Tampere University of Technology Korkeakoulunkatu 10, FI-33720 Tampere, Finland; 4Department of Physics and Energy, University of Limerick Limerick, Ireland).

Chapter 4 is written specifically for this dissertation, though some of its content will be adapted for publication as part of a larger review for *Critical Reviews in Biochemistry and Molecular Biology*.

TABLE OF CONTENTS

LIST OF TABLES

LIST OF FIGURES

LIST OF ABBREVIATIONS

Akt	Ak strain transforming
AngII	angiotensin II
ARF	ADP-ribosylation factor 1
ARFGAPs	ARF GTPase activating protein
ATP	Adenosine triphosphate
BAR	Bin1/amphiphysin/Rvs167
BSA	Bovine serum albumin
Cas9	CRISPR associated protein 9
CDP-DAG	cytidine-diphospho-diacylglycerol
CERT	ceramide transfer proteins
CMP	cytidine-monophosphate
CRISPR	clustered regularly interspaced short palindromic repeats
CTP	cytidine-trisphosphate
DAG	diacylglycerol
DHFR	dihydrofolate reductase
DIC	Differential interference contrast
DCC	deleted in colorectal cancer
DMSO	Dimethyl sulfoxide
DOPC	1,2,-dioleoyl-PtdCho
EGF	epidermal growth factor
EGFR	epidermal growth factor receptor
ENTH	epsin N-terminal homology
ER	endoplasmic reticulum

FAPP1	Four-phosphate-adaptor protein 1
FM4-64	N-[3-Triethylammoniumpropyl]-4-[p-diethylaminophenylhexatrienyl] pyridinium dibromide
FYVE	Fab1/YOTB/Vac1/EEA1
GAP	GTPase-Activating Protein
GEF	Guanine Nucleotide Exchange Factor
GFP	green fluorescent protein
GOLPH3	Golgi Phosphoprotein 3
HAD	haloacid dehalogenase
HER2	human epidermal growth factor receptor 2
HT	Host Targeting
Hr	hour
HR	Homologous recombination
IGFBP2	insulin-like growth factor binding protein 2
Ins	inositol
IP$_3$	Ins-1,4,5-trisphosphate
LNS2	Lipin/Ned1/Smp2
MCS	membrane contact site
MDS	molecular dynamics simulations
MERTK	c-Mer tyrosine kinase
mRNA	messenger RNA
miRNA	micro RNA
NHEJ	Non-Homologous End Joining
OPLS	Optimized Potentials for Liquid Simulations
OSBP	oxysterol binding proteins
Osh	OSBP homology

ORP	OSBP-related protein
PAP	phosphatidic acid phosphatase
PEXEL	*Plasmodium* Export Element
PEST	proline, glutamic acid, serine, threonine
PH	Pleckstrin homology
PI3K	phosphatidylinositol 3-OH kinase
PI4K	phosphatidylinositol 4-OH kinase
PITP	phosphatidylinositol transfer protein
PIP	phosphoinositide
PIS	phosphatidylinositol synthase
PKC	protein kinase C
PL	phospholipid
PLC	phospholipase C
PLD	phospholipase D
PM	plasma membrane
PtdCho	phosphatidycholine
PtdIns (or PI)	phosphatidylinositol
PtdIns3P	phosphatidylinositol-3-phosphate
PtdIns(3,4)P_2	phosphatidylinositol-3,4-bisphosphate
PtdIns(3,4,5)P_3	phosphatidylinositol-3,4,5-trisphosphate
PtdIns4P	phosphatidylinositol-4-phosphate
PtdIns(4,5)P_2	phosphatidylinositol-4,5-bisphosphate
PtdIns5P	phosphatidylinositol-5-phosphate
PtdOH	phosphatidic acid
PTEN	phosphatase and tensin homolog

PyrPtdCho	1-Palmitoyl-2-decapyrenyl-sn-glycero-3-phosphocholine
PyrPtdIns	1-Palmitoyl-2-decapyrenyl-sn-glycero-3-phosphoinositol
RdgB	retinal degeneration B
RFP	red fluorescent protein
RMSD	root mean square deviation
RMSF	root mean square fluctuation
Sfh	Sec fourteen homology
StAR	Steroidogenic acute regulatory protein
TET	Tetracycline
TGN	*trans*-Golgi Network
TNP-PtdEtn	2,4,6-trinitrophenyl-phosphatidylethanolamine
WHAM	weighted histogram analysis method
WT	wild type
YFP	yellow fluorescent protein
YPD	yeast peptone dextrose
Vps34	vacuolar protein sorting 3

CHAPTER 1: PHOSPHATIDYLINOSITOL TRANSFER PROTEINS AND INSTRUCTURE REGULATION OF LIPID KINASE BIOLOGY

Introduction

Inositol (Ins) and phosphoinositide signaling pathways are major intracellular regulatory systems of eukaryotic cells, and their derangements are underlying causes of many diseases. In spite of how much we have learned about phosphoinositide signaling and its regulation, central mechanisms for how phosphoinositide signaling is diversified are still poorly understood. This chapter addresses one such major gap by focusing on PITPs and their mechanisms for specifying biological outcomes of phosphoinositide signaling. That PITP-deficiencies are relevant to neurological diseases, metabolic syndromes and cancer (e.g. as a pro-angiogenic factor in breast cancer) testifies to the biomedical impact of these proteins. At the cellular levels, evidence that PITPs regulate membrane trafficking, lipid droplet metabolism, developmental programs of polarized membrane biogenesis, and growth factor/morphogen receptor signaling identify exciting areas for inquiry. Yet, it is remarkable how little we know about what cellular processes are controlled by PITPs, or about the mechanistic details for how the conformational dynamics of lipid-exchange reactions catalyzed by these proteins govern the actions of PITPs as regulators of phosphoinositide signaling. This chapter discusses the mechanisms by which PITPs execute novel modes of signal control, i.e. by instructing biological outcomes of PtdIns kinases. Studies of the Sec14-like PITPs provide an accurate picture of what is known, and what remains unknown, regarding mechanisms for how PITPs interface with phosphoinositide signaling in eukaryotic cells. We focus in this chapter primarily on Sec14-like PITPs to illustrate progress that has been made, and what progress still needs to be made, regarding PITPs and how these proteins are integrated into the larger network of phosphoinositide signaling.

Inositol as a versatile signaling scaffold

Roles for phosphorylated D-*myo*-inositols (Ins-phosphates) and phosphoinositides (PIPs) in signal transduction are well documented (Michell 2008; Fruman et al. 1998; Di Paolo and De Camilli 2006; Balla 2013), and phosphoinositides fulfill dual signaling roles in this capacity. First, phosphoinositides are metabolic precursors whose hydrolysis by phospholipases C (PLC) initiates production of the potent second messengers diacylglycerol and soluble Ins-phosphates. Historically, the most celebrated such case is PLC-mediated hydrolysis of phosphatidylinositol-4,5-bisphosphate (PtdIns(4,5)P_2) to produce diacylglycerol and the soluble Ins-1,4,5-trisphosphate (IP$_3$) (Suh et al. 1997; Rhee 2001). The former lipid second messenger regulates activities of protein kinases C, whereas this particular isomer of IP$_3$ both gates intracellular calcium channels and serves as the obligate precursor of the other soluble Ins-phosphates and Ins-pyrophosphates (Berridge and Irvine 1984; Odom et al. 2000).

The chemical diversity of the Ins-phosphates, and the relationship of that diversity to the signaling capacities of these second messengers, lays the groundwork for arguments that Ins is evolution's favorite molecule. As each position of the 6-member Ins ring can be phosphorylated (and, for some positions, pyro-phosphorylated), the potential Ins-phosphate cabal is a large one indeed. A simple binary code allows for 63 distinct molecules monophosphorylated at any position, and a trinary code balloons that potential to 728 distinct molecules if both mono- and pyro-phosphorylation is allowed at any position. Thus, the Ins headgroup is a versatile chemical scaffold upon which can be written a large set of unique signaling states, each distinguished from the others on the basis of how phosphates (or pyro-phosphates) are arranged around the Ins ring. It is therefore not surprising that the large numbers of chemically distinct Ins-phosphates produced by cells translate to diverse biological effects. These soluble compounds regulate a wide spectrum of cellular functions ranging from mRNA transcription, to mRNA transport across nuclear pores, to protein folding, and to regulation of enzyme activities (Alcázar-Román et al. 2006; Macbeth et al. 2005; Tan et al. 2007; Lee et al. 2007).

2

Second, the phosphoinositide molecules themselves have intrinsic signaling capabilities independent of their roles as precursors for other second messenger molecules. This realization came from the discovery that phosphoinositides carrying phosphates on the 3-OH position of the Ins headgroup are not substrates for PLCs. As is the case for the Ins-phosphates, there are distinct phosphoinositide classes that differ in the position and number of phosphate groups that decorate the Ins ring. This chemical information is also decoded by proteins, and this recognition mechanism enables protein recruitment to membranes, and their subsequent activation, with spatial and temporal specificity. Phosphoinositides have roles in addition to recruitment of proteins to membranes. We now appreciate these lipids are important allosteric co-factors that modulate the activities of various enzymes and ion channels (Di Paolo and De Camilli 2006; Hilgemann et al. 2001).

The chemical diversity of the soluble Ins-phosphates is not matched by that of the phosphoinositides. That is, the phosphoinositide cabal is far simpler. Yeast produce only five phosphoinositides (PtdIns3P, PtdIns4P, PtdIns5P, PtdIns(3,5)P_2, and PtdIns(4,5)P_2), of which only the two 4-OH phosphorylated species are essential for viability (Fruman et al. 1998; Di Paolo and De Camilli 2006; Balla 2013). Higher eukaryotes produce seven -- the five listed for yeast with the addition of PtdIns(3,4)P_2 and PtdIns(3,4,5)P_3. The chemical simplicity of phosphoinositides notwithstanding, the biological outcomes of phosphoinositide signaling remain exceedingly diverse. How this diversity in functional outcome is achieved from such a restricted set of molecules remains an important question in contemporary cell biology. It seems clear that solution of the diversification paradox requires a high degree of functional compartmentalization of phosphoinositide signaling pools.

Coincidence detection and phosphoinositide signaling

Functional diversification of phosphoinositide signaling is primarily attributed to the deciphering of phosphoinositide chemical codes by specific phosphoinositide-binding modules

(e.g. PH-, ENTH-, FYVE-, BAR-domains, etc). Binding of a specific phosphoinositide species by such modules is subsequently translated to biological action by register of secondary effector binding cues – thereby generating a combinatorial coincidence detection code that confers signaling specificity Figure 1.1A. There is no question that cells employ this post-production, or 'back-loaded', strategy to diversify biological outcomes for phosphoinositide signaling.

Yet, the 'back-loaded' concept does not satisfactorily account for the remarkable diversity in biological outcomes for phosphoinositide signaling. This shortcoming reflects the failure of this model to address compartmentation of phosphoinositide pools other than by rather low resolutions mechanisms involving differential intracellular localization of lipid kinases, etc. A striking example of the inadequacy of strictly 'back-loaded' mechanisms for diversifying phosphoinositide signaling is provided by the yeast *Saccharomyces cerevisiae*. In the example illustrated in Figure 1.1B, Stt4 PtdIns 4-OH kinase signaling in this organism has at least six distinct biological outcomes, and each outcome tracks with a specific PITP. This example, on stark display in a simple unicellular eukaryote, clearly reports that the biological outcomes of phosphoinositide signaling are neither exclusively determined by the chemical nature of the phosphoinositide, nor by identities of the PtdIns kinases that produce it (Bankaitis et al. 1990; Wu et al. 2000; Routt et al. 2005; Desfougeres et al. 2005; Ren et al. 2014). Rather, PITPs help determine the biological outcomes for phosphoinositide signaling via what we term a 'front-loaded' mechanism (Figure 1.1C). How might 'front-loaded' mechanisms work? Herein, we explore the concept that PITPs specify biological outcomes for PtdIns kinase activities via mechanisms that are coupled to the very act of phosphoinositide synthesis.
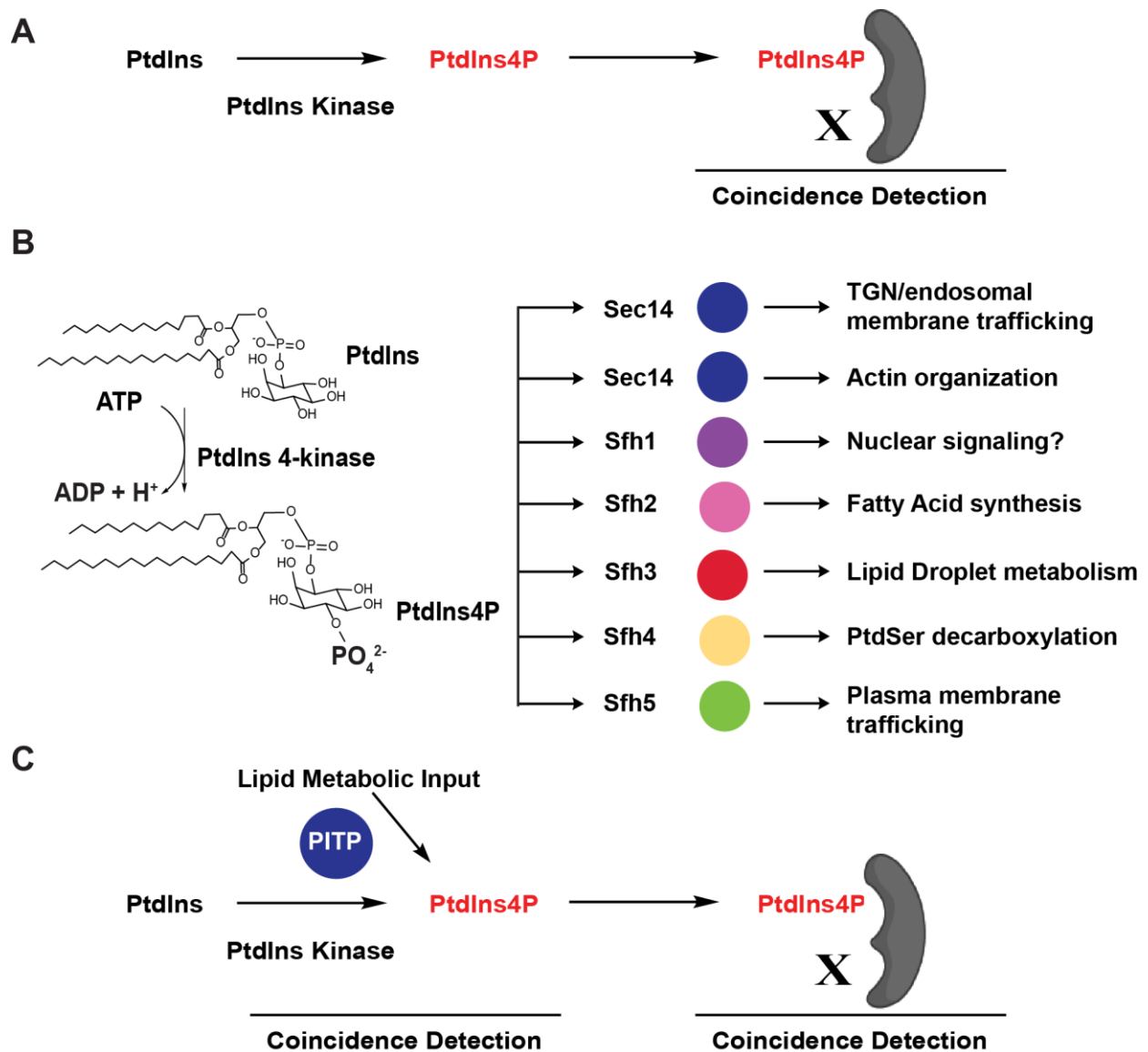
Figure 1.1. Diversity of PtdIns 4-OH kinase signaling in a unicellular cell. **(A)** Back-loaded models for diversifying phosphoinositide signaling interpret determination of biological outcome via a dual coincidence mechanism. In such models, distinction of phosphoinositide chemical identity is linked to recognition of some other effector after phosphoinositide synthesis has occurred (PtdIns 4-OH kinase signaling shown as example here). This combination specifies biological outcome. **(B)** Yeast have two essential PtdIns 4-OH kinases to which can be assigned a larger number of biological outcomes of which seven are shown. Each biological outcome

tracks with a specific Sec14-like PITP. **(C)** PITP-mediated front-loaded model for diversifying phosphoinositide signaling. Front-loaded models for diversifying phosphoinositide signaling interpret determination of biological outcome via a primed channeling of PtdIns to an appropriate kinase (4-OH kinase signaling shown here). The channeling is determined at the synthesis event itself and is determined by the identity of the PITP interacting with the kinase. The differential lipid binding specificities of individual PITPs define the source of metabolic input to the PtdIns kinase, and the PITPs themselves could assemble distinct phosphoinositide binding effectors at the site where the signaling phosphoinositide is (or will be) produced. Such a strategy produces highly integrated signaling circuits with point resolution (dimensions of single protein complexes). This model also identifies PtdIns 4-OH kinases as fundamentally biologically insufficient enzymes, even as wild-type enzymes with all accessory subunits present. Combination of both front- and back-loaded strategies greatly amplifies the simple phosphoinositide chemical code into a large biological outcome space.

Phosphatidylinositol transfer proteins

PITPs are not enzymes, but proteins that mobilize energy-independent transfer of PtdIns, PtdCho and other lipids between membranes *in vitro*, and are therefore also inferred to transfer lipids in a manner not energized by ATP hydrolysis *in vivo* (Karel and Wirtz 2006; Cockcroft and Carvou 2007). PITPs are efficient in this regard as these proteins stimulate cell-free rates of PtdIns transfer between membranes by several orders of magnitude. It is by this operational 'transfer-assay' that PITPs are historically defined. But is this an unfortunate definition that miscasts PITPs as physiologically relevant inter-membrane lipid carriers, thereby sentencing interpretations of these activities to the prison of a superficial and essentially untestable model? We argue such is the case. It is our view that, after some four decades, the lipid transfer protein field still languishes under the conceptual straightjacket imposed upon it by the direct and rather uncritical linkage of in vitro transfer activities to *in vivo* functions as lipid carriers. We discuss alternative interpretations for the lipid-exchange activities, and these ideas suggest powerful new insights into how signaling can be highly compartmentalized – even in circumstances where similar enzymatic reactions are arranged in close quarters on the same membrane surface.

The biochemical and functional questions surrounding these proteins notwithstanding, PITPs are highly conserved across the eukaryotic kingdom. This property implies biological importance, and these proteins fall into 2 families. The Sec14-like PITPs define a superfamily that includes retinaldehyde binding proteins, Ras-GAPs, Rho-GEFs, tyrosine phosphatases, and other phosphoinositide-binding proteins (Phillips et al. 2006; Saito et al. 2007; Bankaitis et al. 2010). The founding member is the major yeast PITP Sec14 (Bankaitis et al. 1990; Bankaitis et al. 1989; Cleves et al. 1991a). Sec14 studies are driving the PITP and lipid transfer protein fields because structural, computational, biochemical and genetic approaches are being productively applied towards elucidation of functional mechanisms. The START-like PITPs belong to the STAR-related lipid transfer protein superfamily and are less well understood.

These proteins are the primary subjects of recent reviews and readers are referred to those summaries for further details (Cockcroft 2007; Cockcroft and Garner 2011; Shadan 2008). Herein, we limit discussion of the START-like PITPs to the question of whether these proteins might also channel PtdIns kinase activities to dedicated biological outcomes (Bankaitis et al. 2010; Schaaf et al. 2008).

PITPs and phosphoinositide signaling from a historical perspective

The experimental origins of lipid transfer proteins lie in studies that identified vesicle-trafficking-independent mechanisms of lipid trafficking in cells. These studies were of various designs, but all relied on measuring inter-compartmental trafficking of lipids in the face of some chemical or conditional inhibition of secretory pathway activity (Sleight and Pagano 1983; Kaplan and Simoni 1985; Vance et al. 1991; Wirtz 1991). Many of the experimental strategies also rested on necessarily rapid purifications of plasma membrane from endoplasmic reticulum using panning techniques. Rapid recoveries of highly purified plasma membrane fractions were absolutely required for interpretation of the data. With the benefit of hindsight informed by the advent of sensitive technologies with which to monitor membrane purity, and the newly rediscovered significance of such complicating structures as intermembrane contact sites (Prinz 2014), it is now apparent that rapid methods for membrane separation and purification were inadequate for the task at hand. The membrane fractions used for readout were not pure, and membrane contaminants preclude confident interpretation of the data. So, the experimental foundation for lipid trafficking via soluble protein carriers is less compelling than previously believed.

With regard to functional interpretations of PITPs, biochemical studies subsequently intersected with theoretical considerations stemming from the knowledge that the metabolic cycle for regenerating phosphoinositide molecules after their consumption by PLC during the course of agonist-stimulated signaling required navigation of a problem of biochemical

8

compartmentation. This problem is grounded on the central presumption that the compartments where PtdIns, the metabolic precursor of all phosphoinositides, is synthesized is physically distant from the location where phosphoinositides are consumed. The specific case under discussion considers replenishment of PtdIns(4,5)P$_2$ pools in the plasma membrane upon agonist stimulation of PLC activity. With respect to synthesis, PtdIns is produced de novo by the enzyme PtdIns synthase which converts Ins and cytidine-diphospho-diacylglycerol (CDP-DAG) to produce PtdIns and cytidine-monophosphate. CDP-DAG is produced from phosphatidic acid (PtdOH) and cytidine-trisphosphate. Both PtdIns- and CDP-DAG-synthases are integral membrane proteins of the endoplasmic reticulum. A solution to this topological problem was suggested where soluble lipid carrier proteins ferry PtdIns from the endoplasmic reticulum to the plasma membrane, and return DAG or PtdOH from the plasma membrane to the endoplasmic reticulum in a retrograde arm of the cycle (Michell 1975; Figure 1.2). This conjecture set a framework for translating the biochemical properties of PITPs to physiological functions in support of phosphoinositide signaling (Paridon et al. 1987). Results from permeabilized cells claiming an obligatory role for soluble PITPs in growth factor receptor signaling were subsequently taken as evidence in support of this basic concept (Kauffmann-Zeh et al. 1995; see below). However, the veracity of such claims in in vivo settings is now uncertain. Recent studies using sophisticated vital imaging studies reveal that the PtdIns synthase enzyme itself may be mobilized from the endoplasmic reticulum via a COPII vesicle-like mechanism, and positioned in the direct proximity of the plasma membrane (Kim et al. 2011). Moreover, available genetic studies with PITP mutant animals and cells also do not support the central predictions of the PtdIns supply model (Alb et al. 2002; Alb et al. 2003; Alb et al. 2007; see below).

Nonetheless, the interpretation of PITPs as lipid carriers remains the prevailing concept for how PITPs execute cellular functions (Prinz 2010; Lev 2010). We view acceptance of this idea to be faith-based because there is no direct evidence that PITPs physically remove a PtdIns monomer from the endoplasmic reticulum and then transport it to the plasma membrane

9

in cells where it is preferentially channeled into phosphoinositide synthesis. The experiment to appropriately test this model in cells is a technically difficult one of course, but there are other reasons to consider alternative ideas. For example, the first PITPs characterized were PtdIns and phosphatidylcholine (PtdCho) transfer proteins and it is for this reason that proteins with those particular properties are often referred to as classical (or canonical) PITPs. In the several cases where the integrity of robust PLC signaling pathways has been interrogated in cells or organisms lacking individual classical PITPs, the results are not consistent with the predictions of the PtdIns transfer cycle (see below).

The designation of PtdIns/PtdCho transfer proteins as classical PITPs will ultimately prove to be an awkward designation as non-classical PITPs (i.e. proteins that transfer PtdIns and some other ligand distinct from PtdCho) have been discovered, and these proteins outnumber the classical PITPs (Saito et al. 2007; Schaaf et al. 2008). Nonetheless, the non-classical PITPs are intriguing in part because the most parsimonious property of a PITP involved in the PtdIns supply cycle illustrated in Figure 1.2 is that of a non-classical PtdIns/DAG or PtdIns/PtdOH transfer protein. Support for PITPs being involved in a PtdIns carrier cycle would additionally involve two experimental demonstrations: (i) that acute loss of a PtdIns/PtdOH transfer protein inhibits sustained PLC signaling, and (ii) that loss of the PITP also reduces flux through the PtdIns biosynthetic pathway. While demonstrations that satisfy both criteria have not been reported to date, PITPs with the appropriate biochemical properties are now identified (see below).
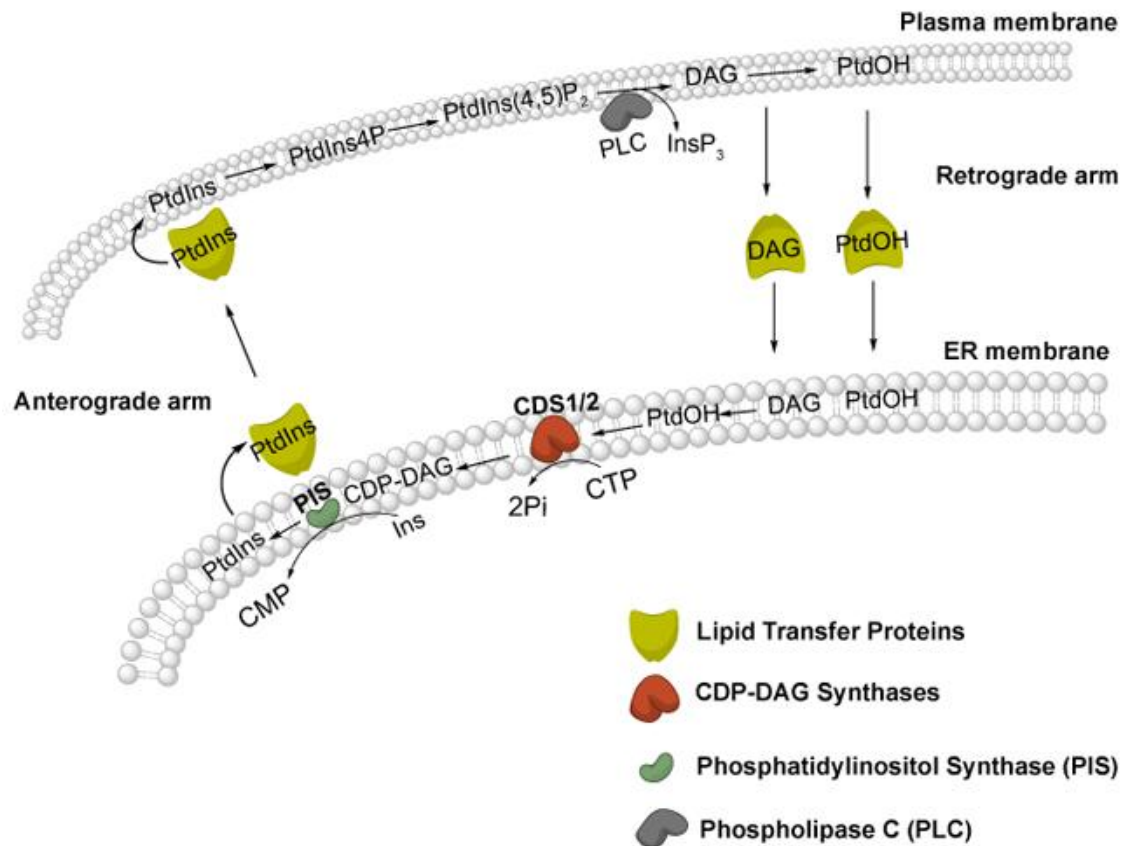
Figure 1.2. A lipid transfer cycle for coupling PtdIns synthesis to phosphoinositide signaling. Lipid-transfer proteins are proposed to drive a cycle of anterograde PtdIns transfer from the endoplasmic reticulum to the plasma membrane, and balanced retrograde transfer of either diacylglycerol (DAG) or phosphatidic acid (PtdOH), to fuel phosphoinositide synthesis and signaling. The model in its simplest and most integrated form predicts PITP deficits will result in reduced phosphoinositide signaling at the plasma membrane with diminished resynthesis of PtdIns at the endoplasmic reticulum.

The anatomy of the Sec14 phospholipid exchange cycle

        To understand the functions of PITPs as molecules, no matter in what specific

physiological settings these functions are discharged, it is essential to understand the complex

dynamics associated with how PITPs execute lipid exchange. Structural and biophysical studies

are contributing strongly in this regard. The superficial shape of the exchange cycle is simple.

The PITP homes onto a membrane surface where it undergoes a conformational change to

expose the hydrophobic pocket so that lipid exchange can ensue. Electron spin-labeling studies

demonstrate the hydrophobicity gradient across the Sec14 lipid-binding pocket closely mimics

that of a membrane leaflet (Smirnova et al. 2007). The exchange process, when viewed in basic

terms, therefore rests on the concept that phospholipid (either bound or to be bound) is

presented with a choice of partitioning into one of two chemically equivalent environments. That

is, from the membrane into the hydrophobic pocket and vice-versa. A simple partitioning

mechanism neatly accounts for the energy-independence of the lipid exchange cycle. However,

PITP binding to the membrane must evoke a highly local destabilization of the membrane

surface in order to 'activate' lipid molecules for chemical partitioning -- thereby identifying those

activated molecules as lipids competent for exchange. The various questions surrounding the

early steps in the exchange cycle remain to be investigated.

        From the protein point of view, crystallographic studies define two major Sec14

conformers – i.e. the 'open' and 'closed' conformers (Schaaf et al. 2008; Sha et al. 1998;

Phillips et al. 1999). The 'closed' conformer is bound to a single phospholipid molecule, and this

conformer is interpreted to represent the protein in its soluble (cytoplasmic) state. The 'open'

conformer is interpreted as representing the membrane-associated PITP engaged in lipid

exchange (Sha et al. 1998; Phillips et al. 1999). In this form, the hydrophobic pocket is exposed

and lipid-free due to an 18Å displacement of a helical gate element that governs access to the

lipid binding pocket (Figure 1.3A). Reversible cross-linking experiments demonstrate that the

large rigid body motions of the helical gate are essential for lipid exchange. Moreover, these

conformational transitions are themselves controlled by a conformational switch element conserved across the Sec14-superfamily, the G-module. Survey of human disease alleles that involve Sec14-like proteins/domains highlight the importance of this element in the context of the Sec14-fold as a number of these alleles represent missense mutations that alter the G-module itself (Ryan et al. 2007). Outstanding questions for future address include how activity of the G-module is regulated by membrane-binding. Indeed, the closer one examines the Sec14 conformational dynamics associated with lipid exchange, the more interesting these become. Directed evolution experiments indicate that G-module conformational transitions regulate the kinetics of gating of the hydrophobic pocket for lipid exchange, and that activation of the G-module responds to water organization and dynamics within the lipid binding pocket itself (Schaaf et al. 2011).

Although we are now beginning to understand the dynamics of the lipid exchange cycle from the Sec14 point of view, we know nothing about the cycle from the perspective of the phospholipid ligands. As will become clear below, evolving concepts for Sec14-like PITP activities not as lipid carriers, but as novel regulators of the biological outcomes of phosphoinositide signaling, demand an atomistic understanding of the mechanics of lipid exchange from both protein and lipid points of view. The challenges include solving how Sec14-like proteins dock onto membrane surfaces, what trajectories are drawn by PtdIns and secondary lipid ligands as these navigate entry and exit from the hydrophobic pocket, of the relative kinetics of lipid ligand entry and exit from the hydrophobic pocket, and how this relates to the interaction between the PITP and the PtdIns 4-OH kinase.

Lipid binding by Sec14-like proteins

Although the Sec14 conformational dynamics associated with lipid exchange provide a useful picture of the cycle from the protein point of view, an equally critical key to understanding mechanisms of PITP function demands understanding how the lipid ligands enter and exit the

13

hydrophobic pocket. The fact that PtdIns and PtdCho are chemically similar molecules (with the

exception of their respective headgroups) would seem to suggest that the trajectories with which

these two phospholipids enter and/or exit the Sec14 hydrophobic pocket. But, the advent of high

resolution crystal structures of Sec14 and other closely related Sec14-like proteins indicate this

is not at all the case (Schaaf et al. 2008). Structural studies with Sec14 and its close homolog

Sfh1 reveal the PtdCho and PtdIns headgroups are bound at physically distant sites. Whereas

the PtdCho headgroup and glycerol backbone are buried deep within the hydrophobic pocket,

the corresponding regions of bound PtdIns are positioned much closer to the protein surface

(Figure 1.3B). Although Sec14 has a much higher affinity for PtdIns than for PtdCho, the

selectivity for PtdIns vs PtdCho is estimated to be sufficiently small in energetic terms so that

H_2O rearrangements within the hydrophobic pocket are sufficient for negotiating the energy

barriers that confront the heterotypic phospholipid exchange cycle. Of particular mechanistic

relevance, a functional Sec14 molecule must house both PtdCho and PtdIns binding/exchange

capability in order to stimulate production of PtdIns4P in cells (Schaaf et al. 2008; Schaaf et al.

2011). Those data demonstrate that both homotypic PtdCho- and homotypic PtdIns-exchange

reactions are biologically futile activities, and that Sec14-mediated stimulation of PtdIns 4-OH

kinase activity requires heterotypic exchange reactions (e.g. PtdIns for PtdCho or vice versa).
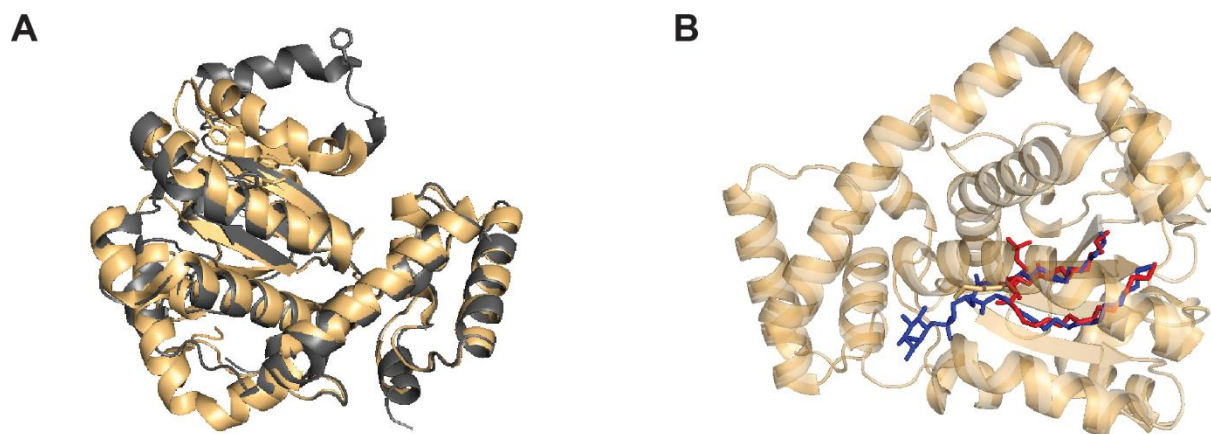
Figure 1.3. Structural engineering of Sec14-like PITPs. **(A)** Access to lipid binding pocket is controlled by the dynamics of a helical gate. The α-carbon backbones of the open (silver) and closed (gold) structures of Sec14 and Sfh1 are rendered in ribbon diagram and superposed. The respective positions of the helical element that gates access to the lipid binding pocket, and the displacement of the gating element between the two conformers, are highlighted. **(B)** Classical Sec14-like PITPs bind PtdIns and PtdCho at distinct sites. The binding poses of PtdIns (blue) and PtdCho (red) within the closed Sec14 (Sfh1) conformer are shown. The respective headgroups are identified by the corresponding solid colored circles.

Sec14-like proteins and instructive regulation of PtdIns kinase activity

Why is a heterotypic exchange cycle essential for Sec14-mediated support of optimal PtdIns 4-OH kinase activity and stimulated phosphoinositide synthesis in yeast cells? It is difficult to argue that PtdIns transfer mechanisms are involved because PtdIns naturally constitutes 20-25 mol% of bulk glycerophospholipid in yeast. Why would there be an obligate need for a PITP-driven PtdIns supply mechanism in membranes so rich in PtdIns? Alternative concepts need to be considered. In that regard, a kinetic trap model is proposed where slow PtdCho egress from the pocket results in abortive PtdIns entries – thereby exposing a frustrated PtdIns that is registered by the lipid kinase as an accessible substrate for phosphorylation (Bankaitis et al. 2010; Schaaf et al. 2008).

This model has several key ideas, three of which are emphasized here. First, PITPs are required for biologically sufficient PtdIns4P production because PtdIns 4-OH kinases (at the least) are biologically inadequate interfacial enzymes when substrate PtdIns resides in a bilayer. This inadequacy is manifest even when PtdIns is a major bulk membrane phospholipid in the cell. Second, it describes stimulation of PtdIns 4-OH kinase activity in terms of a PITP-mediated PtdIns presentation mechanism where effective PtdIns presentation by Sec14 requires PtdCho binding. Third, the model identifies the optimal PtdIns substrate for PtdIns 4-OH kinase action as a lipid molecule that is frustrated in its entry into the Sec14 pocket. That is, a PtdIns molecule that never successfully enters the Sec14 pocket. In this model, Sec14 operates as a PtdCho sensor that couples PtdCho metabolic information to activation of PtdIns as a substrate for production of a dedicated signaling pool of PtdIns4P. The ability of Sec14 to prime PtdIns4P production in response to PtdCho metabolic cues outlines the basic principle of what we term instructive regulation of PtdIns 4-OH kinase activity. A detailed example of this idea is presented in the following section using Sec14-mediated regulation of membrane trafficking through the TGN/endosomal system as biological context.

The base concept that Sec14-like proteins specify privileged phosphoinositide signaling pools via instructive regulation of lipid kinases has interesting implications, and structural studies indicate this type of regulation might be very broad indeed. The structural signatures, or bar codes, that identify the elements directly involved in PtdIns headgroup coordination are conserved throughout the Sec14 superfamily, while the PtdCho-binding bar code is recognized only in a subset of these proteins (Bankaitis et al. 2010; Schaaf et al. 2008; Nile et al. 2010). These features portend conservation of inositol-lipid binding capacity throughout the Sec14-superfamily with an accompanying diversification in the binding specificities for secondary lipid ligands. Using this idea to extend the principle of instructive lipid kinase regulation, Sec14-like proteins/domains can be interpreted as adaptors that interface the metabolism of diverse lipids/lipophiles with stimulated phosphoinositide synthesis for formation of functionally compartmentalized lipid signaling pools.

The concept of instructive regulation of inositol lipid kinases is gaining momentum from the recognition that naturally occurring human disease alleles of Sec14-superfamily proteins, including the most common inherited alleles associated with human retinal degeneration and acute vitamin E deficiencies, directly involve PtdIns (or phosphoinositide) binding bar-code residues (Bankaitis et al. 2010; Schaaf et al. 2008; Nile et al. 2010; He et al. 2009; Kono et al. 2013). That remarkable correlation implies an inositol phospholipid is a genuine physiological ligand for the Sec14-like protein in question (cellular retinadehyde binding protein and α-tocopherol transfer protein, respectively). Indeed, recent structural and functional analyses of the α-tocopherol transfer protein strongly reinforce this concept (Kono et al. 2013). Other Sec14-like proteins/domains associated with human disease include caytaxin and neurofibromin, and loss-of-function mutations that compromise the presumptive PtdIns-binding bar-code motifs of these proteins have now been identified (Bankaitis et al. 2010; Schaaf et al. 2008; Nile et al. 2010).

Instructive regulation from the perspective of yeast Sec14-like PITPs

The yeast system offers strong opportunities for exploring instructive regulation of PtdIns kinases by Sec14-like proteins. As discussed above, each of the six *Saccharomyces* Sec14-like PITPs specify unique biological outcomes for PtdIns 4-OH kinase signaling, and four of the six are non-classical on the basis of failing to exhibit measurable PtdCho-transfer activities and not displaying recognizable PtdCho-binding bar-codes (Ren et al. 2014; Schaaf et al. 2008; Nile et al. 2010; Li et al. 2000). The Sfh3 PITP represents a particularly interesting case in this regard as, even though it is a PITP that activates PtdIns 4-OH kinase activity in a fashion analogous to the one discharged by Sec14 in the same cell, it nonetheless acts in a biologically antagonistic way to Sec14 (Ren et al. 2014). This functional antagonism reflects competing activities by these PITPs in channeling PtdIns 4-OH kinase activities towards disparate biological outcomes. Whereas Sfh3 directs PtdIns 4-OH kinase signaling towards developmental regulation of lipid droplet metabolism, Sec14 trains lipid kinase activity on membrane trafficking through the TGN/endosomal system. The idea of instructive stimulation of PtdIns 4-OH kinases by Sec14-like proteins posits that channeling of PtdIns 4-OH kinase activity to distinct biological outcomes is determined in part by the binding of these two PITPs to distinct secondary ligands. Indeed, the dimensions and chemical environment of the Sfh3 hydrophobic pocket differ radically from those of the classical PITPs Sec14 and Sfh1 (Ren et al. 2014; Schaaf et al. 2008) – i.e. a property consistent with diverged secondary lipid binding specificities. Identification of the secondary ligands hypothesized to prime PtdIns presentation to the lipid kinases is now an important endeavor, and there are data to suggest that such a ligand for Sfh3 may be a sterol (Holič et al. 2014).

How do Sec14-like PITPs interact with PtdIns 4-OH kinases? An enzyme::PITP complex offers the simplest solution for PtdIns presentation. In some instances, this may well be the case. One such example involves the dual requirements for a Sec14-like PITP (Sfh4) and the Stt4 PtdIns 4-OH kinase in regulation of phosphatidylserine decarboxylation in yeast (Wu et al.

2000). The Sfh4 requirement shows high PITP-specificity as no other Sec14-like protein can operate as functional surrogate in this metabolic reaction (Routt et al. 2005), and the PITP specificity may reflect the need for a physical interaction between the Sfh4 and the decarboxylase enzyme (Riekhof et al. 2014); although the functional requirement for this interaction has not been shown. In other cases, a tight physical interaction does not seem essential. Stimulation of yeast Pik1 and Stt4 PtdIns 4-OH kinases by Sec14 are two cases in point. The possibility that PITPs might present PtdIns to the lipid kinase *en passant*, and thereby facilitate a 'drive-by' phosphorylation of the headgroup, is consistent with demonstrations that the structurally unrelated vertebrate START-like PITPs can perform as functional Sec14 surrogates in stimulating PtdIns 4-OH kinase activities when expressed at high levels in yeast (Skinner et al. 1993; Ile et al. 2010).

Sec14 and the interface between lipid metabolism and membrane trafficking

Why would cells employ specific Sec14-like PITPs to serve as PtdCho sensors when PtdCho is the most abundant cellular phospholipid? What possible signaling information could come from this curious design? This paradox can be examined by reviewing the results of genetic studies of Sec14 function in vivo, and interpreting those results through the conceptual lens of instructive regulation of the Pik1 PtdIns 4-OH kinase. The PITP activity of Sec14 is essential for yeast cell viability because this activity is required for efficient transport of secretory cargo from the trans-Golgi network (TGN) to the cell surface (Bankaitis et al. 1990; Bankaitis et al. 2010). Sec14 promotes TGN function primarily by regulating a retrograde membrane trafficking pathway that returns components of the anterograde trafficking machinery to the TGN from endosomes (Mousley et al. 2008). Seminal insights into Sec14 function in the TGN/endosomal system came from study of 'bypass Sec14' mutations that circumvent the normally essential Sec14 requirement for membrane trafficking and cell viability (Cleves et al. 1989; Cleves et al. 1991b; Fang et al. 1996). All of the 'bypass Sec14' alleles ultimately proved

19

to be recessive – identifying these as loss-of-function mutations that inactivate functional antagonists of Sec14 activity. These mutations fall into two general categories; those that ablate enzymes of the CDP-choline pathway for PtdCho biosynthesis (Cleves et al. 1991a; Cleves et al. 1991b; McGee et al. 1994), and those that ablate proteins whose activities either degrade (e.g. the Sac1 PtdIns4P phosphatase) or sequester (e.g. the oxysterol binding protein homolog Kes1/Osh4) from PtdIns4P its pro-trafficking downstream effectors (Cleves and Novick 1989; Guo et al. 1999; Rivas et al. 1999; Li et al. 2002; Mousley et al. 2012; Mesmin et al. 2013; Figure 1.4). Those genetic data revealed that Sec14 coordinates PtdCho metabolism with PtdIns4P signaling to promote membrane trafficking through TGN/endosomal compartments, and the PtdCho sensor function is proposed to constitute a mechanism for sensing metabolic flux through the CDP-choline pathway as a proxy for consumption of a pro-trafficking lipid diacylglycerol (Bankaitis et al. 2010; Kearns et al. 1997; Ile and Schaaf 2006). Thus, the PtdCho sensor activity translates to activation of the Sec14 heterotypic exchange cycle for production of a second pro-trafficking lipid, PtdIns4P, by the Pik1 PtdIns 4-OH kinase (Figure 1.4). In this way, Sec14 facilitates the tuning of PtdIns4P production in response to PtdCho synthesis via the CDP-choline pathway and the consumption of DAG in the process. This model provides a coherent and physical picture for the general concept of crosstalk between PtdCho and PtdIns4P metabolic pathways.
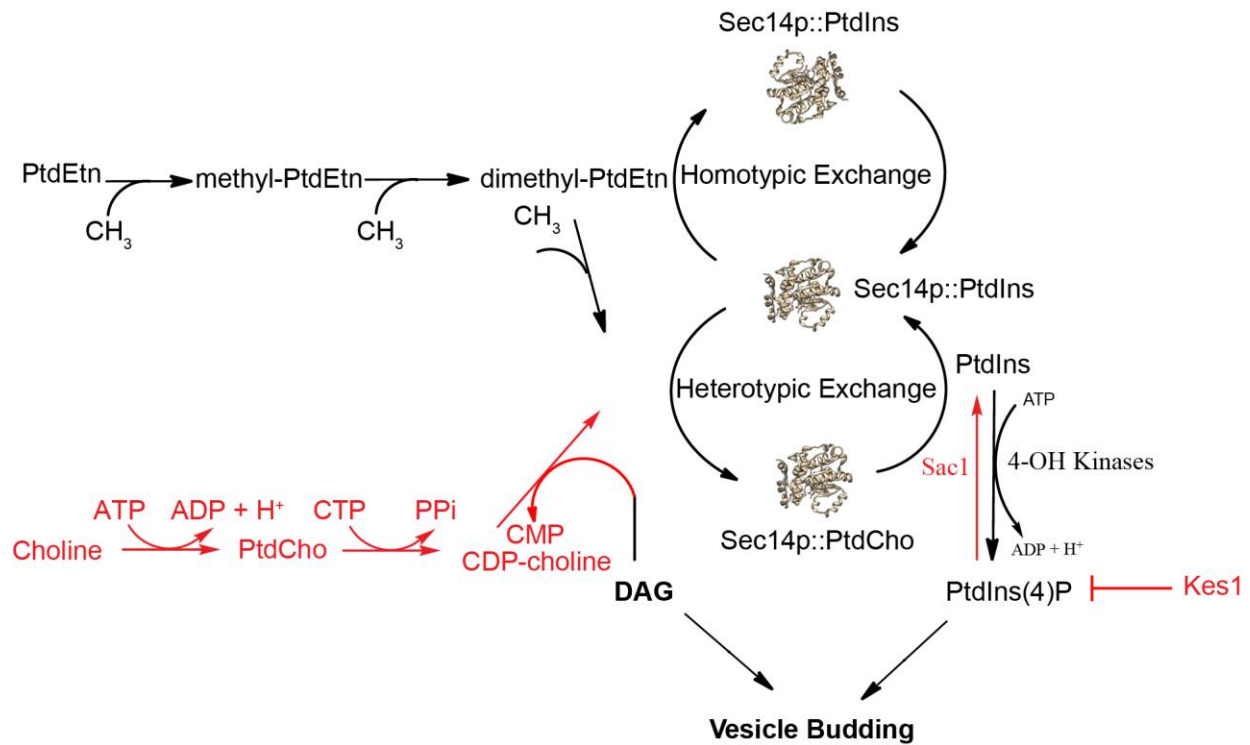
Figure 1.4. Instructive regulation of PtdIns 4-OH kinase by Sec14 and TGN/endosomal membrane trafficking. A model is drawn where Sec14 interfaces PtdCho metabolism (and consumption of the pro-secretory lipid DAG) with the amplitude of PtdIns-4-phosphate pro-secretory signaling in the yeast TGN/endosomal membrane trafficking pathway. Sec14 serves as a sensor for flux through the CDP-choline pathway for PtdCho biosynthesis and, via PtdCho binding and activation of heterotypic exchange cycles, stimulates activity of the Pik1 PtdIns 4-OH kinase to produce PtdIns-4-phosphate in response to CDP-choline pathway activity. Cellular activities whose loss of function result in 'bypass Sec14' are highlighted in red (see text).

Metazoan START-like PITPs

Metazoan START-like PITPs consist of either a free-standing PITP domain, or are multiple domain proteins (Figure 1.5). Numerous lines of evidence indicate that they also regulate phosphoinositide signaling. Several of those annotated physiological contexts recapitulate the Sec14 case in that membrane trafficking events are involved. These include regulated and constitutive secretory processes in neuroendocrine and mast cells (Hay and Martin 1993; Ohashi et al. 1995; Pinxteren et al. 2001), and non-excitatory cells (Jones et al. 1998; Simon et al. 1998), retrograde membrane trafficking from the Golgi complex regulated by the START-domain protein PITPα (Carvou et al. 2010), speculation that endocytic trafficking of the angiotensin II receptor may be regulated by another START-domain protein PITPnc1 (Garner et al. 2011; Garner et al. 2012), and potentiation of anterograde trafficking from the mammalian TGN via regulation of diacylglycerol metabolism by a multi-domain START-like PITP termed PITPnm1. The TGN trafficking activity of PITPnm1 is of interest in that it, like Sec14, counters the antagonistic effects of the CDP-choline pathway for PtdCho biosynthesis on vesicular transport (Litvak et al. 2005). Other signaling circuits that show START-like PITP-dependence include the *Drosophila* visual and olfactory phototransduction pathways, and chemosensation in the worm. These sensory systems depend on activity of the multi-domain START-like PITPs – e.g. fly RdgB and worm pitp-1, respectively, although a requirement for PITP activity in PITP-1 biological function has not been demonstrated (Vihtelic et al. 1991; Milligan et al. 1997; Iwata et al. 2011). There are also reports of an obligate role for the START-domain PITPα and multi-domain PITPnm1 proteins in forward signaling of the epidermal growth factor receptor, and for PITPα in both epidermal growth factor receptor and netrin receptor signaling (Kauffmann-Zeh et al. 1995; Kim et al. 2013; Larijani et al.2003; Xie et al. 2005).
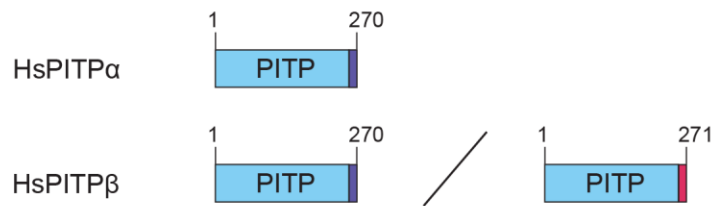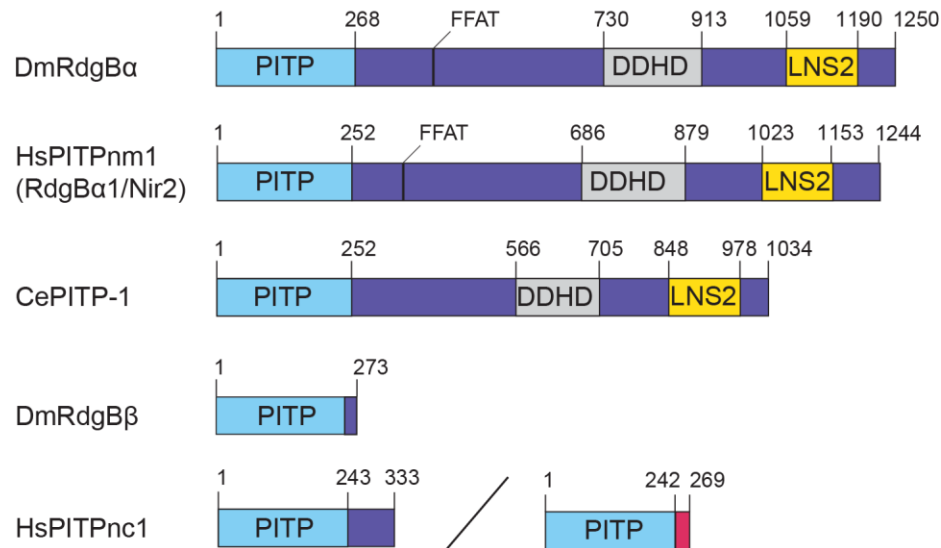
Figure 1.5. Domain architecture of START-like PITPs. Class I PITPs include PITPα and two splice variants of PITPα. Class II PITPs are orthologs of the *Drosophila* DmRdgBα and include the multi-domain human and *C. elegans* HsPITPnm1 and CePITP-1, respectively, the single domain fly DmRdgBα and two splice variants of HsPITPnc1. Alternative nomenclature is indicated in parentheses. Spliceoforms are designated by a diagonal line, and variant C-termini are indicated in pink. Domain location and length of proteins is marked in superscript: PITP (light blue), phosphatidylinositol transfer protein; DDHD (grey); Lipin/Ned1/Smp2; LNS2; FFAT, diphenylalanine in an acidic tract.

START-like PITPs and phosphoinositide signaling

The prevailing thought is these proteins are intracellular PtdIns carriers (Cockcroft and Carvou 2007; Cockcroft 2007; Prinz 2010; Lev 2010). In the case of the START-domain versions, these PITPs are considered to be soluble carriers while the membrane-associated multi-domain proteins are posited to act as shuttle factors that operate in focal areas of close membrane apposition – i.e. intermembrane contact sites (Prinz 2014; Holthuis and Levine 2005; Lev 2012). Unfortunately, the available data from model metazoan organisms – both vertebrate and invertebrate – are rather confusing from the perspective of offering some unified mechanism of function. There is little solid evidence from animal systems to show that growth factor or morphogen receptors obligatory require START-domain PITPs (e.g. PITPα) for forward signaling from the plasma membrane. In cases where the question has been put to the acid experimental test, soluble canonical PITPs (e.g. PITPα) do not score as significant components of PtdIns supply pathways for sustained phosphoinositide signaling at the plasma membrane (Alb et al. 2002; Alb et al. 2003; Alb et al. 2007).

There is clear evidence of the physiological importance of the soluble START-like PITPs, however. Zebrafish PITPβ and PITPα hypomorphs show defects in establishment and/or maintenance of photoreceptor outer segments and embryogenesis, respectively (Ile et al. 2010). PITPα-deficient mice are born alive but suffer perinatal death brought on by multiple pathologies. These include a dramatic spinocerebellar neurodegenerative disease marked by a fulminating course of aponecrotic cell death and neuroinflammation, an inability of the animals to process and transport lipoproteins from the enterocyte, striking lipid homeostatic defects in the liver, and degeneration of pancreatic islets that leads to a catastrophic hypoglycemia (Alb et al. 2003). Interestingly, the high flux phosphoinositide-driven synaptic cycle remains fully intact in *pitpα* null neurons – even in performance assays where such cells are subjected to excitation trains of such intensities that the synaptic capacities of the test neurons are ultimately overwhelmed (Alb et al. 2007). A biologically functional PITPα must bind PtdIns as evidenced by

the demonstration that mouse strains expressing a mutant protein specifically defective in PtdIns (but not PtdCho) binding, as sole source of PITPα activity in the animal, phenocopy the null mouse (Alb et al. 2007). Those data demonstrate an authentic role for PITPα in regulating inositol lipid signaling in the mouse, although there are no obvious derangements in bulk phosphoinositide pools in deficient cells or tissues (Alb et al. 2003).

Recently, the mammalian PITPnc1 and its fly cognate RdgBβ were recognized to be PtdIns/ PtdOH transfer proteins (Garner et al. 2012), and that the multi-domain PITPnm1 also binds PtdOH. In this case, PtdOH binding activity resides in a C-terminal LNS2 domain, in addition to PtdOH being the counter-ligand for the PITP domain (Kim et al. 2013; Cockcroft et al. 2016). Non-canonical proteins such as PITPnc1 display the biochemical properties expected of a lipid shuttling activity involved in the phosphoinositide consumption-regeneration cycles depicted in Figure 1.2, and PITPs such as these will be particularly interesting to analyze with regard to the integrity of phosphoinositide signaling and capacity for PtdIns resynthesis in genuine *in vivo* contexts. In that regard, there is growing interest in PITPnc1 from the perspective of cancer biology. The microRNA mir-126 exhibits tumor suppressor activity (Tavazoie et al. 2008; Guo et al. 2008; Feng et al. 2010), and one of its target genes is PITPNC1 (Png et al. 2012). Downregulation of mir-126 and consequent elevation of PITPnc1 levels promotes recruitment of endothelial cells to tumors with subsequent increase in angiogenesis and increased metastatic potential (Png et al. 2012), and we will discuss this in more detail in Chapter 4.

START-like PITPs at inter-membrane contact sites

The multi-domain PITPs (e.g. PITPnm1) are envisioned to participate in such capacities via endoplasmic reticulum::plasma membrane contact sites that organize and integrate the calcium signaling machineries of those two membrane systems in response to cell stimulation (Prinz 2010; Lev 2010). The primary physiological activities of these multi-domain PITPs are

likely restricted to excitatory cells where the amplitudes of induced signaling are very high (e.g. neurons). Several observations are consistent with such a view. First, the *Drosophila* RdgBα is functionally important only in sensory organs involved in vision and olfaction. The null fly is otherwise viable. The PITP-1, also the sole multi-domain PITP in the worm, is similarly nonessential for base viability of this organism (Iwata et al. 2011). Third, siRNA-mediated knockdown of PITPnm1 does not affect viability of the hypomorphic mammalian cells in an *ex vivo* context (Litvak et al. 2005). This result is congruent with genetic data as the PITPnm1 null mice are viable – albeit with defects in cholesterol and calcium homeostasis and altered auditory functions (http://www.informatics.jax.org/marker/MGI:1197524; Carlisle et al. 2013). An obligate role for the PITP-domain in discharge of these physiological activities remains to be demonstrated. The cellular and animal viability data are puzzling given the reported obligatory roles for this protein in promoting growth factor signaling and anterograde protein trafficking from the TGN. It remains formally possible that there is some functional redundancy between PITPnm1 and its close homolog PITPnm2 (Lu et al. 2001). However, the tissue expression profile for PITPnm2 is restricted to retina and dentate gyrus, and is therefore much more limited than that of the widely expressed PITPnm1. As such, PITPnm2 is likely the true mammalian ortholog of fly RdgBα. However, mice lacking PITPnm2 are healthy and show no defects in photoreceptor function (Lu et al. 2001).

START-like PITPs and instructive regulation of phosphoinositide signaling

Sec14-like and START-like PITPs exhibit completely unrelated structural folds (Figure 4.1) (Yoder et al. 2001; Schouten et al. 2002; Tilley et al. 2004), so it remains an open question as to whether or not these proteins execute mechanistically homologous activities. So, do START-like PITPs also instruct biological outcomes for PtdIns kinase signaling in metazoans? The question cannot be answered at this time because the appropriate experimental test has yet to be devised for the metazoan systems to which these proteins are native. The fact that the

START-like PITP family is far more sparse than is the Sec14 superfamily in even the most complex vertebrates, suggests that instructive regulation is either not a physiologically important activity of these PITPs, or that the biological scope of any such activity is limited for these proteins. However, there are indications these PITPs can execute an instructive regulation when interrogated under quasi-physiological conditions. That evidence comes from yeast systems where both zebrafish and mammalian START-like PITPs efficiently stimulate PtdIns 4-OH kinase activities to produce PtdIns4P under conditions of PtdIns surfeit and high-level expression of the PITP (Ile et al. 2010). The fact that the RdgBα PITP domain can also perform Sec14-like functions when expressed at high levels in yeast, although it cannot fully substitute for Sec14, forecasts that it too has that biochemical capability (unpublished data).

That instructive regulation is a viable alternative for interpreting how the START-like PITPs function is also suggested by an old and puzzling observation. Although RdgBα is a multi-domain PITP of which the START-like PITP domain comprises only some 20% of the total protein sequence (Vihtelic et al. 1991), expression of the RdgBα PITP domain alone is sufficient to fully complement the dramatic retinal degeneration phenotype of null flies (Milligan et al. 1997). By contrast, expression of PITPα in RdgBα-deficient retinal is completely ineffective in this regard. The non-exchangeability of these two PITP modules is also on display in domain-swap experiments where PITPα replaced the RdgBα PITP domain in the context of the full-length protein (Milligan et al. 1997). Perhaps the functional non-equivalence of these two PITPs reflects an ability of the RdgBα PITP to bind PtdOH whereas PITPα lacks this capacity (Yadev et al. 2015). This biological specificity of PITP action, a result usually on display when PITP functions are interrogated in authentic biological contexts, and a central feature of instructive regulation models, is not recapitulated in permeabilized cell experiments where PITP functional promiscuity is the dominant theme (Hay and Martin 1993; Ohashi et al. 1995; Pinxteren et al. 2001; Jones et al. 1998; Cunningham et al. 1996).

That intermembrane contact sites are privileged sites of signaling and lipid transfer is an attractive model, and incorporation of multi-domain PITPs into such structures suggests how these proteins might facilitate intermembrane lipid transfer. Can instructive regulation work within the framework of a contact site? We suggest yes. Localization of the PITP to a contact site physically organizes where instructive regulation of a lipid kinase occurs in response to PtdOH production. In this scenario the PITP serves as a PtdOH sensor that monitors phosphoinositide signaling flux and couples PtdOH production to instruction of enhanced on-demand production of phosphoinositide at a precise site on the plasma membrane. There is much to be learned about the relationship between PITPs and contact sites, however. That expression of the PITP module alone is sufficient to satisfy the demands of the animal for multi-domain PITP function, in the two cases where the issue has been rigorously queried (i.e. fly RdgBα and worm pitp-1; Milligan et al. 1997; Iwata et al. 2011), remains a remarkable and an altogether perplexing result.

PITPs as targets for chemical interference with phosphoinositide signaling

Finally, the concept of instructive regulation of PtdIns 4-OH kinases by PITPs identifies these proteins as highly discriminating portals through which privileged phosphoinositide signaling pools can be interrogated. Proof-of-concept is provided by recent discoveries of small molecule inhibitors with validated specificity for Sec14 (Nile et al. 2014; Lee et al. 2014). Treatment of yeast with biologically active inhibitors recapitulates the phenotypes associated with *sec14* loss-of-function mutations, and there are no obvious off-target effects. Interestingly, Sec14 is subject to specific inhibition by several different chemical scaffolds (Lee et al. 2014), and the available data show that PITP-directed small molecule inhibitors offer superior strategies for interfering with phosphoinositide signaling pools that interface with specific biological pathways. Moreover, these PITP-targeted interventions can be applied with far greater specificities than those afforded by even the most specific inhibition of individual PtdIns-kinases (Figure 1.6), or even enzyme dimerization-based (e.g. rapalog) depletion of compartment-specific pools of individual phosphoinositides.

Two objections against the idea of targeting PITPs for inhibition by small molecules can be imagined: (i) the concern that these proteins will bind lipophilic compounds nonspecifically due to the hydrophobic nature of the lipid binding pocket, and (ii) that candidate inhibitors will fail to discriminate between PITPs or even other unrelated proteins that bind lipophiles. What is particularly interesting is that even very closely-related Sec14-like PITPs are not inhibited by Sec14-active compounds. The available data indicate the biologically active small molecule inhibitors enter the Sec14 hydrophobic pocket in an exchange reaction and are trapped there by a set of specific Sec14::inhibitor interactions (Nile et al. 2014). The geometry of these interactions is both key to the binding mechanism and to the high specificity of these inhibitors for Sec14 as opposed to the other Sec14-like proteins. Inhibitor binding is not only sterically incompatible with Sec14::phospholipid interactions, but the interaction also effectively locks Sec14 into its closed conformer – thereby prohibiting lipid exchange.

The advent of strategies for discovery of PITP-directed inhibitors, and downstream exploitation of such inhibitors as experimental tool compounds, offers exciting new prospects for studying both PITP function and phosphoinositide signaling in a wide variety of experimental systems. First, the availability of appropriate and well-characterized inhibitors will enable functional analyses of PITPs and phosphoinositide signaling in organisms not amenable to application of standard genetic or gene-silencing approaches. Many eukaryotic parasites fall into this category. Second, PITP-directed inhibitors will facilitate genome-scale functional interaction screens in even the most complex cells by facilitating acute and specific inhibition of the target at the onset of the screen (Kampmann et al. 2013). This feature promises to effectively minimize the complications that arise when compensatory mechanisms come into play. Finally, PITP-directed inhibitors promise to facilitate resolution of biochemical systems where lipid signaling circuits have been biochemically reconstituted from wild-type components. Chemical intervention approaches obviate the need for biochemically reconstituting conditionally functional systems from mutant components – i.e. a strategy that, even when available, often proves problematic.
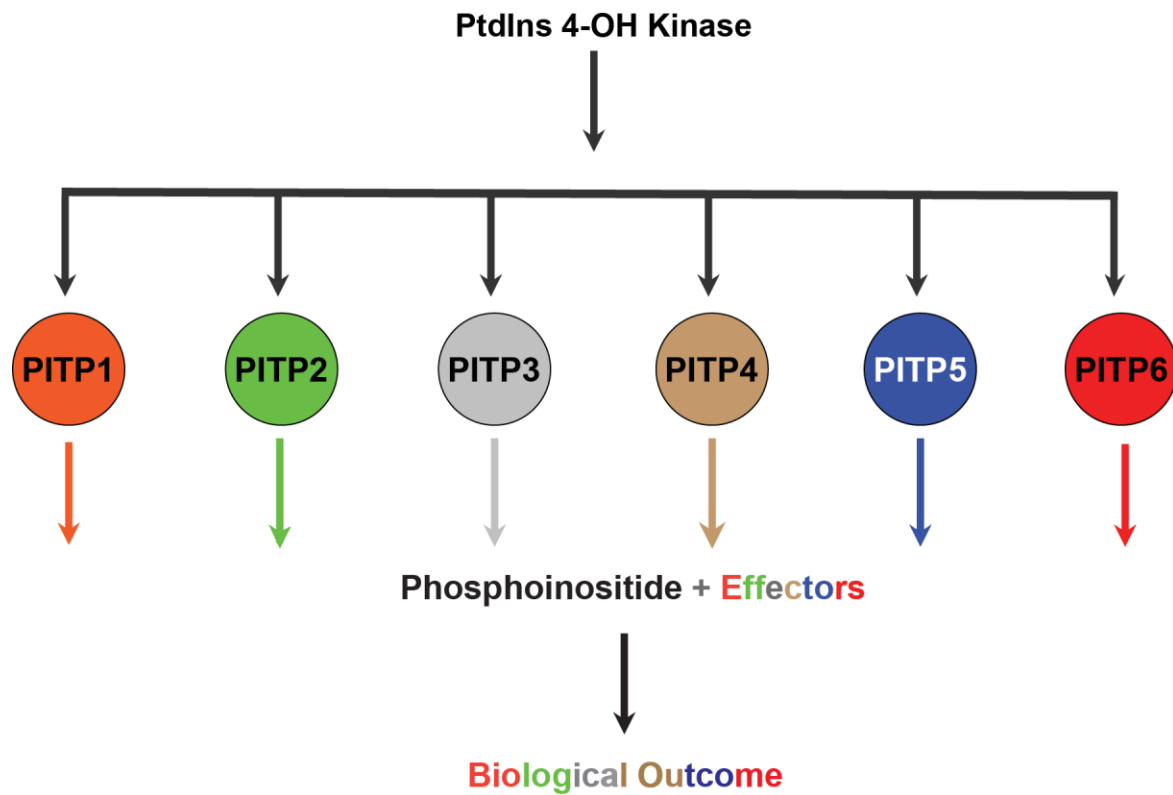
Figure 1.6. PITPs as targets for chemical inhibition of phosphoinositide signaling. A diversity tree for biological outcomes of signaling via a PtdIns 4-OH kinase that produces only PtdIns-4-phosphate but interfaces with multiple PITPs. Chemical inhibition of the kinase, even with absolute specificity, will compromise the entire outcome tree. Inhibition of any individual PITP offers a more surgical approach to dissecting phosphoinositide signaling.

Conclusions

PITPs and other lipid transfer proteins, such as homologs of oxysterol binding proteins (Osh) and ceramide transfer proteins (CERT), have burst onto the main cell biology stage in the past few years. The growing interest in these enigmatic transfer proteins makes this an appropriate time to consider what it is that we actually know about how these proteins operate, what we do not know, and what has not yet been rigorously established. In this chapter, we used PITPs as a case study for discussing alternatives to the historical lipid carrier models that have dominated, and still dominate, the scene. Concepts such as instructive regulation of lipid metabolic enzymes, and roles for such mechanisms of metabolic control in diversifying biological outcomes for lipid signaling, offer new frameworks for interpreting the physiological actions of transfer proteins. Will there be a unifying resolution to how these various transfer proteins execute their biological functions? Perhaps other than general agreement for a central role for the lipid exchange cycle, we feel this unlikely. Whereas some proteins exhibit modes of action suggesting sensing roles, rather than transfer functions, others appear to be most readily interpreted in the context of transfer proteins. The various possibilities will need to be evaluated for each protein class on their own experimental merits. What is clear is that authentic physiological assays are needed for progress and, in the few cases where such assays have been exploited in detail, the results of such assays testify to the remarkable biology of these proteins. We anticipate that the emergence of as yet unappreciated linkages of PITPs to mammalian diseases will guide important future efforts.

CHAPTER 2: A NOVEL COUPLING OF PHOSPHATIDYLINOSITOL-TRANSFER, PLECKSTRIN-HOMOLOGY AND OXYSTEROL-BINDING-PROTEIN-RELATED DOMAINS INTO AN INTEGRATED PHOSPHOINOSITIDE SIGNALING CIRCUIT IN *TOXOPLASMA*

Introduction

Toxoplasma gondii is an obligate intracellular parasite that belongs to the eukaryotic phylum Apicomplexa, which is responsible for many common diseases of humans and animals, including malaria (*Plasmodium*), Cryptosporidiosis (*Cryptosporidium*), and Cyclosporiasis (*Cyclospora*) (Levine 1970). *Toxoplasma* infects one-third of humans worldwide, causing fatal encephalitic disease in immunocompromised individuals. In order to establish a productive infection, *T.gondii* must invade a host cell, elaborate an intracellular compartment called the parasitophorous vacuole (PV) in which to replicate, eventually egress from the host cell, and repeat the process. *Toxoplasma* utilizes a set of specialized late secretory organelles – the micronemes, rhoptries, and dense granules – at all stages of infection to secrete parasite effectors into the host cell or PV. Because the secretory system is unique to Apicomplexa, it presents a promising target for therapeutic intervention. Studies of early and late secretory compartments in Apicomplexa reveal that fundamental regulatory mechanisms are conserved as compared to other eukaryotes such as yeast or mammals, but these parasites have repurposed conserved molecular networks to fit their specialized secretory requirements (Liendo and Joiner 2000, Liendo et al. 2001, Pieperhoff et al. 2013, Tomavo 2014).

In this work, we describe for the first time PtdIns4P pools on *Toxoplasma* secretory membranes. Distinct membranes are coded by unique PtdIns4P pools which can be identified by specific phosphoinositide biosensors derived from known PIP binding domains. We identify a

33

PtdIns4P pool on Golgi/ECL membranes, as well as higher order PIPs (PtdIns(4,5)P_2 and

PtdIns(3,4)P_2) on the plasma membrane. Of particular interest is the identification of PtdIns4P

pools on specialized secretory organelles, the dense granules.

PtdIns4P in yeast is synthesized by one of two PtdIns 4-OH kinases: Pik1 on Golgi

membranes and Stt4 at the plasma membrane. PI4Ks in yeast are biologically insufficient

enzymes due to their inability to access PtdIns inside the lipid bilayer (Schaaf et al. 2008; Ile et

al. 2006). The productive synthesis of PtdIns4P levels high enough to support trafficking from

secretory membranes requires cooperation of PI4Ks with phosphatidylinositol transfer proteins

(PITPs), particularly Sec14 in the case of yeast TGN/endosomal membranes (Bankaitis et al.

1989). Sec14 is a coincidence detector that is primed for PI4K stimulation by binding of PtdCho,

thereby coupling PtdCho metabolism to PtdIns4P-dependent trafficking (Fang et al. 1996;

Mousley et al. 2008; Schaaf et al. 2008). Sec14 is antagonized specifically by a member of the

Oxysterol binding proteins (OSBPs), Kes1/Osh4 (Li et al. 2002, Fairn et al. 2007, Stefan et al.

2011). Kes1 blocks PtdIns4P-dependent secretion from TGN/endosomes by sequestering the

Sec14-dependent pool of PtdIns4P, and itself integrates signals from other pathways including

sterol, sphingolipid, and TORC1 and nitrogen signaling pathways (Mousley et al. 2012).

We describe the *Toxoplasma* cohort of PITPs in an effort to understand whether

PtdIns4P pools on *Toxoplasma* secretory membranes might be subject to similar regulation. The

Toxoplasma genome codes for three Sec14 homology (Sfh) proteins, and one unique

multidomain START-like PITP, which we termed PITP Multidomain Protein (PIMP). The TgPIMP

PITP domain contains the PtdIns-binding barcode of metazoan START-like PITPs, transfers

PtdIns between membranes in a manner dependent on that barcode, and utilizes

phosphatidylcholine (PtdCho) as a counterligand *in vitro*. PIMP localizes to dense granules in

Toxoplasma but is not a secreted protein, suggesting that *T.gondii* has adapted a PITP signaling

network to its specialized secretory system. PIMP harbors a PH domain that binds PtdIns4P and

PtdIns(4,5)P_2 *in vivo*, and this domain alone is sufficient to localize to dense granules in a PIP-

binding dependent manner. PIMP has a C-terminal OSBP-related protein (OSBP) module, and the PIMP PITP domain can substitute for Sec14 in yeast, suggesting it has the capacity to function in instructive regulation of PtdIns 4-OH kinases, and may be subject to the same antagonistic signaling as the Sec14/Kes1 network in yeast. TgPIMP is thus a physical platform for integration of multiple lipid signaling pathways in *Toxoplasma* and is the first known example of a PITP physically coupled to an OSBP domain.

Materials and Methods

Molecular biology reagents.

All *Toxoplasma* expression vectors utilized the pTUB system, wherein gene expression is driven by the *tubulin* promoter and stable populations can be selected with chloramphenicol. In all cases, the genes were cloned between a 5' BglII site and a 3' AvrII site. These were tagged with YFP or RFP, and the nature of the tag as well as its orientation is indicated directly in the figure legends. The cloning primers used are as follows: Fapp1-PH (F: 5'-ga AGATCT aaaatggaggggggtgttgtacaag-3'; R: 5'- ga CCTAGG agtccttgtatcagtcaaacatgc-3'); GOLPH3 (F: 5'-aa AAGATCT atgacctcgctgacccag-3'; R: 5'- aaa CCTAGG ttacttggtgaacgc-3'); TgROP1 (F: 5'-gga AGATCT aaaatggagcaaaggctgcca -3'; R: 5'- gtt CCTAGG aaattgcgatccatcatcctg-3'); PIMP-PH (F: 5'-aaa AGATCT cgctcagacgctggagc-3'; R: 5'-aaa CCTAGG aaaagacttggggaggaag-3'); full length PIMP (F: 5'-aaa AGATCT atgaaggtgttcgagtaccgcctcgtgctg-3'; R: 5'-aaa CCTAGG agcaggagaggcggtgactcccg-3').

Site-directed mutagenesis was performed using standard techniques. Primers used for mutagenesis are as follows: PIMP-PITP-T65E (F: 5'-gacaccggccagtac GAA cacaagcgcatcaac-3'; R: 5'-gttgatgcgcttgtg TTC gtactggccggtgtc-3'); PIMP-PH-R503A (F: 5'-gaatacgacgtggaacttg GCA tacgtcgtgctgcgaaac-3'; R: 5'-gtttcgcagcacgacgta TGC caagttccacgtcgtattc-3'); FAPP1-PH-K7A (F: 5'-ggagggggtgttgtac GC tggaccaactatctcac-3'; R: 5'-gtgagatagttggtccac GC gtacaacaccccctcc-3'); FAPP1-PH-R18L (F: 5'-ctcacaggctggcagcctc T ttggtttgtttagataatgg-3'; R: 5'-ccattatctaaaacaaaccaa A gaggctgccagcctgtgag-3').

Yeast strains and media.

Yeast strains utilized are described in detail elsewhere (Bankaitis et al. 1989, 1990; Cleves et al. 1991; Ghosh et al. 2015), and included CTY182 (*MATα ura3-52 lys2-801 his3Δ-200, CTY1-1Aa SEC14+*), CTY1-1A (*MATa ura3-52 lys2-801 Δhis3-200 sec14-1ts*), CTY558 (*MATa ade2 ade3 leu2 his3Δ ura3-52 sec14Δ1::HIS3*), CTY1537 (*MATa ura3-52 leu2 Gal+*

36

pik1-101ᵗˢ), CTY1568 (*MATα leu2 ura3 his3 trp1 ly2s suc2-Δg stt4Δ::HIS, YCp(LEU2, stt4-4ts)*), CTY100 (CTY1-1A *sac1-26*), RG4 (pRS315-*mss4-25ᵗˢ*; *mss4Δ::kanR, ura3-52, his3-Δ200, ade2*), RG5 (MAT*α his3Δ1 leu2Δ0 lys2Δ0 ura3Δ0 vps34Δ::kanMX*).

Methods for culturing yeast in standard yeast peptone dextrose (YPD) or minimal SD media, for gene eviction, and standard lithium acetate transformation were as previously described (Sherman et al. 1983; Rothstein 1984; Ito et al. 1983). For experiments using a Doxycycline (Dox)-repressible expression system (pCM189), cells were grown in selective SD media with 10ug/mL Dox or in selective SD liquid media with 10ug/mL Dox and supplemented with 0.5% casamino acids. Expression from pCM189 was induced by washing cells 2X and incubating in Dox-free selective SD/casamino acids media for 18hrs.

Homology modeling.

Homology models of PIMP domains were generated with MOE 2013.08 Modeling package. The target sequence for PIMP-PITP domain was aligned to the PITPα bound to PtdIns (PDB I.D. 1UW5; 2.90 Å) and unbound form (1KCM, 2.00 Å resolution) with a sequence similarity of ~35% to generate models in closed and open conformation respectively. For PIMP-PH domain, solution structure of pleckstrin homology domain containing protein family A member 5 from human (PDB I.D. 2DKP) and crystal structure of FAPP1 pleckstrin domain was used as a template. The ligands were included in the environment to generate induced fit homology models of the complexes. By default, 10 independent intermediate models were generated as a result of permutational selection of different loop candidates and side chain rotamers. The intermediate model that scored best according to the selected forcefield (Amber99), was chosen as the final model and was subjected to further optimization.

Protein purification.

Recombinant His-tagged proteins expressed from pET28b-His8-PITP^{PIMP} and pET28b-His8- PITP$^{PIMP(T65E)}$ were produced from *E.coli* BL21 (RIL/DE3; New England BioLabs Inc, Ipswich, MA). Transformed cells were cultured overnight at 37°C, and subcultured into 8L of TB media supplemented with 30µg/mL kanamycin and 25µg/mL chloramphenicol. Cells were grown for 4hrs at 37°C, shifted to 16°C, and protein expression was subsequently induced with IPTG (100µM final concentration). Cultures were harvested after 18hrs and cells lysed either by bead-beating or flash-freezing with liquid nitrogen and thaw. Clarified lysates were incubated with TALON metal affinity beads (Clontech, Mountain View, CA), and bound proteins were eluted using a 25–200mM imidazole step gradient regime. Peak fractions were identified by analyzing individual fractions by SDS-PAGE, pooled and dialyzed against 300mM NaCl, 25mM Na_2HPO_4 (pH=7.5), 5mM 2-mercapthoethanol (Prod # 68100, Thermo Scientific, Rockford, IL). Protein mass was estimated by SDS-PAGE and Coomassie staining using BSA titration series as standards.

Lipid transfer assays.

Methods for measuring protein-mediated transfer of [^{3}H-]PtdIns from rat liver microsomes to PtdCho liposomes, and transfer of [^{14}C]-PtdCho from liposomes (98 mol% PtdCho, 2mol% PtdIns) to bovine heart mitochondria, have been described (Aitken et al. 1990; Bankaitis et al. 1990; Schaaf et al. 2008).

Tissue culture and propagation of *Toxoplasma* cells.

HFFs and MRC cell lines were cultured in Dulbecco's modified Eagle's medium with 10% fetal bovine serum (FBS), incubated at 37°C with 5% CO_2 in humidified air. All *T. gondii* strains were maintained by serial passage in MRC or HFF monolayers. Parasites were grown to egress and purified from host cell lysate by passage through 18G and 25G needles and

pelleting at 2K rpm for 5 minutes. Media for selection and maintenance of transgenic parasites was supplemented with chloramphenicol to a final concentration of 20µM.

Production of total *Toxoplasma* cDNA fractions by reverse transcription.

To generate total cDNA from *Toxoplasma*, parasites were cultured to egress in HFF or MRC monolayers, and purified passage through 18G and 25G needles and pelleting at 2K rpm for 5 minutes. RNA was isolated using Qiagen RNeasy and quantified by 260nm absorbance and quality assessed by agarose gel electrophoresis. RNA was converted to cDNA using the Bio-Rad iScript Select cDNA Synthesis kit. Presence of full-length PIMP transcripts in the cDNA library was probed by PCR using total cDNA as template and primers for1 (5'-aaggtgttcgagtaccgcc-3'), rev1 (5'-ggagtcaccgcctctcc-3'), for2 (5'- ggcctcgtcgacgtctcc-3'), rev2 (5'-agcaggagaggcggtg-3').

***Toxoplasma* transfection and selection of transgenic parasites.**

Parasites were transfected by electroporation as previously described (Soldati and Boothroyd 1993). Briefly, ca. 10^7 tachyzoites (*Toxoplasma gondii* RH strain) were freshly purified from host cells and mixed with 20µg of plasmid in transfection buffer (120mM KCl, 150µM $CaCl_2$, 5mM $MgCl_2$, 2mM EDTA, 25mM HEPES KOH, 10mM KPO_4). For co-transfections, 20µg of each plasmid were used. Parasite/DNA solution was subjected to an electrical pulse in 25uF and 1.3kV using the Bio-Rad Gene Pulse II electroporation apparatus. Parasites were allowed to recover on MRC or HFF monolayer in the absence of drug for 24 hours after which transgenic cells were selected in the presence of 20µM chloramphenicol.

Immunofluorescence imaging of *Toxoplasma*.

MRC or HFF host cells were seeded onto glass-bottom dishes and infected with parasites for 18-24hrs. Monolayers containing intracellular parasites were washed twice with

PBS, fixed with 4% paraformaldahyde (v/v) for 15min at RT, permeabilized with 0.2% Triton-X (v/v) for 4min at RT, blocked with 2% BSA in PBS 1hr at RT or overnight at 4°C, incubated with primary antibody diluted in blocking buffer (mouse GRA3 at 1:500, mouse MIC3 at 1:500, or rat TgSORTLR at 1:250) over night at 4°C, washed 3X with PBS, incubated with fluorophore-conjugated anti-mouse or anti-rat secondary antibody at 1:1000 – 1:2000 dilution in blocking buffer for 1hr at RT, washed 3X with PBS, and imaged in PBS without mounting within 24hrs.

Confocal imaging.

Confocal imaging was performed using NikonA1R and Olympus FV-1000 confocal microscopes. Images were processed in Nikon Elements Viewer 4.0, ImageJ and Adobe Photoshop CS. The styryl dye FM4-64 was used to label yeast vacuolar membranes as previously described (Vida and Emr 1995). Coverslips for imaging yeast were coated with 0.5mg/mL concanavalin A (Sigma-Aldrich L7647) and washed with PBS.

Results

Toxoplasma PIMP couples PITP, PH and OSBP domains.

The coding of adjacent PITP and OSBP genes on chromosome IX suggests transcriptional co-regulation of these two modules. Indeed, these were annotated as a single open reading frame (gene ID TGME49_289570), predicted to be transcribed as a 5739bp mRNA whose primary translation product is a 1912-amino acid protein with a molecular mass of ca. 210kDa (Figure 2.1A). What is striking about the modular organization of this P̲ITP M̲ultidomain P̲rotein (PIMP) is that the predicted primary translation product physically joins three distinct domains -- all of which fall into families of known inositol lipid binding proteins. Proceeding from the N-terminus, the three domains include: (1) the N-terminal 347 residues that share 28% primary sequence identity and 40% similarity to the mammalian single-domain START-like PITPα (PITP^{PIMP}), (2) a putative pleckstrin homology (PH) domain for binding of phosphoinositides (residues 482-581; PHPIMP), and (3) a C-terminal OSBP-domain (residues 1605-1912; OSBP^{PIMP}) that shares 19.5% primary sequence identity and 29.3% similarity, across the entire 434 residue sequence, to one of the seven yeast ORPs Kes1/Osh4. In addition, PIMP harbors what is predicted to be a four-helix hydrophobic domain that separates The PITP^{PIMP} and PH^{PIMP} domains from the OSBP domain, as well as three potential HT ("host targeting") sequences (or PEXEL in _Plasmodium_) that reside immediately upstream of the OSBP^{PIMP} domain. The three potential HT sequences in PIMP $_{1603}$RGLVD$_{1607}$, $_{1556}$RRLPE$_{1560}$, and $_{1433}$RWLGE$_{1437}$ conform closely to the HT consensus sequence RxLxD/E (Figure 2.1A) (Hiller et al. 2004; Bhattacharjee et al. 2008; Haase et al. 2010; Hsiao et al. 2013).

To confirm that the predicted transcript is produced _in vivo_, parasites were cultured in mammalian cells to egress, total RNA fractions were prepared, and PIMP-specific cDNAs were produced by reverse transcription. Along with a complete 5.7kb transcript, two overlapping fragments representing the 5` 5056bp of the predicted transcript as well as the terminal 927bp were recovered (Figure 2.1B). Thus, we conclude the entire _PIMP_ gene is transcribed in

Toxoplasma with the potential to encode the predicted PITP-PH-OSBP polyprotein. That

Toxoplasma can translate a full-length PIMP polypeptide was confirmed by immunoblotting

experiments using extracts prepared from transgenic parasites expressing the full-length cDNA

at elevated levels (data not shown).
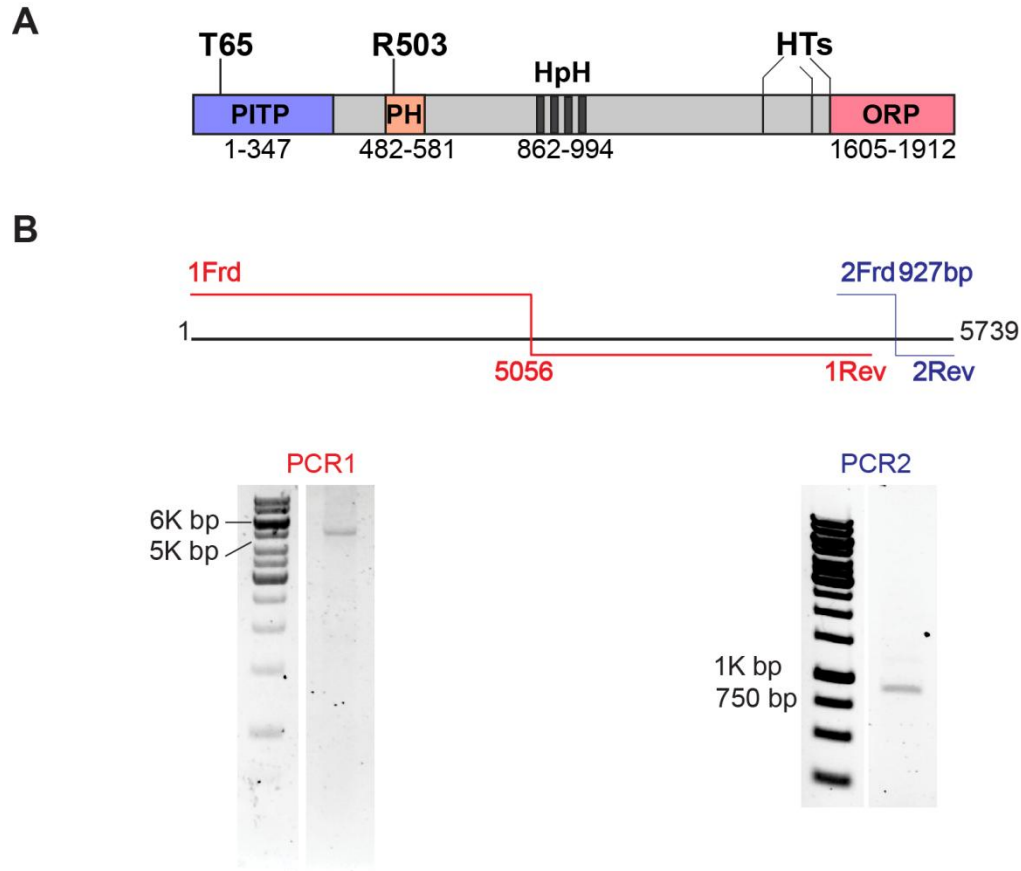
Figure 2.1. PIMP domains are co-transcribed as a single mRNA. (A) A diagram of the PIMP

domain structure. PIMP is comprised on a PITP domain (residues 1-347), PH domain (residues

482-581), a region containing predicted hydrophobic helices (HpH) (residues 862-994), and an

OSBP domain (residues 1608-1912). Three predicted HT sites are identified: HT1

($_{1433}$RWLGE$_{1437}$), HT2 ($_{1556}$RRLPE$_{1560}$), and HT3 ($_{1603}$RGLVD$_{1607}$). Location of lipid-binding

residues for the PITP and PH domains are designated (T65 and R503, respectively). **(B)**

Overlapping primer pairs used to confirm PIMP transcript are depicted below (1Frd/1Rev and

2Frd/2Rev) with the predicted product size. PIMP gene is transcribed in a single transcript.

Toxoplasma RH RNA was converted to cDNA and used as a template for PCR using primer

pairs 1Frd/1Rev and 2Frd/2Rev. The resulting PCR products (5056bp and 927bp for PCR2) are

shown in the lower panel.

The PITP^{PIMP} domain exhibits PITP-like activities

Threading of the PITP[PIMP] primary sequence onto a high resolution PITPα crystal structure predicted significant structural similarity between these polypeptides (Figure 2.2A). Like PITPα, the LBD of PITP[PIMP] is composed of β sheets that form the hydrophobic pocket floor onto which the phospholipid binds. These are flanked by three α helices and a lipid exchange loop that acts as a "lid" to the binding cavity. The lipid exchange loop is formed between β strand 3 and 4 of PITP[PIMP], however, unlike PITPα there is another small insertion in PITP[PIMP] which forms a loop between β-strand 2 and α-helix and is next to lipid exchange loop. Another distinguishing feature of PITP[PIMP] is a 77-residue insertion loop between β-strand 7 and 8 (Figure 2.2A). Residues in the lipid-binding pocket of PITPs that specifically coordinate the inositol headgroup of bound PtdIns are referred to as the PtdIns-binding bar code. These are highly conserved between the members of a PITP family. Indeed, superimposition of the modeled PITP[PIMP] lipid binding pocket onto that of PITPα revealed conservation of this structural motif (Figure 2.2B). The PtdIns-binding barcode involves residues T_{59}, K_{61}, E_{86}, N_{90} for PITPα, and T_{65}, K_{67}, E_{92} and N_{96} for PITP[PIMP], respectively (Figure 2.2B) (Alb et al. 1995; Tilley et al. 2004).

Two independent assays were used to assess whether PITP[PIMP] has intrinsic phospholipid exchange activity. One, we used a biological assay where the ability of PITP[PIMP] expression to act as functional surrogate for the essential yeast PITP Sec14 was tested. There were two versions of the biological assay. The first experimental paradigm took advantage of yeast strains carrying a conditional *sec14[ts]* allele where the essential Sec14 PITP is rendered nonfunctional at 37°C -- resulting in an inability of the yeast mutant to grow at that restrictive temperature (Figure 2.2C, left panel). Expression of either wild-type Sec14 (the positive control) or of PITP[PIMP] rescued growth of *sec14[ts]* cells at 37°C. As the essential function of Sec14 depends on its ability to bind PtdIns (Schaaf et al. 2008), these data indicated PITP[PIMP] has intrinsic ability to bind and/or exchange PtdIns. Mammalian PITPα residue T_{59} is required for

coordination of the PtdIns headgroup within the lipid-binding pocket, and missense substitutions at that position selectively inactivate the PtdIns binding activity of the protein with no compromise of PtdCho-binding (Alb et al. 1995; Tilley et al. 2004). This residue is invariant amongst the metazoan START-like PITPs and, in the cases where the experiment has been done, it is required for PtdIns-binding and biological function of these proteins (Milligan et al. 1997; Alb et al. 2007; Ile et al. 2010). The corresponding residue in PITP^{PIMP} is T$_{65}$ (Figure 2.2B). Expression of the PITP$^{PIMP (T65E)}$ mutant, which is expected to be ablated for PtdIns-binding activity, failed to rescue $sec14^{ts}$ mutant growth at restrictive temperatures (Figure 2.2C, left panel).

These results were reproduced using a second, more rigorous, biological paradigm where the ability of PITP^{PIMP} to restore viability to $sec14\Delta$ mutants was tested using a well-characterized plasmid shuffle assay (Phillips et al. 1999; Schaaf et al. 2008). In this system, viability of $sec14\Delta$ cells is supported by a plasmid-borne copy of a wild-type *SEC14* gene. A second plasmid driving high-level expression of a query PITP is introduced into the yeast strain, and all nutritional selection pressures maintaining either plasmid are subsequently relieved by culturing cells in rich medium. Loss of the *SEC14* plasmid is recorded by white colonies and white colony sectors in a background of red colonies. This outcome reports viability of the white segregants in the absence of any Sec14 contribution, and is only possible if expression of the query PITP fulfills all essential Sec14 functions. While ectopic high-level expression of mammalian PITPα supported high frequency loss of the *SEC14* plasmid, introduction of a PITP^{PIMP} expression plasmid was only able to do so at low frequency (Figure 2.2C, right panel). Given PITP^{PIMP} expression was driven by a constitutive and powerful *PMA1* promoter, and the expression cassette was maintained on a high copy episomal plasmid, the shuffle data suggest PITP^{PIMP}, while having PITP activity, is an inefficient PITP -- at least when expressed in yeast.

PITP^{PIMP} exhibits both PtdIns- and PtdCho-exchange activities

Biochemical assays with recombinant PITP^{PIMP} demonstrated this module catalyzes significant transfer of both [^{3}H]-PtdIns and [^{3}H]-PtdCho between membranes *in vitro* in a concentration-dependent manner (Figure 2.2D, E). In the membrane system employed, and consistent with the plasmid shuffle data, PITP^{PIMP} scored as an inefficient PtdIns-transfer protein relative to Sec14. Whereas Sec14 transferred ca. 30% of input [^{3}H]-PtdIns in assays with 10μg of protein, PITP^{PIMP} assays saturated at 8% [^{3}H]-PtdIns transfer with 200μg of protein. PITP^{PIMP}-mediated PtdCho-transfer activity was more efficient as ~30% of input [^{3}H]-PtdCho was transferred with 200μg of protein. In accord with previous demonstrations, the $T_{65}E$ PITP^{PIMP} mutant domain was completely inactive for PtdIns-transfer activity *in vitro* (Figure 2.2D) while maintaining undiminished PtdCho-transfer activity (Figure 2.2E). Moreover, missense substitution of the neighboring PITP^{PIMP} T_{61} residue did not reduce PtdIns- or PtdCho-transfer activity -- further confirming PITP^{PIMP} residue T_{65} is orthologous to the PtdIns headgroup coordinating PITPα residue T_{59} (data not shown).

Figure 2.2. **PITP^PIMP is a *bona fide* START PITP. (A)** PITP^PIMP retains the START PtdIns-

binding barcode. The PIMP PITP domain (residues 1-347) was threaded onto the crystal

structure of RnPITPα bound to PtdIns (PDB 1UW5) using SWISS-MODEL

(http://swissmodel.expasy.org). The structure was visualized in UCSF Chimera. The crystal

structure of PITPα is shown in red, and the predicted PITP^PIMP is shown in blue. **(B)** PtdIns-

coordinating residues (in PITPα: T59, K61, E86, N90; for PITPPIMP: T65, K67, E92, N96) are

high-lighted. **(C, left panel)** PITP^PIMP complements Sec14 deficiency in yeast in a PtdIns-

barcode dependent manner. PITP^PIMP or PITP^PIMP (T65E) was over-expressed in Sec14^ts (CTY1-

1A) cells from an episomal plasmid under the *PMA1* promoter. Cells were grown in selective SD media and spotted onto YPD agar in 10-fold dilutions starting with OD 1. Plates were incubated at 30°C or 37°C for two days and imaged with ChemiDoc (Bio-Rad). Images were processed in Bio-Rad ImageLab software. **(C, right panel)** PITPPIMP substitutes for SEC14 in yeast in a PtdIns-barcode dependent manner. PITPPIMP or PITPPIMP(T65E) was over-expressed in CTY558 from an episomal plasmid under the *PMA1* promoter. Cells were grown in SD media and spotted onto YPD agar in 10-fold dilutions starting with OD 1. Plates were incubated at room temperature for three days and imaged with ChemiDoc (Bio-Rad). Purified recombinant 8xHis-PITPPIMP transfers **(D)** ^{3}H-PtdIns and **(E)** ^{3}H-PtdCho between membranes *in vitro* in a concentration-dependent manner (amounts of PITP tested: 10, 25, 50, 75, 100, 200µg). The predicted PtdIns-barcode mutant T65E ablates PtdIns transfer but not PtdCho transfer.

PITP-like genes in *Toxoplasma*

The PIMP PITP domain belongs to the START structural family, though it cannot be clearly assigned to either Class of PITPs currently defined in that family (Figure 2.3A). The *Toxoplasma* genome database identifies three candidate PITPs other than PIMP, all of which belong to the Sec14-like protein superfamily (Figure 2.3A). These Sec Fourteen Homologs are designated TgSfhA (TGME49_246330), TgSfhB (TGME49_269390), and TgSfhC (TGME49_213790). Primary sequence similarity comparisons to the *Saccharomyces* Sec14-like PITPs show TgSfhA is most homologous to the yeast Sfh3 and Sfh4 PITPs exhibiting ca. 29% primary sequence similarity to both (E values: 1e^{-23} and 2e^{-23}, respectively). These yeast Sfh PITPs are involved in control of fatty acid mobilization from lipid droplet stores and in decarboxylation of phosphatidylserine to phosphatidylethanolamine in TGN/endosomal compartments, respectively. While TgSfhB shares most primary sequence homology to Sec14 (E value: 1e^{-10}), that level of primary sequence homology was also apparent in comparisons of

TgSfhB to all of the Sfh PITPs (22-25%) excluding Sfh5. Thus, we cannot confidently assign a

yeast ortholog for TgSfhB. TgSfhC is most homologous to Sec14 and Sfh1 sharing 28-30%

primary sequence similarity to each (E value: 7e^{-05} when aligned with Sfh1). However, in no

case could we demonstrate PITP-like activities in functional complementation experiments

where the abilities of these proteins to act as functional surrogates for yeast Sec14 was

assayed (Figure 2.3B). The PIMP PITP domain, therefore, is the only *Toxoplasma* PITP that

can function in the Sec14 cellular context.
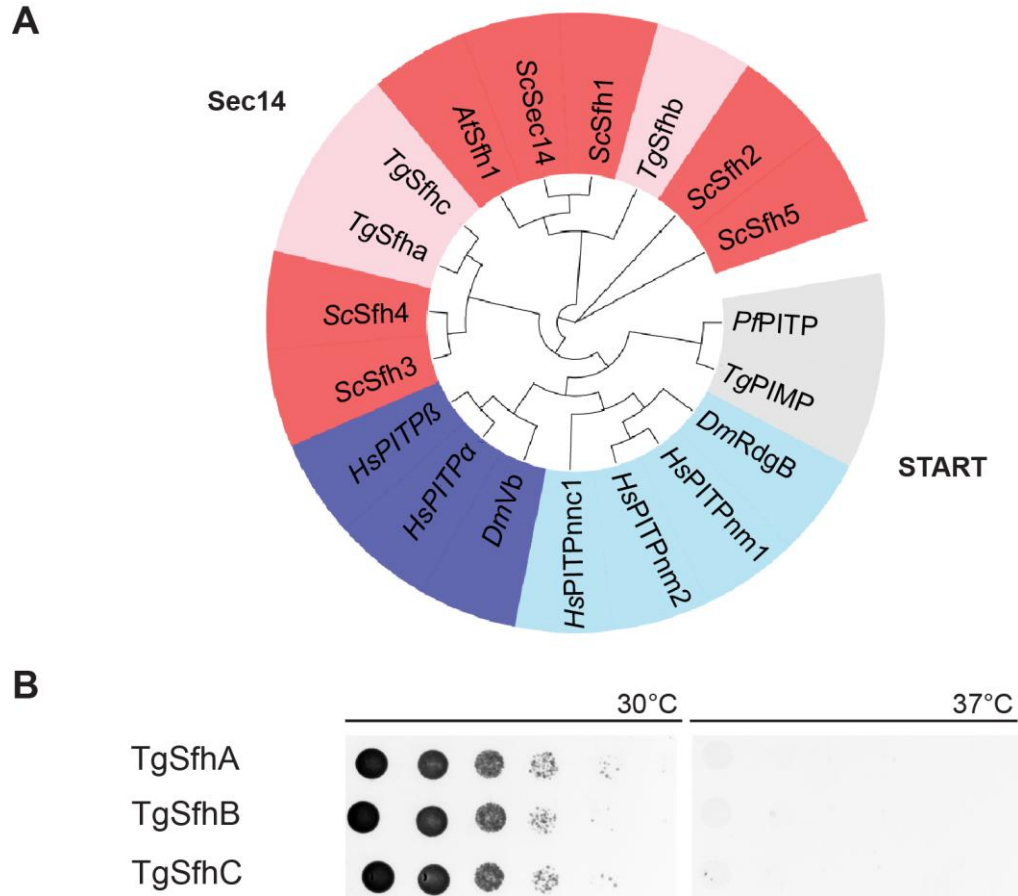
Figure 2.3. *Toxoplasma* **PITPs. (A)** Circular cladogram of *Toxoplasma* PITPs and known

orthologs. Sequences from BLAST homology searches (http://www.ncbi.nlm.nih.gov/BLAST)

against either HsPITPβ (for the START family) or ScSec14p (for the Sec14 family) were aligned

in VectorNTI to define node distances. Data were visualized using EvolView software

(www.evolgenius.info/**evolview***).* The Sec14 family is in red/pink, where yeast Sfhs and

Arabidopsis AtSfh1 are in red, and the Toxoplasma Sec14 homologs (TgSfha, TgSfhb and

TgSfhc) are in pink. The START family is in blue/grey, where human and Drosophila Class I

PITPs are in dark blue, human and Drosophila Class II PITPs are in light blue, and T.g. PIMP

and its Plasmodium ortholog are in grey*.* **(B)** *Toxoplasma* Sfhs do not complement Sec14

deficiency in yeast. TgSfhA, TgSfhB or TgSfhC were over-expressed in Sec14[ts] (CTY1-1A) cells

from an episomal plasmid under the *PMA1* promoter. Cells were grown in selective SD media

and spotted onto YPD agar in 10-fold dilutions starting with OD 1. Plates were incubated at 30°C or 37°C for two days and imaged with ChemiDoc (Bio-Rad). Images were processed in Bio-Rad ImageLab software.

PH^{PIMP} is a PtdIns4P and PtdIns(4,5)P$_2$ binding module

PH domains are phospholipid-binding modules with varying selectivity and affinity for individual phosphoinositide species (Lemmon et al. 1995; Lemmon 2007). The PH^{PIMP} domain was threaded onto the known crystal structures of homologous proteins, the pleckstrin homology domain containing protein family A member 5 (PDB I.D. 2DKP) and the PH domain of FAPP1. A consensus model was built from the two templates (Figure 2.4A). Similar to the PH^{FAPP1} structure, PH^{PIMP} domain folds into seven-strand β-barrel flanked by an α-helix and β loops highlighting the overall fold similarity. Residue Arg$_{503}$ is predicted to lie within the PH^{PIMP} domain lipid-binding pocket and this residue is conspicuous as it is highly conserved among PH domains (Figure 2.4A). Structural studies of the PH domain of GRP1 provide a rationale for this conservation by demonstrating that the orthologous Arg residue coordinates phosphoinositide headgroup binding within the PH^{GRP1} lipid binding pocket (He et al. 2008).

To determine whether PH^{PIMP} has the capacity to bind phosphoinositides, the isolated domain was tagged with GFP and expressed in a series of yeast strains that exhibited deficiencies in specific phosphoinositide pools. PHPIMP localized to the plasma membrane and punctate structures reminiscent of TGN/endosomal compartments in WT yeast cells (Figure 2.4B). That this localization was dependent on phosphoinositide binding was suggested by the inability of the PH$^{PIMP(R503A)}$ mutant to target to those compartments (Figure 2.4B). This defect in membrane targeting was not the trivial result of proteolysis of the chimeric proteins as immunoblot analyses confirmed stability of the GFP-tagged PH$^{PIMP(R503A)}$.

PH^{PIMP} localization profiles recorded in WT yeast cells resembled the distribution of PtdIns4P as read out by a variety of PH domain-based PtdIns4P biosensors (Roy and Levine 2004; Baird et al. 2008; Wood et al. 2009; Dowler et al. 2000: Garcia et al. 2000). To determine whether PH^{PIMP} has PtdIns4P binding activity, we tested its response to perturbations of specific PIP enzymes in yeast (Figure 2.5). First, we determined whether accumulation of PtdIns4P in ER membranes could effect a relocalization of GFP- PH^{PIMP} to that compartment. To that end, the chimera was expressed in *sac1* mutants defective for the Sac1 phosphatase, the major PtdIns4P phosphatase of yeast. These mutants accumulate high levels of PtdIns4P in precocious compartments such as ER membranes (Li et al., 2002; Nile et al., 2014). Indeed, a significant localization of PH^{PIMP} to ER membranes was scored in the Sac1-deficient cells (Figure 2.5A, quantified in 2.5C). As expected, PH^{PIMP(R503A)} was unable to localize to membranes in this strain, indicating that the lack of PtdIns4P binding ability of this mutant is the property that affects plasma membrane and endosomal localization in WT cells (Figure 2.5C). Though there are also PtdIns3P pools on endosomal membranes, we found that the PH^{PIMP} domain was not sensitive to these. PH^{PIMP} localization to either the plasma membrane or the punctate compartments was unaffected in *vps34Δ* mutants genetically ablated for the single yeast PtdIns 3-OH kinase activity and therefore completely devoid of 3-OH phosphorylated phosphoinositides (i.e. PtdIns3P and PtdIns(3,5)P$_2$) (Figure 2.5A, quantified in 2.5C).

In a second approach to determine the PIP binding capacity of the PIMP PH domain, we tested whether PtdIns4P is required for membrane binding by PH^{PIMP}. The two major PtdIns 4-OH kinases of yeast are Pik1, which is primarily responsible for producing TGN/endosomal pools of this PH^{PIMP}, and Stt4, the enzyme required for synthesis of plasma membrane pools of PtdIns4P. Thus, GFP- PH^{PIMP} was expressed in yeast mutants carrying either *pik1-101^{ts}* or *stt4^{ts}* alleles, and localization of the reporter was analyzed by GFP imaging. The *pik1-101^{ts}* is a strong allele that exhibits PtdIns4P deficits even at temperatures permissive for growth of the mutant strain (Walch-Solimena & Novick 1999). Indeed, PH^{PIMP} failed to localize to punctate

compartments in the *pik1-101^{ts}* mutant -- even when cells were cultured at a growth-permissive temperature of 30°C. The effect was specific in that plasma membrane targeting was unaffected under those same conditions (Figure 2.5A). When queried in the *stt4^{ts}* mutant challenged with the restrictive temperature of 37°C for 1.5hrs, a partial loss of PH^{PIMP} from the plasma membrane was scored, while localization to the punctate TGN/endosomal compartments remained uncompromised (Figure 2.5B, quantified in 3.5C).

Because the plasma membrane PtdIns4P pool is a major source of metabolic precursor for PtdIns(4,5)P$_2$ synthesis, we considered the possibility that PtdIns(4,5)P$_2$ and not PtdIns4P is the primary determinant for PHPIMP targeting to that membrane system. Consistent with this idea, PH^{PIMP} failed to bind to the plasma membrane of *mss4^{ts}* mutants conditionally defective for the single yeast PtdIns4P 5-OH kinase activity upon shift of those cells to the restrictive temperature of 37°C for 30 min (Figure 2.5B, quantified in 2.5C). Taken together, the data demonstrate PH^{PIMP} exhibits significant affinity and selectivity for both PtdIns4P and PtdIns(4,5)P$_2$ when functionally queried using an authentic biological system as experimental platform.

53
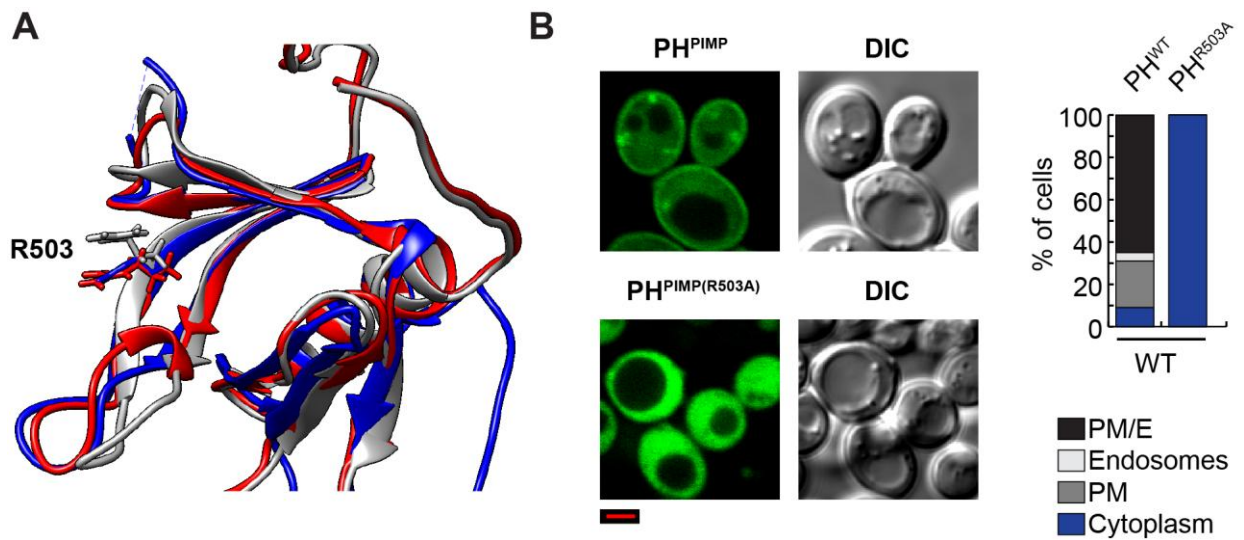
Figure 2.4. The PH^{PIMP} domain localizes to membranes in yeast in a manner dependent on a predicted PIP-binding residue. (A) The PH^{PIMP} domain was modeled on the crystal structure of human PEPP2 PH domain (PDB 2DKP) as described in materials and methods. The structure was visualized in UCSF Chimera. Predicted lipid-binding residue Arg503 is highlighted in blue. **(B)** GFP-tagged PH^{PIMP} or PH^{PIMP (R503A)} was expressed in WT cells by removal of Dox from the media and culturing at 30°C. The PH domain localizes to plasma membrane and puncta in an R503-dependent manner. Quantification of GFP- PH^{PIMP} and GFP- PH^{PIMP (R503A)} in wild-type yeast. Localization is quantified as percent of cells localized to the specified compartment, with at least 100 cells counted. DIC and GFP confocal image panels are shown. Scale bars: 2 μm
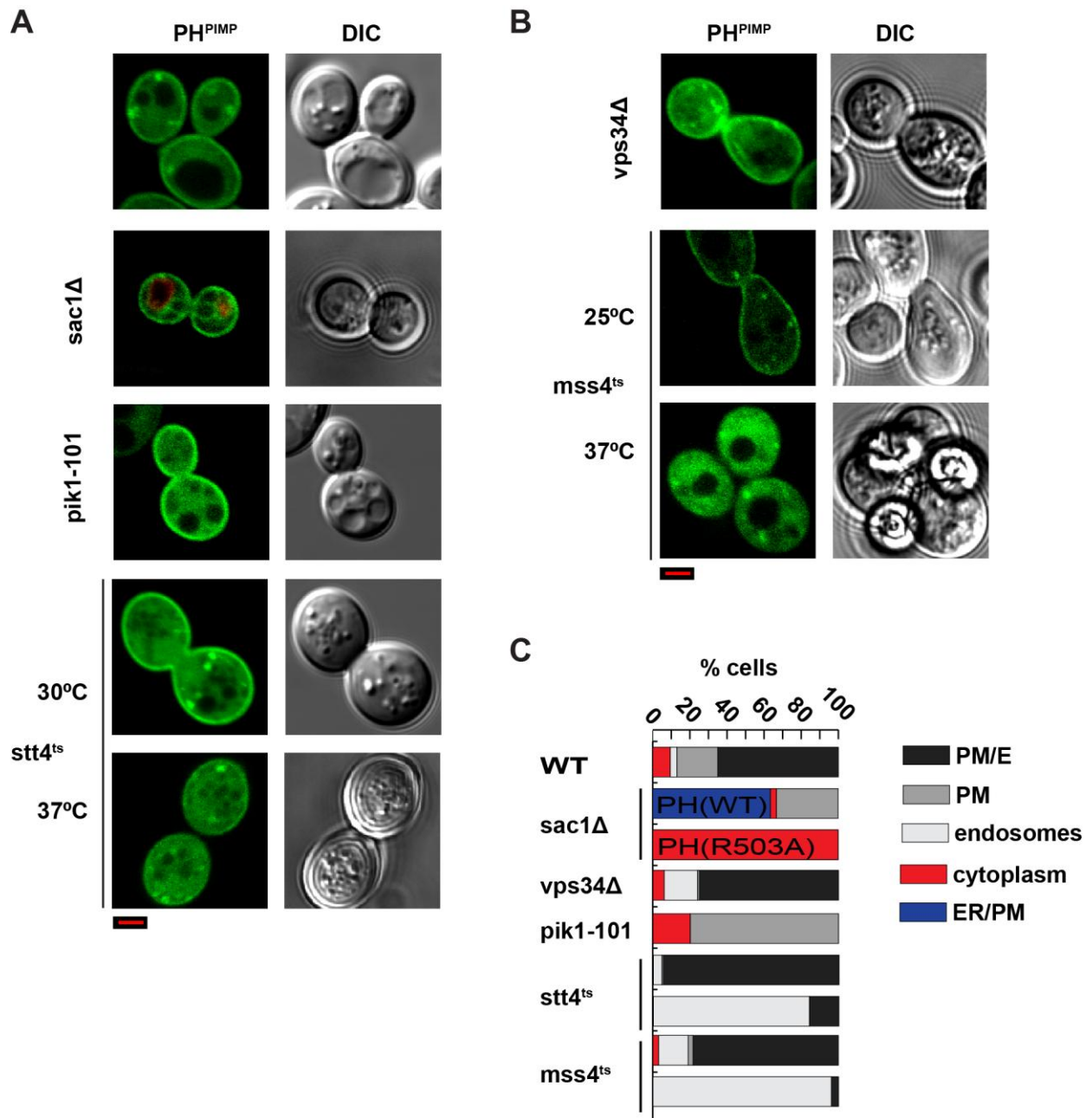
Figure 2.5. The PH^{PIMP} domain PI4P and PI(4,5)P₂ *in vivo*. (A) GFP- PH^{PIMP} expressed in

PtdIns-4-P phosphatase *sac1-26* cells at 30ºC relocalizes to the ER. GFP- PH^{PIMP} is delocalized

from puncta when expressed in the PtdIns-4-OH kinase mutant Pik1-101 strain at 30°C while

retaining localization to the plasma membrane Localization in the Stt4^{ts} strain at 30°C permissive

temperature is WT with some loss from the plasma membrane at 37C (1hr). **(B)** Localization of

GFP- PH^{PIMP} in PtdIns-3-OH kinase *vps34Δ* cells at 30°C does not change localization from the

WT pattern. Plasma membrane-bound GFP- PH^{PIMP} is delocalized to the cytoplasm in PtdIns-4P 5-OH kinase mss4ts cells with 30min incubation at 37°C restrictive temperature. **(C)** Quantification of GFP- PH^{PIMP} and GFP- PH$^{PIMP\ (R503A)}$ in yeast. Localization is quantified as percent of cells localized to the specified compartment, with at least 100 cells counted. DIC and GFP confocal image panels are shown. Scale bars: 2 µm

Toxoplasma secretory pathway is coded by specific PtdIns4P pools

How might a PITP with specific PIP sensing capacity affect signaling in _Toxopaslama_?
To address this question, it was necessary to map PtdIns4P and PtdIns(4,5)P$_2$ distribution in
Toxoplasma. Other than superficial description of a presumptive PtdIns4P pool on an
unidentified membrane compartment in _Plasmodium_ (McNamara et al. 2013), neither the nature
nor the distribution of phosphoinositide pools has been characterized in Apicomplexans.
Although PH domains are useful biosensors for phosphoinositide availability in living cells, the
PIP-dependent membrane-binding activities of these proteins are also modulated by other, often
undefined, variables that diversify their organelle targeting properties beyond those that can be
explained by lipid-binding specificity. To that end, we engineered a series PtdIns4P biosensors
using well-characterized PIP-binding domains for expression in _Toxoplasma_. These included
the PtdIns4P biosensors PH^{FAPP1} (Dowler et al., 2000), GOLPH3 (Wood et al. 2009), and
Legionella SidM-P4M (Hammond et al. 2014), the PtdIns(3,4)P$_2$ biosensor PH^{TAPP1} (Thomas et
al. 2001), and the PtdIns(4,5)P$_2$ reporter PH^{PLC} (Garcia et al. 2000).

Discrete PtdIns4P pools were detected on specific _Toxoplasma_ secretory organelles
including the dense core granules and Golgi/endosome-like compartments, as well as higher-
order PIP pools on the plasma membrane. Moreover, consistent with the behaviors of these
reporters in other cell types, different PtdIns4P biosensors reported different pools of this
phosphoinositide. For instance, PH^{FAPP1} homed onto structures situated both anterior and
posterior to the cell nucleus, and these organelles were marked with GRA3 -- identifying them
as dense granules (Figure 2.6A). Dense granule targeting of PH^{FAPP1} was dependent on
PtdIns4P binding as substitution of R18L and K7A (i.e., substitutions previously shown to ablate
binding of PH^{FAPP1} to PtdIns4P _in vitro_ and _in vivo_, abolished PH^{FAPP1} targeting to _Toxoplasma_
membranes (Figure 2.6A) (He et al. 2011). PH^{FAPP1} was mostly excluded from SORTLR-marked
Golgi/endosomal compartments and MIC3-positive micronemes, indicating that the PtdIns4P
pool on dense granules is specific among the _Toxoplasma_ secretory pathway (Figure 2.6A).

This pool was confirmed with a second PtdIns4P-specific biosensor, the *Legionella* SidM-P4M domain, which also localized to GRA3-positive dense granules (Figure 2.6A, bottom panel). Representative line scan analysis confirms co-localization of PH^{FAPP1} and SidM-P4M with GRA3, while PH^{FAPP1} does not co-localize with TgSORTLR (Figure 2.6B). In *Toxoplasma*, DAPI stains both the nucleus and the apicoplast genome, and none of the biosensors tested co-localized with DAPI (data not shown).

We identified distinct PtdIns4P pools on other secretory membranes. PH^{GOLPH} localized to SORTLR-marked Golgi/endosomal compartments (Figure 2.7A). A striking feature of this PtdIns4P biosensor was the exquisite intercalation of PH^{GOLPH}-containing membranes with those marked by SORTLR, suggesting the existence of PtdIns4P pools in membranes of earlier stage secretory pathway organelles (Figure 2.7A). Eukaryotic cells have a pool of PtdIns4P at the plasma membrane that is used to replenish higher order PIPs, and this pool is recognized by the SidM(P4M) domain in mammalian cells (Hammond et al. 2014). In our studies, this domain localized only to dense granules, suggesting that the plasma membrane PtdIns4P pool is *Toxoplasma* has some unique properties compared to other eukaryotes, or perhaps that the dense granule PtdIns4P levels are high enough to sequester this biosensor. We were able to identify phosphorylated derivatives of PtdIns4P, PtdIns(4,5)P$_2$ and PtdIns(4,3)P$_2$, at the *Toxoplasma* plasma membrane (Figure 2.7B). Though in mammalian cells, these can be generated by phosphorylation of PtdIns5P, or the degradation of PtdIns(3,4,5)P$_3$, the major contribution to either pool comes from PtdIns4P phosphorylation (Czech 2000). These data offer indirect evidence of a PtdIns4P pool at the plasma membrane. We conclude that the *Toxoplasma* secretory pathway is coded by distinct PtdIns4P pools, and that these are likely used in regulation of secretory functions.
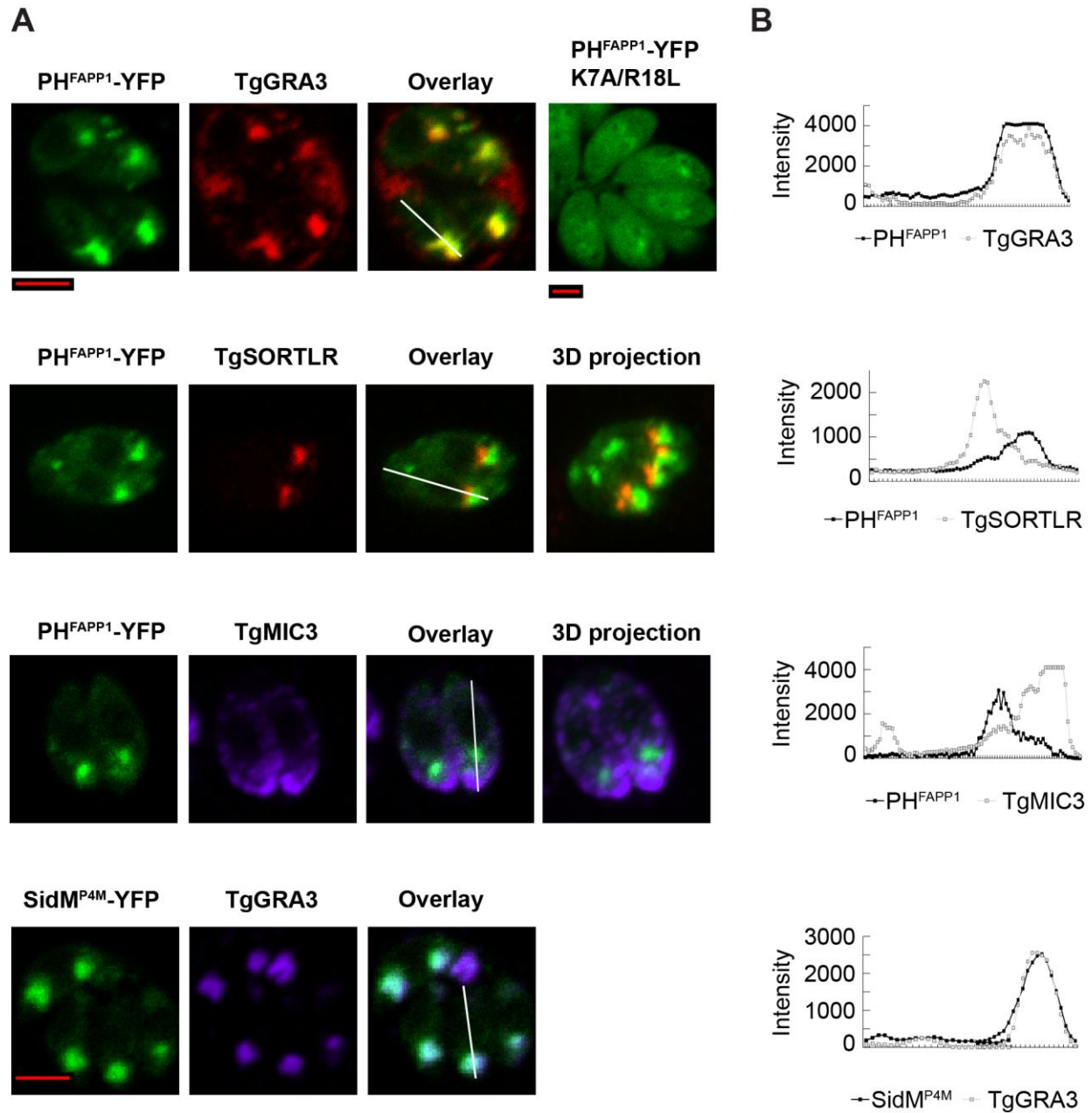
Figure 2.6. There are specific PtdIns4P pools on dense granules in *Toxoplasma*.

(A) Immunofluorescence of *Toxoplasma* cells transiently expressing either the PH^{FAPP1}-YFP or SidM (P4M)-YFP biosensors, stained against TgGRA3, TgSORLR, or TgMIC3. The PtdIns4P-binding mutant of PH^{FAPP1}-YFP (K7A/R18L) is delocalized to the cytoplasm. TRITC or far red and YFP confocal image panels are shown. TRIC/YFP co-localization appears yellow, far

red/YFP co-localization appears blue. Scale bars: 2 µm. **(B)** Representative line scan analysis,

where the line is defined in the respective overlay image in (A).
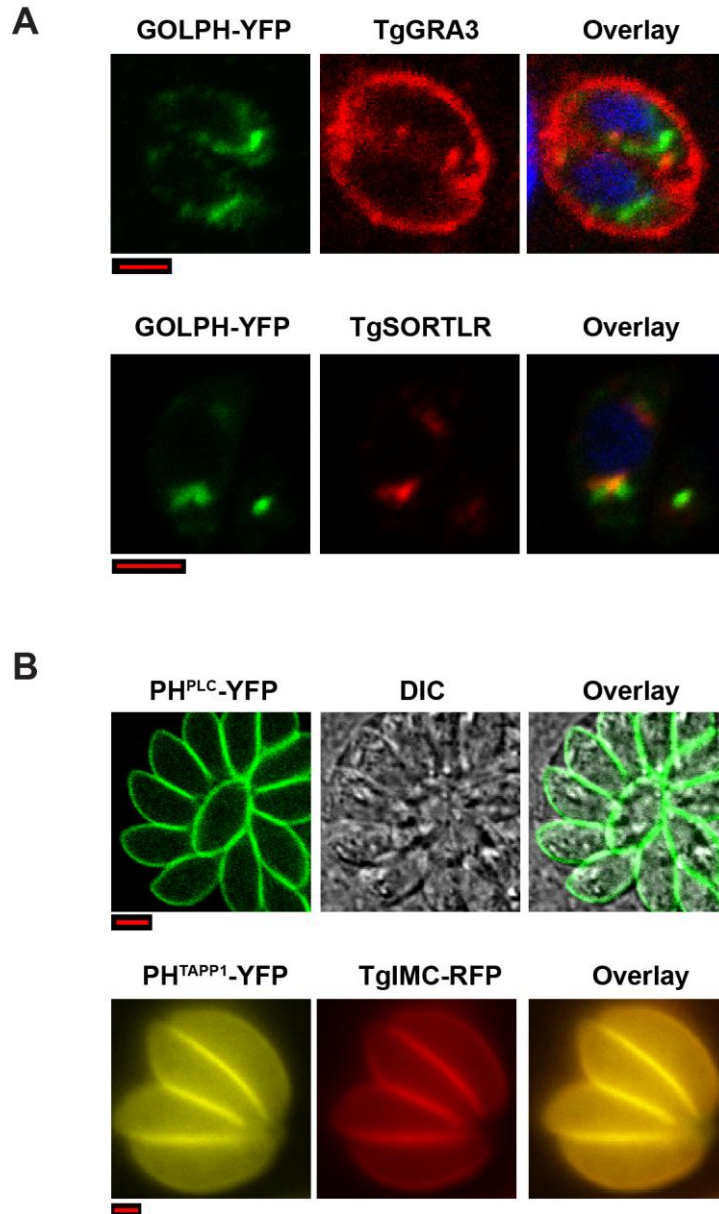
Figure 2.7. There are distinct PtdIns4P pools on early and late secretory membranes in *Toxoplasma*. **(A)** Immunofluorescence against TgGRA3 or TgSORTLR of *Toxoplasma* cells expressing GOLPH3-YFP reveals a PtdIns4P pool on early secretory membranes but not on dense granules. **(B)** Biosensors that recognize higher order PIPs: PtdIns(4,5)P_2 (PH^{PLC}-YFP, top panel shown against DIC) or PtdIns(3,4)P_2 (PH^{TAPP1}-YFP, bottom panel shown against cell surface marker Inner Membrane Complex (IMC)) localize to the plasma membrane. TRITC and YFP confocal image panels are shown, co-localization appears yellow. Scale bars: 2 μm.

PH^{PIMP} preferentially registers a dense-granule pool of phosphoinositide

To determine whether PH^{PIMP} displays an *in vivo* localization profile that overlaps with

any of the PtdIns4P biosensors, we expressed YFP-tagged PH^{PIMP} in *Toxoplasma*. Indeed,

PH^{PIMP} co-localized with the GRA3 dense granule marker, as well as with RFP-tagged PH^{FAPP1}

when the two constructs are co-expressed (Figure 2.8A). Localization of PH^{PIMP} to dense

granules was sensitive to missense substitution of Arg$_{503}$ as the mutant R$_{503}$A domain exhibited

a cytoplasmic distribution under those same experimental conditions (Figure 2.8B). Taken

together, the collective data suggest PH^{PIMP} is alert to a pool of PtdIns4P deployed on the

surface of dense granules, and suggest PH^{PIMP} functions primarily as a PtdIns4P binding

module in *Toxoplasma*. Though we did not detect PtdIns(3,4)P$_2$ and PtdIns(4,5)P$_2$ pools on

dense granules, it's possible that a PI(4,5)P$_2$ pool exists on dense granules to which our

biosensors are insensitive, and that the PIMP PH domain recognizes this pool together with, or

in exclusion of, PtdIns4P.
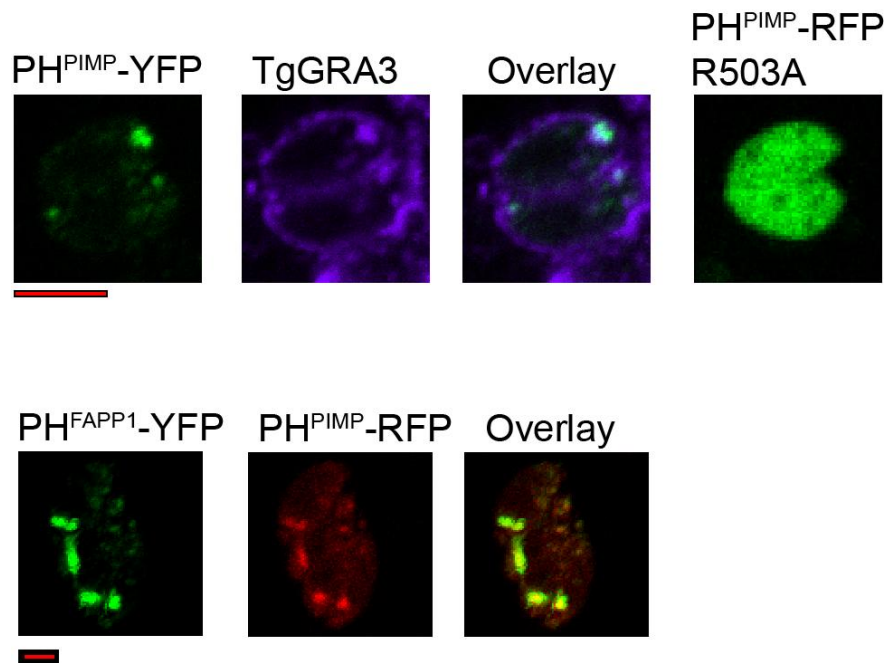
Figure 2.8. PH^PIMP senses PIP pools on dense granules in *Toxoplasma*. PH^PIMP -YFP was

expressed in *Toxoplasma* and immune-stained against TgGRA3, showing co-localization in the

overlay. PH^PIMP(R503A)-YFP did not bind membranes in live cells. Co-expression of PH^PIMP-RFP

and PH^FAPP1-YFP confirmed the PIP pools detected by both domains overlap (overlay). TRITC

or far red and YFP confocal image panels are shown. TRIC/YFP co-localization appears yellow,

far red/YFP co-localization appears blue. Scale bars: 2 μm.

PIMP is a dense granule protein

Does PH^{PIMP} contribute to PIMP recruitment to specific *Toxoplasma* secretory organelles as a function of PtdIns4P and/or PtdIns(4,5)P$_2$ availability? We exogenously expressed full-length PIMP tagged on the C-terminus and immunostained against GRA3. Full length PIMP does indeed localize to dense granules, as well as other intracellular structures not marked with GRA3 (Figure 2.9A). The coincidence of PIMP localization with that of its isolated PH domain suggested that the PtdIns4P-binding activity of PH^{PIMP} might contribute to the spatial and temporal recruitment of the full-length protein to the surface of dense granules. That hypothesis was tested by incorporating the R$_{503}$A missense substitution into the context of the full-length PIMP and assessing the consequences on PIMP localization. Inactivation of the PtdIns4P-binding activity of the PH^{PIMP} domain compromised targeting of the full-length PIMP to GRA3(+) dense granules (Figure 2.9B). PIMP^{R503A} still localized to distinct intracellular structures, but these were separate and adjacent to GRA3(+) membranes (Figure 2.9B). These data indicate PIMP is recruited to dense granules, or to a certain subset of dense granules, in a manner dependent on the PIP-binding activity of its PH domain. Other double-label experiments showed that PIMP does not localize to Golgi/ECL membranes, rhoptries, or micronemes as marked by SORTLR (Sloves, et al. 2012), TgROP1-RFP (Hajj et al. 2007) and TgMIC3 (Garcia-Reguet et al. 2000), respectively (Figure 2.10).
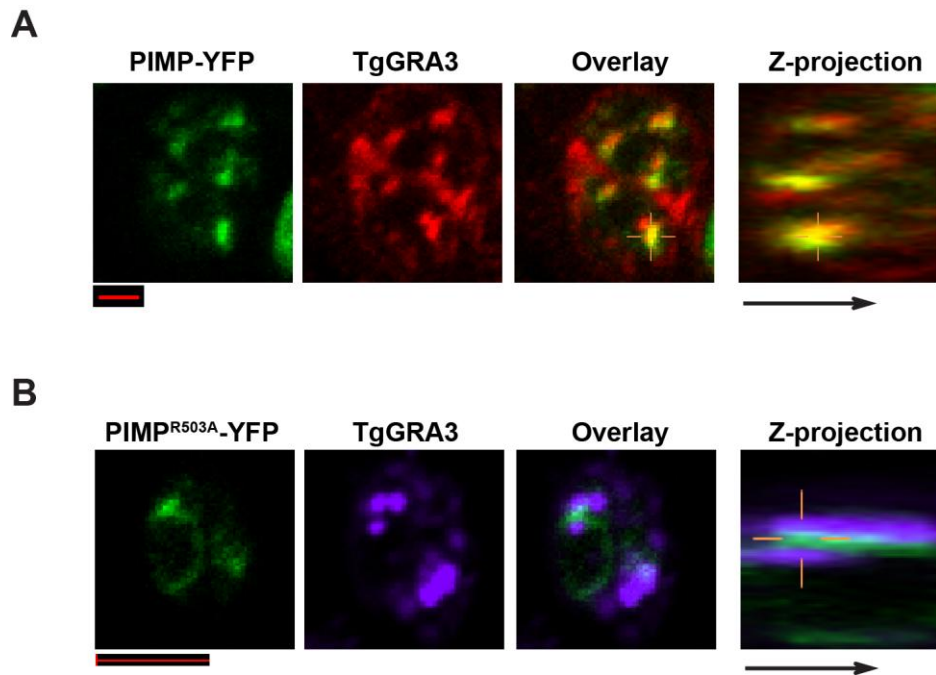
Figure 2.9. PIMP is a dense granule protein. (A) PIMP-YFP was expressed in *Toxoplasma*

and immune-stained against TgGRA3. **(B)** PIMP[R503A]-YFP was expressed in *Toxoplasma* and

immune-stained against TgGRA3. TRITC or far red and YFP confocal image panels are shown.

TRIC/YFP co-localization appears yellow, Far red/YFP co-localization appears blue. Z-

projection indicates signal along the z-stack horizontal to the indicated cross-hairs.

Scale bars: 2 μm.
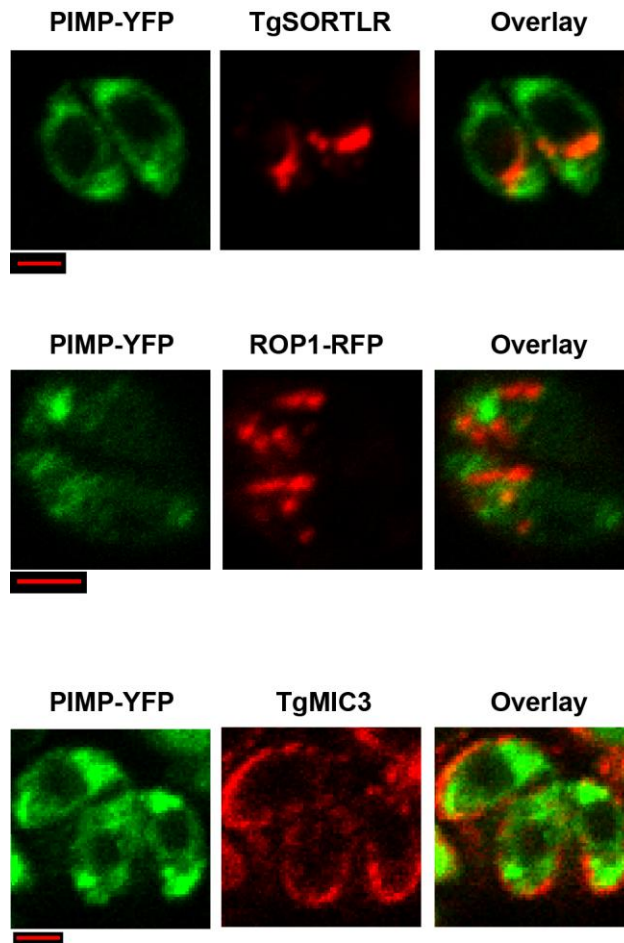
Figure 2.10. PIMP is unique to dense granules. PIMP-YFP was expressed in *Toxoplasma*

and immune-stained against TgSORTL or TgMIC3, or co-expressed with rhoptry marker

construct ROP1-RFP. TRITC or far red and YFP confocal image panels are shown. TRIC/YFP

co-localization appears yellow, Far red/YFP co-localization appears blue. Z-projection indicates

signal along the z-stack horizontal to the indicated cross-hairs. Scale bars: 2 μm.

Discussion

      Toxoplasma are obligate intracellular parasites with a complex life cycle that includes

several stages of differentiation, multiple hosts and a wide host cell range (Boothroyd and Grigg

2002). Many eukaryotic signaling pathways are conserved in *Toxoplasma* and adapted to its

unique requirements (Liendo and Joiner 2000; Nagamune et al. 2008; Tomavo 2014). We can

therefore use what's known about other eukaryotes as a template from which to understand

Toxoplasma signaling pathways. We identify for the first time PtdIns4P pools in *Toxoplasma*,

including a pool on specialized secretory organelles that are involved directly in pathogenesis,

the dense granules. PIMP is a multi-domain PITP/PH/OSBP protein, which senses PtdIns4P

and PtdIns(4,5)P$_2$ through its PH domain and localizes to dense granules. PIMP is a *bona fide*

PITP with PtdIns/PtdCho transfer activity. We propose a model wherein PIMP represents the

hub of an Apicomplexan signaling network that mirrors the Sec14/Kes1 network in yeast.

PIP signaling in the *Toxoplasma* secretory system

      Though *Toxoplasma* acquire many essential biomolecules from their host cells, they are

capable of synthesizing their own PIP network as evidenced by the presence of a functional

PtdIns Synthase encoded in the *Toxoplasma* genome (Schwab 1994; Coppens et al. 2000;

Seron et al. 2000; Charron and Sibley 2002). However, phosphoinositide signaling networks

within Apicomplexa are poorly understood. Analysis of PtdIns3P signaling in *Toxoplasma* has

focused on the prediction that this PIP will regulate late secretory signaling (Tawk et al. 2011).

Surprisingly, PtdIns3P pools in *Toxoplasma* were only detected at the apicoplast, a non-

photosynthetic chloroplast that is not part of the secretory pathway (Tawk et al. 2011; Daher et

al. 2015). Though this work reveals an important function of PtdIns3P*,* the question of how PIP

signaling regulates late secretory membranes in *Toxoplasma* remained unanswered.

      PtdIns4P signaling is also a major regulator of secretion in eukaryotes (Bankaitis et al.

2010; Cleves et al. 1989). PtdIns4P networks have hitherto not been described in *Toxoplasma*.

Using PtdIns4P biosensors known to recognize their substrate in the context of different membranes in yeast or mammalian cells, we show distinct pools of PtdIns4P associated with the *Toxoplasma* Golgi/ELC (according to GOLPH3 domain), and on dense granules (according to SidM-P4M and the FAPP1 PH domain) (He et al. 2011; Dippold et al. 2009; Hammond et al. 2014). The GOLPH3 domain also localizes to cytoplasmic structures distinct from rhoptries, micronemes, the apicoplast, or the nucleus. The positive identification of these structures will further reveal processes subject to regulation by the PtdIns4P network. We also describe a plasma membrane pool of the higher order PIP, PtdIns(4,5)P$_2$, which is generated in other eukaryotes by the phosphorylation of PtdIns4P (and to a lesser extent, the phosphorylation of PtdIns5P), implying the presence of a plasma membrane PtdIns4P pool. These analyses show that distinct pools of PtdIns4P are used to code the *Toxoplasma* secretory pathway, and open novel avenues for study of Apicomplexan secretory processes, especially how these relate to secretion of specialized parasite effector proteins from the dense granules.

PIMP as the hub of a Sec14/Kes1-like signaling network in Apicomplexa

The physical coupling of the PITP and OSBP modules in PIMP suggests conservation of the privileged Sec14/Kes1 relationship not only between eukaryotes, but also across mechanism. Sec14 and Kes1 are separate gene products, and there is no evidence they ever physically interact. Furthermore, the PIMP PITP domain is a START domain with no homology to Sec14 proteins. This suggests that PIMP in *Toxoplasma* and the Sec14/Kes1 signaling hub in yeast came to exist by distinct evolutionary paths, converged on a common useful mechanism. How much of what we know about the Sec14/Kes1 signaling hub can be translated to PIMP function in *Toxoplasma*?

Evidence that PIMP is found on dense granules and binds PtdIns4P through its PH domain mirrors aspects of how Sec14/Kes1 regulate late secretory signaling in yeast in a way that centers on the production and availability of PtdIns4P (Bankaitis et al. 1990; Bankaitis et al.

1989; Cleves et al. 1991a; Fang et al. 1996). The PITP domain of PIMP can substitute for Sec14 in yeast. Like Sec14, and some START PITPs, PITP[PIMP] transfers both PtdIns and PtdCho between membranes *in vitro*, making it capable, at least on principle, of stimulating PtdIns4P synthesis in response to membrane DAG levels as per PtdCho proxy. The GTPase Arf1 controls vesicle biogenesis at Golgi membranes by recruitment of coat proteins (Serafini et al. 1991). ARF-GTPase activating proteins (ARFGAPs) Gcs1p and Age2p are downstream effectors of Sec14 signaling (Yanagisawa et al. 2002). The *Toxoplasma* ortholog of Arf1 has been identified and localized to the Golgi (Liendo et al. 2001). Exogenous expression of dominant negative mutants of TgArf1 inhibit transport of a reporter protein to dense granules, while supplementation of wild-type TgArf1 into a permeabilized cell system augments dense granule secretion, suggesting that dense granule biogenesis as well as secretion are regulated by an Arf1-dependent mechanism (Liendo et al. 2001). This pathway might work in parallel with PIMP signaling, as yeast Arf1 does with Sec14 to coordinate PtdIns4P and vesicle biogenesis.

The yeast OSBP Kes1 binds both sterol and PtdIns4P (Li et al. 2002; Im et al. 2005; de Saint-Jean et al. 2011). The instability of the PIMP OSBP domain when expressed in isolation of the full-length protein has precluded our ability to assay its antagonism of PITP[PIMP] or of Sec14. We have also been unable to test its capacity to bind sterol or PtdIns4P. Several features of the OSBP primary sequence suggest that the domain is competent to bind sterol and an inositol lipid, though perhaps not PtdIns4P. The Kes1 PtdIns4P-binding bipartite motif including K109/K336 and H142/H144 are mostly aliphatic in OSBP[PIMP], and are likely not able to stabilize the PtdIns4P inositol phosphate groups (de Saint-Jean et al. 2011). OSBP[PIMP] may be able to accommodate a different inositol lipid, however, as the orthologous residues that stabilize the general inositol structure in Kes1 are conserved. Some "long ORPs" fulfill the PIP binding function through an N-terminal PH domain, and indeed that may be the case for the binding PH[PIMP].

The two residues of Kes1 known to stabilize sterol H202/E204 lose sterol-binding capacity when mutated to aliphatic residues (de Saint-Jean et al. 2011). The cognate residues in the PIMP OSBP domain are K1755 and S1757, which retain the ability to form hydrogen bonds and may therefore be capable of binding sterol. *Toxoplasma* is considered an obligate intracellular parasite because it requires certain key essential nutrients that it cannot itself synthesize and must therefore scavenge from the host cell. A key role of effector proteins secreted from dense granules is to maintain the intracellular compartment in which the parasite divides and scavenge nutrients from the host cell. Cholesterol is one essential metabolite that the parasites cannot efficiently synthesize themselves, and *Toxoplasma* acquires cholesterol from the host cell by concentrating low density lipoprotein-derived cholesterol into the parasitophorous vacuole from the host cell (Coppens et al. 2000). Sterol sensing in *Toxoplasma* may therefore be coupled directly to nutrient scavenging pathways. If OSBP^{PIMP} has the capacity to bind sterol, it may translate this metabolic input to PtdIns4P-regulated secretion pathways on dense granules to stimulate secretion of effector proteins involved in nutrient scavenging pathways.

PIMP architecture is suited for specific coding of membrane signaling pixels

Eukaryotic cells use membranes as signaling platforms to organize specific biological events, such as exchange of material between the cell and the environment, polarity, and developmental control of cell morphogenesis (Lecuit and Pilot 2003). Because these events demand spatial and temporal precision, a signaling membrane cannot be a blanket of signaling components. In the case of PIP signaling, PITPs have emerged as important organizers of membrane signaling "pixels" across eukaryotes (Bankaitis et al. 2010; Ghosh et al. 2015).

The PIMP PH domain is a PtdIns4P-binding domain, with co-specificity for PtdIns$(4,5)P_2$. When expressed exogenously in live *Toxoplasma*, PH^{PIMP} localizes exclusively to dense granules in a PIP-binding dependent manner as evidenced by delocalization to the cytoplasm of

the PIP-binding mutant (R503A). Though we did not identify any pools of higher order PIPs anywhere but on the cell membrane in our biosensor analysis, the possibility remains that a PI(4,5)P$_2$ pool exists on dense granules, and that PH^{PIMP} senses both this pool and the PtdIns4P pool, perhaps to their mutual exclusion. Mutation of the PH domain at Arg503 in the context of full-length PIMP delocalizes PIMP from GRA3(+) structures. The mutant protein remains associated with cytoplasmic structures that resemble dense granules, though it's not clear whether these structures are some other organelle or a distinct subset of dense granules. This suggests that the PIMP PH domain has a function as a localization determinant that targets PIMP to a specific PtdIns4P pool, i.e., one that is present on dense granules or a subset thereof. The ability to distinguish between PtdIns4P pools equips PIMP with the capacity to specify a membrane signaling pixel.

The PIMP PH domain may regulate PIMP function as a PIP sensor. PH^{PIMP} domain binding of PtdIns4P on dense granule membranes may inhibit the PIMP PITP domain as a mechanism for controlling PtdIns4P production. Conversely, lack of PH^{PIMP} binding to the membrane may activate the PITP domain in an effort to replenish the PtdIns4P pool. This could happen through PH domain-mediated induction of conformational changes to the full-length protein. Alternatively, PH^{PIMP} may bind directly to the PIMP PITP domain, wherein PITP^{PIMP} and dense granule PtdIns4P effectively compete for PH^{PIMP}. There is precedent for regulatory interactions of PITP and PH domains. The mammalian multi-domain Rho-GEF Dbs has an N-terminal Sec14 domain and a downstream PH domain. In this protein, intramolecular contacts between the Sec14 and PH domains must be alleviated for Dbs to affect a cellular function (Kostenko et al. 2005). The PIMP PITP domain has a unique insertion that is well-poised to interact with other proteins and represents a possible platform for intramolecular interactions with the PH domain (described below). An ability to sense PtdIns4P levels and affect downstream synthesis of PtdIns4P may therefore be another mechanism by which PIMP can specify a signaling pixel on dense granule membranes.

The PIMP PITP domain exhibits a "loop" region (residues 193-261) that does not align with any known mammalian START PITP. PITP^{PIMP} with the loop deleted did not substitute for Sec14 in the yeast complementation assay, suggesting that the loop is important for PITP activity or proper folding (data not shown)/ A marked feature of the loop is a highly charged tract (203-REETEEKREETEEKREET-220) that may serve as an interaction domain for a PIMP effector protein. The full 77-residue loop does not exist in the Aconoidasida *Plasmodium* and *Babesia* orthologs of PIMP, nor does it exist in a putative PITP from *Perkinsus*, a protozoan outside of, but related to, the Apicomplexa. Two Coccidia closely related to *Toxoplasma*, *Neospora* and *Eimeria*, encode for START PITPs that do have an insertion in this region; however, each sequence is unique, and only *Toxoplasma* PIMP exhibits the full charged tract described above. *Toxoplasma*, *Neospora* and *Eimeria* all infect a wide range of mammalian hosts, but each has a unique definitive host (felines, canines, and chickens, respectively). Furthermore, each preferentially infects a different tissue and causes a different disease: encephalitis with *Toxoplasma*, neuromuscular degeneration with *Neospora*, and diarrhea with *Eimeria* (Donahoe et al. 2015). The lack of homology to other START proteins suggests that this region is suited to a function specific to *Toxoplasma*, and may reflect binding to specific effectors that contribute to its unique host and cellular tropisms. Conformational exposure of the loop may allow PITP^{PIMP} to bind an effector protein or to one of the other PIMP domains, which could contribute to the pixel identity of a specific signaling domain on dense granule membranes.

Regulation of PIMP signaling by coupling of the PITP and OSBP domains

Immediately N-terminal to the OSBP domain in PIMP are three HT consensus sites (Figure 2.1A). Called PEXELs in *Plasmodium* for *Plasmodium* Export Elements, these are protease cleavage sites recognized by the Apicomplexan-specific aspartic acid protease Plasmepsin V (Horrocks and Muhia 2005). PEXEL sequences target their proteins to the ER by

specifically binding PtdIns3P on ER membranes, which makes the site accessible to ER-resident Plasmepsin V (Bhattacharjee et al. 2012; Bullen et al. 2012; Goldberg 2012). Following cleavage, these proteins are targeted for secretion and export to the host cell (Horrocks and Muhia 2005; Bhattacharjee et al. 2012). HT sequences in *Toxoplasma* are also protease cleavage sites; however, these proteins are not exported into the host cell following cleavage but rather remain cytoplasmic (Hsiao et al. 2013). Most of the HT-containing proteome in *Toxoplasma* are dense granule proteins, wherein the N-terminal domains of the proteins remain associated with the dense granules following protease cleavage of the HT sequences, and the cleaved C-terminal domains remain in the *Toxoplasma* cytoplasm (Hsiao et al. 2013).

HT sites do not exist anywhere else in PIMP but in the ~175 residues upstream of the OSBP domain, and are consistent with the identity of PIMP as a dense granule protein. These sites pose two interesting possibilities for PIMP regulation: (1) that PIMP integrates PtdIns3P signaling into the dense granule circuit, and (2) that the PIMP OSBP domain is evicted from the full length protein under certain signaling conditions. We were unable to express or purify a stable recombinant region that encompasses these sites specifically, and were therefore unable to assay its ability to bind PtdIns3P directly. Our preliminary experiments argue that at least one of these sites is cleaved *in vivo* when PIMP is exogenously expressed in *Toxoplasma* (data nor shown).

Interestingly, two of the three HT sites are coded for on exon/intron boundaries of the PIMP gene: at the boundary of exons 15 and 16, and at the start of exon 17, raising the possibility that these regions are also subject to regulation on the transcriptional level. We did not detect distinct splice forms in our reverse-transcriptase experiments; however, that does not exclude the possibility that such regulation occurs at stages of the parasite life cycle not included in our analyses.

The biological role of PIMP in *Toxoplasma*

Herein, we describe a multi-domain PITP that has the potential to act as a platform for the integration of parasite metabolism sensing pathways with secretion of dense granule proteins specialized for maintaining pathogenesis. How does PIMP regulate dense granule functions? And how is this translated to the cell biology of *Toxoplasma* and other Apicomplexa? We discuss these questions, our findings, and future directions in greater detail in Chapter 4.

CHAPTER 3: ATOMISTIC INSIGHTS INTO THE DYNAMICS AND ENERGETICS OF THE MAMMALIAN PHOSPHATIDYLINOSITOL TRANSFER PROTEIN PHOSPHOLIPID EXCHANGE CYCLE

Introduction

Phosphatidylinositol (PtdIns) is a metabolic precursor of phosphoinositides, and these lipids function as critical intracellular chemical signals in eukaryotes. While much effort is invested in understanding the enzymes that produce and consume phosphoinositides, fundamental aspects for how phosphoinositide production is regulated and physically organized define unappreciated gaps in our understanding of how inositol lipid signaling is prosecuted in cells. It is in those contexts that PtdIns transfer proteins (PITPs) command increasing interest as activities that functionally channel lipid metabolic information to dedicated and tightly integrated phosphoinositide signaling circuits. It is therefore no surprise that the biological importance of PITPs is on striking display in both uni- and multi-cellular organisms. Phenotypes associated with defects in individual PITPs include: (i) non-redundant functions of individual PITPs in channeling phosphoinositide signaling to Golgi/endosomal membrane trafficking, lipid droplet metabolism, and endosomal phosphatidylserine metabolism in yeast (Bankaitis et al. 1990; Cleves et al. 1991; Wu et al. 2000; Ren et al. 2014), (ii) collapse of 'extreme' polarized plant membrane growth programs required for tissue organogenesis (Vincent et al. 2005; Huang et al. 2013; Ghosh et al. 2015), (iii) defects in embryogenesis and retinal degeneration disease in both *Drosophila* and zebrafish (Vihtelic et al. 1991; Milligan et al. 1997; Giansanti et al. 2006; Ile et al. 2010), and (iv) neurodegeneration, chylomicron retention disease, liver steatosis, and hypoglycemia in neonatal mice (Hamilton et al. 1997; Alb et al. 2003; Alb et al. 2007).

The biological importance of these proteins notwithstanding, PITPs remain poorly characterized with respect to how these proteins work as molecules. PITPs are not enzymes, but proteins that mobilize energy-independent transfer of PtdIns and PtdCho between membranes *in vitro* (Helmkamp et al. 1974; Wirtz 1991). On the basis of this operational assay, PITPs have historically been described to function as lipid carriers that transport PtdIns from its site of synthesis in the endoplasmic reticulum to the plasma membrane where agonist-stimulated phospholipase C-dependent pathways consume phosphoinositides -- for which PtdIns is a metabolic precursor (Wirtz 1991). An alternative mechanistic framework for thinking about how PITPs function as molecules is gaining strong momentum, however, and it conceptualizes a very different mechanism which does not involve inter-membrane PtdIns-transfer at all. Rather, PITPs are proposed to chaperone a tightly channeled 'on-demand' synthesis of privileged, and spatially highly organized, phosphoinositide pools dedicated to specific biological outcomes (Schaaf et al. 2008; Bankaitis et al. 2010; Grabon et al. 2015).

Regardless of whether PITPs function as PtdIns presentation modules, or as *bona fide* PL-transfer proteins, there is no question that the PL-exchange reaction is central to their biological activity. The exchange reaction, in summary, includes the PITP ejecting bound PL upon docking onto a membrane surface, followed by reloading of the PITP with another PL molecule prior to its disengagement from the surface. Studies in purified systems with defined liposomes and recombinant PITP show that abstraction of PL from a membrane bilayer during the exchange reaction occurs in the absence of any co-factors or ATP (Helmkamp et al. 1974; Wirtz 1991). Thus, PITPs lower the activation energy of PL desorption from the bilayer and couple protein conformational transitions to a cycle of PL unloading and loading. However, the fundamental details of the protein and PL dynamics associated with the exchange reaction are proving exceptionally challenging to dissect using conventional wet biochemistry approaches.

Initial insights into the conformational dynamics of PL-exchange were obtained from unrestrained MD simulations and biochemistry of the yeast PITP Sec14 (Ryan et al. 2007). Although the MD time course was short (32 ns), oscillations between 'open' and 'closed' Sec14p conformers were simulated and Sec14 structural elements were identified that control the conformational pathway associated with such oscillations (Ryan et al. 2007; Schaaf et al. 2011). While informative, those simulations are limited. First, the MD simulations were conducted in the absence of a membrane bilayer, revealing no information about PL::PITP interactions during the exchange reaction (Ryan et al. 2007). It is those interactions that must be understood. Second, the detailed information from the Sec14 MD does not translate to the START-domain PITPs since the two classes of PITPs are structurally unrelated. This issue takes on added force given the severe developmental and neurodegenerative phenotypes associated with genetic deficiencies in START-domain PITP function in vertebrates and other metazoans (Vihtelic et al. 1991; Milligan et al. 1997; Giansanti et al. 2006; Ile et al. 2010; Hamilton et al. 1997; Alb et al. 2003). As first address of these major gaps in our knowledge, we describe MD simulations that reveal the protein and PL dynamics, and the free energy landscape, of PtdIns and PtdCho exchange by the mammalian START-domain PITPα. The MDS offers key descriptions of PITPα mechanism: (1) interaction of PITPα with the membrane is spontaneous and mediated by four specific substructures, (2) the ability of PITPα to close around the phospholipid ligand correlates to loss of flexibility of two helix/loop regions as well as the C-terminal helix, (3) extraction of the phospholipid by PITPα is stabilized mostly by hydrogen bonds, and (4) the trajectory of PtdIns or PtdCho into the lipid binding pocket is mediated by overlapping but unique sets of PITPα residues. We rationally engineered altered versions of PITPα based on MDS predictions and tested them for function *in vivo* and *in vitro*. These analyses support the MDS predictions. Together, the data provide a platform from which START PITP phospholipid exchange can be understood and further analyzed.

Materials and Methods

Atomistic molecular dynamics simulations.

Molecular dynamics simulations (MDS) were performed for PITPα in a system

reconstituted with a lipid bilayer consisting of either pure 1,2-dioleoyl-PtdCho (DOPC) or a

90%/10% molar mixture of DOPC and PtdIns. PITPα structures in the open (PDB 1KCM) and

closed (PDB 1FVZ) conformations were retrieved from the RCSB Protein Data Bank (Yoder

et al. 2001; Schouten et al. 2002). The former structure is lipid-free whereas the latter

describes PITPα in complex with a single bound PtdCho molecule. These two starting

structures were each introduced into each of the two bilayer systems to generate a total of

four systems that were run in 1 µs all-atom simulations. In all cases, PITPα was positioned

above the bilayer in the water phase. Simulations were run at physiological salt

concentrations (150 mM KCl) and counter ions were introduced to neutralize the total charge

of the system. Details of the compositions of each simulated system are provided in Table

3.1.

Table 3.1. Composition of simulated systems.

System/number of molecules	PITP	DOPC	PI	water	K^+	Cl^-	Simulation time (microseconds)
1	1 (1FVZ – closed)	192	0	27593	81	77	1
2	1 (1FVZ – closed)	190	18	26235	93	73	1
3	1 (1KCM – open)	192	0	27519	79	77	1
4	1 (1KCM – open)	190	18	27212	98	76	1

The OPLS all-atom force field was used to describe the interactions between all

molecules (Jorgensen and Tirado-Rives 1988). For water, the TIP3P model that is

compatible with the OPLS parameterization was employed (Jorgensen et al. 1983). The

system structure used in this study is identical to those employed in our previous simulations

of lipid bilayers (Kaiser et al. 2011; Orlowski et al. 2011). Further, to parameterize lipid molecules, improved parameters specifically derived for lipids were used (Maciejewski et al. 2014; Kulig et al. 2015; Kulig et al. 2016). Periodic boundary conditions with the usual minimum image convention were employed in all three dimensions. The length of each hydrogen atom covalent bond was preserved by the LINCS algorithm (Hess et al. 1997). The integration time step was set to 2 fs and the simulations were carried out at constant pressure (1 bar) and temperature (310 K). The temperature and pressure were controlled by the Parrinello-Rahman and velocity-rescale methods, respectively (Parrinello and Rahman 1981; Bussi et al. 2007). The temperatures of the solute and the solvent were coupled separately. For pressure, a semi-isotropic scaling was employed. The Lennard-Jones interactions were cut off at 1.0 nm. For the electrostatic interactions, the particle mesh Ewald method (Essmann et al. 1995) was employed with a real space cut-off at 1.0 nm, beta-spline interpolation (6th order), and a direct sum tolerance of 10^{-6}. The simulations were performed with the GROMACS 4.5.5 simulation package (Hess et al. 2008; Pronk et al. 2013).

Free energy calculations.

Free energies of DOPC and PtdIns uptake by PITPα were obtained by umbrella sampling simulations of two model systems. The starting structure of the first system was obtained from the final structure after a 1 µs production run of simulation 3 (Table 3.1). The second system was generated from the first by replacing the DOPC molecule positioned closest to the binding site with a PtdIns molecule.

Free energy profiles for DOPC and PtdIns uptake by PITPα were calculated using the umbrella sampling method (Kästner 2011). The starting structures were obtained as follows. First, a single PL (DOPC or PtdIns) was pulled from the bilayer towards the PITPα lipid-binding pocket along the z-axis (membrane normal) in 20 ns simulation with a constant pulling force constant of 1000 kJ x mol^{-1} x nm^{-2} and a pulling rate of 0.00075 nm x ns^{-1}

exerted on the lipid headgroup. Next, the position of the lipid headgroup was adjusted by lateral pulling such that it was positioned in the near vicinity of PITPα residues Cys_{95} and Phe_{225} reported to be important for PtdCho binding (Yoder et al. 2001; Garner et al. 2012), of residues Thr_{59}, Lys_{61}, Glu_{86}, and Asn_{90} known to coordinate the inositol headgroup (Alb et al. 1995; Tilley et al. 2004). After the PLs were optimally positioned within the PITPα binding pocket, the constraints imposed on the respective headgroups were released. The DOPC and PtdIns systems were then simulated for an additional 150 and 240 ns, respectively.

In umbrella sampling simulations, 28 and 26 windows with a spacing of 0.1 nm were employed for PtdIns and DOPC systems, respectively. The reaction coordinate (ζ) was chosen as z-coordinate of the lipid headgroup with boundaries at the plane of the membrane-water interface and at the upper regions of the lipid binding pocket. In each window, a harmonic restraining potential of 1000 kJ x mol^{-1} x nm^2 was applied in the z-direction on the distance between the center of mass of the given headgroup and the DOPC bilayer bound with PITPα. Finally, the free energy profile for both PLs was constructed with the weighted histogram analysis method (WHAM) (Kumar et al. 1992) based on the biased distribution of the given PL and magnitude of the umbrella biasing potential along the reaction coordinate. All free energy calculations were performed with an identical set of simulation parameters as described above for the equilibrium simulations.

Visualization.

All the snapshots and movies presented in this work were prepared using the VMD package (Humphrey et al. 1996). Molecular graphics and analyses of *PITPNA* single-nucleotide polymorphisms were performed with the UCSF Chimera package developed by the Resource for Biocomputing, Visualization, and Informatics at the University of California, San Francisco.

Lipid reagents.

For radiolabeled lipid transfer assays, preparation of [³H]-PtdIns rat liver microsomes has been described (Bankaitis et al. 1990; Schaaf et al. 2008). [³H]-PtdCho (L-α-dipalmitoyl [choline methyl-³H], ART 0284) was purchased from American Radiolabeled Chemicals, Inc. (ARC). For fluorescence-based lipid transfer assays, L-α-PtdCho and L-α-phosphatidic acid from chicken egg of highest available quality, were purchased from Avanti Polar Lipids (Alabaster, AL, USA), and used without further purification. 1-Palmitoyl-2-decapyrenyl-sn-glycero-3-phosphocholine (PyrPtdCho) was synthesized from 1-palmitoyl-2-hydroxy-sn-glycero-3-phosphocholine (Avanti Polar Lipids) and parinaroyl anhydride (Salinger and Lapidot 1966; Gupta et al. 1977), and purified by reverse phase HPLC chromatography (Beckman Ultrasphere ODS outfitted with 4.6 x 25 cm column (Patton et al. 1982). 1-Palmitoyl-2-decapyrenyl-sn-glycero-3- phosphoinositol (PyrPtdIns) was prepared from yeast PtdIns and parinaroyl anhydride as described (Somerharju et al. 1982). 2,4,6-trinitrophenyl-phosphatidylethanolamine (TNP-PtdEtn) was prepared as described (Gordesky and Marinetti 1973), and purified by silica gel column chromatography. Stock solutions of lipids were prepared in methanol and kept at -20 °C. The concentrations of PyrPtdIns and PyrPtdCho were determined spectroscopically, while the concentrations of L-α-PtdCho, L-α-phosphatidic acid and TNP-PtdEtn solutions were determined according to Rouser et al. (Rouser et al. 1970). All lipid solutions were taken to ambient temperature before use. All other chemicals used were of highest available quality and the organic solvents were of spectroscopic grade.

Yeast strains and media.

Yeast were grown in YPD liquid media (1% yeast extract, 2% bactopeptone, and 3% glucose), or SD liquid media (0.67% nitrogen base, 3% glucose with appropriate amino acids supplemented) (Sherman et al. 1983). The respective plate media included 2% agar. Yeast strains CTY182 (*MATa ura3-52 lys2-801 Δhis3-200*), and CTY1-1A (*MATa ura3-52 lys2-801*

Δ*his3-200 sec14-1^ts*) were previously described (Bankaitis et al. 1990; Cleves et al. 1991; Bankaitis et al. 1989). *PITPNA*–expressing yeast strains were constructed by genomic integration of a single copy cassette where the *PITPNA* open reading frame was expressed under the control of the powerful and constitutive *PGK1* promoter (P_{PGK}) and configured in tandem with a functional *HIS3* selection marker. The integration cassette was recombined into the *LEU2* locus of the appropriate recipient yeast strain by standard lithium acetate transformation methods (Gietz et al. 2002). Transformants were selected on media lacking histidine and correct integration of the cassette was confirmed by screening for leucine auxotrophy as unselected phenotype. *PITPNA* over-expression strains were generated by transformation of the *PITPNA* expression cassette (driven by the powerful constitutive *PMA1* promoter) subloned into a yeast *URA3* episomal plasmid pDR195 (Rentsch et al. 1995) by the lithium acetate method. Transformants were selected on uracil-free media.

Site-directed mutagenesis.

The *Rattus norvegicus PITPNA* gene was mutated by site-directed mutagenesis in the P_{PGK1}-*PITPNA HIS3::LEU2* yeast integration vector, the pDR195 (P_{PMA1}-*PITPNA*) vector, and in the pET28b-*His8-PITPNA* protein expression plasmid. Mutations were confirmed by DNA sequencing. Nucleotide sequences for primers for the site-directed mutagenesis experiments are available from the authors by request.

Protein purification.

Recombinant PITPα and mutant versions were expressed from pET28b-*His8-PITPNA* vectors propagated in *E.coli* BL21 (RIL/DE3; New England BioLabs Inc, Ipswich, MA). Bacteria were cultured in 4L TB + kanamycin/chloramphenicol media for 4hrs at 37°C, shifted to 16°C and induced for recombinant protein expression with IPTG (100μM final concentration). Cultures were harvested after 18hrs, and cells disrupted by passage through

a French Press in low-phosphate lysis buffer (300mM NaCl, 25mM Na-phosphate, 5mM 2-mercaptoethanol, pH 7.5). Clarified lysates were incubated with TALON metal affinity beads (Clontech, Mountain View, CA), and bound proteins step-eluted with imidazole (25mM–200mM). Proteins were concentrated using the Amicon Ultra filter system (EMD Millipore), and concentration determined by SDS-PAGE and comparison against a BSA standard mass series.

Lipid transfer assays.

End-point assays measured transport of [^{3}H]-PtdIns from rat liver microsomes to PtdCho liposomes or [^{3}H]-PtdCho from liposomes (98 mol% PtdCho, 2mol% PtdIns) to bovine heart mitochondria as described (Bankaitis et al. 1990; Schaaf et al. 2008).

Pyrene-labeled PtdCho (PyrPtdCho) and PtdIns (PyrPtdIns) binding and transfer measurements were performed using a real-time de-quenching assay as described by Somerharju *et al.* (Somerharju et al. 1987) with modification. For the transfer measurements two vesicle populations were used. The donor (with TNP-PtdEtn quencher) and acceptor (without TNP-PtdEtn quencher) vesicles were prepared as follows. For the acceptor vesicles stock solutions of egg PtdCho and egg phosphatidic acid were mixed in a 291/9 nmol (97/3 mol%) ratio and dried under a stream of N$_2$. The resulting lipid film was then hydrated with 2 ml low phosphate buffer (25 mM Na$_2$HPO4, 300 mM NaCl, pH 7.5) and sonicated on ice for 10 min. For the donor vesicles stock solutions of egg PtdCho, PyrPtdCho/PyrPtdIns and TNP-PtdEtn were mixed in a 4/0.5/0.5 nmol ratio, solvent was evaporated and the lipid film re-suspended in 10 µl EtOH. The solution was injected into the buffer containing the acceptor vesicles. After a 5-10 min equilibrium period, the fluorescence intensity (excitation 346 nm, emission 378 nm) was measured as a function of time at 37°C using a ISS K2 fluorimeter (ISS Inc., Champaign, IL).

To measure transfer from donor to acceptor, 1 μg protein was injected every 250 s for a total of 4 injections. To obtain relative transfer efficiency, the initial slope after each protein injection was calculated and the mean slope values for each protein (n=4) was normalized to that calculated for purified PITPα. For binding measurements, donor vesicles were injected into 2 ml low phosphate buffer. After a 5-10 min equilibrium period the solution was titrated 10x with 0.1 nmol recombinant protein and fluorescence intensity was measured as a function of wavelength (excitation 343 nm, emission 360-450 nm) at 37 °C (K2 fluorimeter). The intensity at 348 nm was then plotted against protein amount and the slope value for each protein was calculated and normalized against PITPα in order to obtain the relative binding efficiency.

Results

PITPα binding to the membrane bilayer.

Both open apo-PITPα and closed PtdCho-bound holo-PITPα forms have been crystallized and the structures solved (Yoder et al. 2001; Schouten et al. 2002). The protein consists of four domains. The PL-binding cavity includes: (i) an 8-stranded β-sheet capped by two long α-helices, (ii) a regulatory loop speculated to be involved in mediating protein interactions, (iii) the C-terminal domain suggested to participate in closure of the PL-binding pocket, and (iv) a small lipid exchange loop speculated to form a lid over the PL binding pocket and thereby gate access to it. To examine the PITPα lipid exchange cycle at an atomistic level, extensive all-atom MD simulations of both the open and closed PITPα conformers were run in systems reconstituted with bilayers consisting of DOPC or PtdIns/DOPC. Root mean square deviation (RMSD) and Root mean square fluctuation (RMSF) plots of PITPα Cα-atoms showed that both conformers were stable during the simulations (Figure 3.1A & B). Higher flexibility was observed for the open conformer in the presence of the DOPC/PtdIns membrane (Figure 3.1A, blue line), and this was primarily accounted for by the increased flexibility of the PITPα extreme C-terminus (Figure 3.1B – blue line). That is, the substructure suggested to gate access to the PITPα hydrophobic pocket. Two substructures bounded by residues 25-38 and 65-83, respectively, similarly exhibited enhanced flexibilities in the open conformer relative to the closed holo-PITPα. Indeed, it is in that latter substructure that the most striking conformational change was observed during the MD simulations. This region bounded by residues 65-83, which corresponds to the lipid-exchange loop, was in the form of a turn in the starting structure and transformed into a 3_{10}-helical conformation during the MD. As described below, this conformational change coincided with insertion of that loop into the bilayer upon PITPα association with the membrane.

Firm and spontaneous PITPα binding to membrane was observed for both conformers, in both membrane systems, within the first 200-300 ns of simulation -- as scored by the number of H-bonds established between protein and PL (Figure 3.1C). Initial (0 ns) and final (1000 ns) snapshots for all four simulations are presented in Figure 3.2. Detailed analyses of the occurrence of H-bond interactions between individual PITPα residues and PLs are compiled in Table 3.2. Although the residues identified for membrane binding differed between the open and closed conformers in the DOPC systems, some residues were consistently highlighted and these identified three common regions involved in membrane association. Those regions were defined by: (i) the lipid exchange loop (residues 68-81), (ii) residues 135-163, and (iii) residues 204-220. With regard to specific interactions, Tyr_{103} of the open conformer engaged DOPC in H-bond interactions whereas the C-terminal lid domain of the closed conformer (residues 259-264) interacted with DOPC. Parallel analyses in the DOPC/PtdIns systems identified residues 147-153 and 208-219 in PITPα-PtdIns interactions (Table 3.3).

Occurrence of contacts between PITPα and PL atoms were similarly monitored throughout the MD course where contact was set as an inter-atomic distance of $\leq$ 0.35 nm (Figure 3.3A-C). Those analyses indicated that, in addition to the regions identified by H-bond analyses, both conformers showed that residues 28-41 constituted another region of membrane association. Moreover, the open conformer uniquely presented one additional membrane interaction subdomain (residues 99-110), and this particular set involved interactions other than H-bonds (e.g. charge pairs). This unique membrane association area was able to interact with the bilayer surface due to the slightly different dock orientation of the open PITPα conformer on the membrane surface relative to that of the closed form -- a difference which renders this protein region more accessible to the membrane for binding.
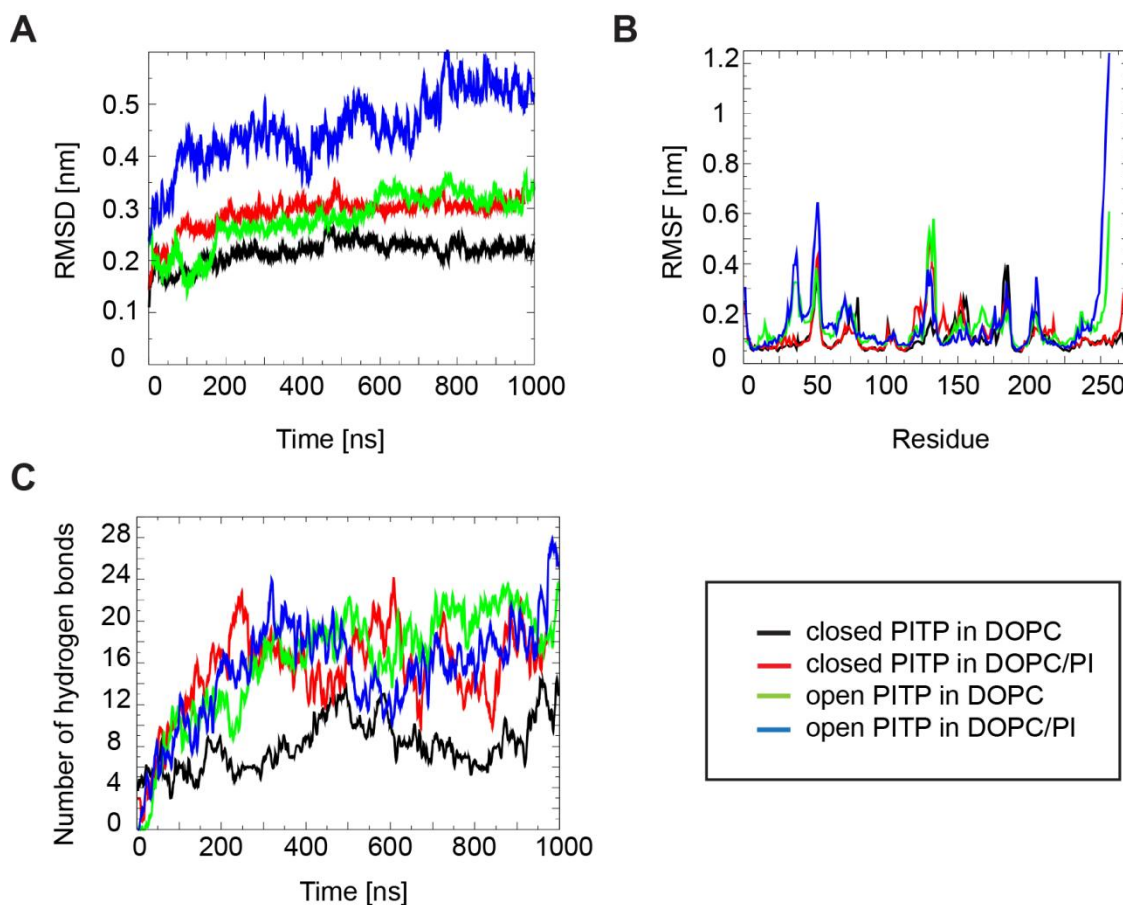
Figure 3.1. PITPα is stable during simulations. (A) RMSD of open and closed PITPα conformers in MD simulations (as described in Table 3.1). **(B)** RMSF of open and closed PITPα conformers in MD simulations (as described in Table 3.1). **(C)** Overall number of hydrogen bonds between the protein and lipids in time for MD simulations (as described in Table 3.1).1 – black line, 2 – red line, 3 – green line, 4 – blue line.
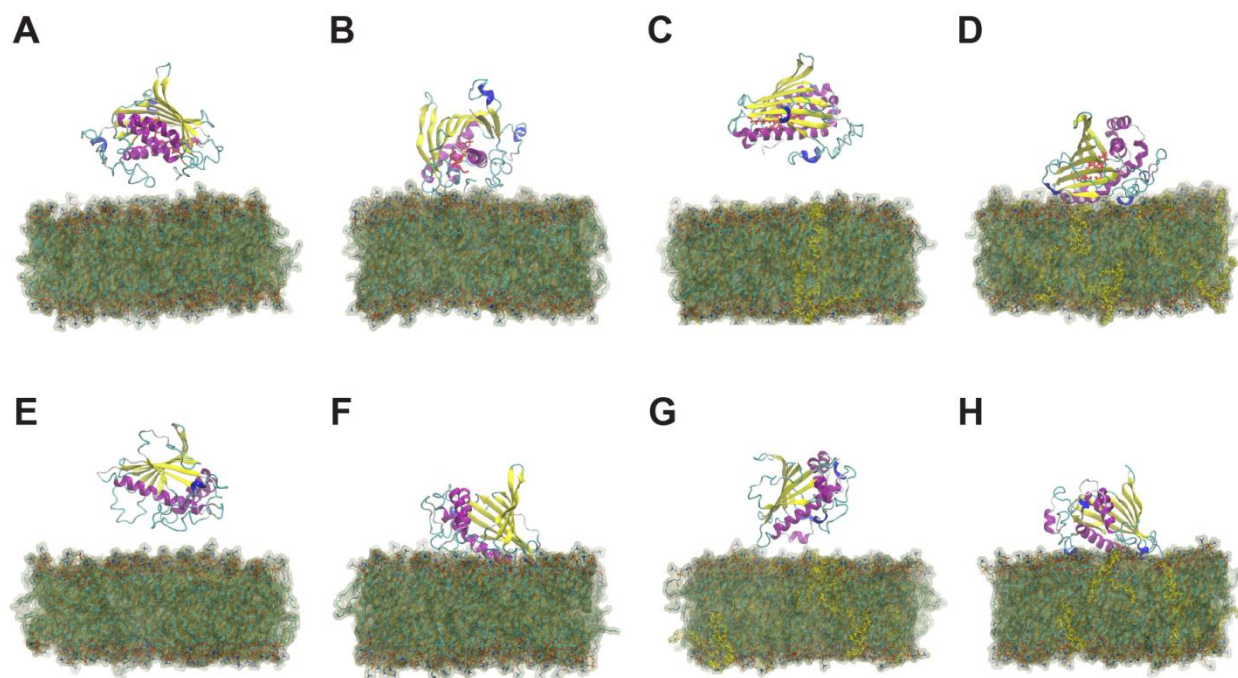
Figure 3.2. **PITPα changed conformations during simulations.** Initial (0 ns – **A, C, E, G**) and final (1000 ns – **B, D, F, H**) snapshots from the simulations of systems: 1 **(A, B)**, 2 **(C, D)**, 3 **(E, F)** and 4 **(G, H)** - as described in Table 3.1. Lipids shown in licorice (PtdIns in yellow and PtdCho inside the binding pocket of PITPα in red) and transparent brown surface. PITPα is presented in new cartoon representation in colors representing secondary structure. Water molecules and ions not shown for clarity.

Table 3.2. Number of hydrogen bonds protein-DOPC lipids in 300-1000ns. The least frequent hydrogen bonds were neglected.

Residue	Closed in DOPC	Closed in DOPC/PI	Open in DOPC	Open in DOPC/PI
Lys68	-	-	-	1.39 (+/- 0.003)
Thr71	-	-	1.36 (+/- 0.005)	1.40 (+/- 0.005)
Arg74	1.30 (+/- 0.005)	-	0.95 (+/- 0.004)	-
Glu79	0.22 (+/- 0.002)	-	0.51 (+/- 0.003)	-
Ala81	0.28 (+/- 0.003)	-	-	-
Tyr103	-	-	0.86 (+/- 0.002)	0.51 (+/- 0.003)
Lys135	-	1.42 (+/- 0.006)	0.54 (+/- 0.003)	-
Tyr141	-	1.14 (+/- 0.002)	-	-
Arg147	-	-	-	1.97 (+/- 0.006)
Ser152	-	1.93 (+/- 0.002)	1.36 (+/- 0.005)	1.88 (+/- 0.003)
Lys153	-	1.87 (+/- 0.006)	1.82 (+/- 0.003)	0.93 (+/- 0.004)
Tyr155	-	-	-	0.27 (+/- 0.002)
Lys156	-	-	-	0.40 (+/- 0.003)
Lys163	-	-	-	0.79 (+/- 0.003)
Trp204	-	0.37 (+/- 0.003)	0.32 (+/- 0.002)	-
Gly205	-	-	0.33 (+/- 0.002)	-
Gln207	-	0.46 (+/- 0.003)	-	-
Asn208	-	1.00 (+/- 0.004)	1.77 (+/- 0.003)	-
Lys209	-	1.92 (+/- 0.004)	1.76 (+/- 0.003)	0.98 (+/- 0.004)
Asn212	-	0.42 (+/- 0.003)	1.23 (+/- 0.003)	-
His215	-	0.88 (+/- 0.002)	-	-
Lys216	-	0.63 (+/- 0.003)	1.80 (+/- 0.004)	0.78 (+/- 0.003)
Gln217	-	-	-	0.30 (+/- 0.002)
Lys219	-	0.73 (+/- 0.003)	-	-
Arg220	-	-	1.25 (+/- 0.004)	1.38 (+/- 0.003)
Arg259	1.48 (+/- 0.003)	-	-	-
Gln260	1.18 (+/- 0.003)	-	-	-
Lys261	1.82 (+/- 0.002)	-	-	-
Val264	0.10 (+/- 0.002)	-	-	-

Table 3.3. Number of hydrogen bonds protein-PI lipids in 200-1000ns. The least frequent hydrogen bonds were neglected.

Residue	Closed in DOPC/PI	Open in DOPC/PI
Arg147	-	0.50 (+/- 0.003)
Ser148	0.11 (+/- 0.002)	-
Lys153	0.12 (+/- 0.002)	-
Gln207	-	0.13 (+/- 0.003)
Asn208	-	-
Lys209	-	1.72 (+/- 0.003)
Asn212	0.32 (+/- 0.003)	-
His215	0.13 (+/- 0.002)	-
Lys216	0.35 (+/- 0.003)	0.56 (+/- 0.003)
Lys219	0.11 (+/- 0.002)	-
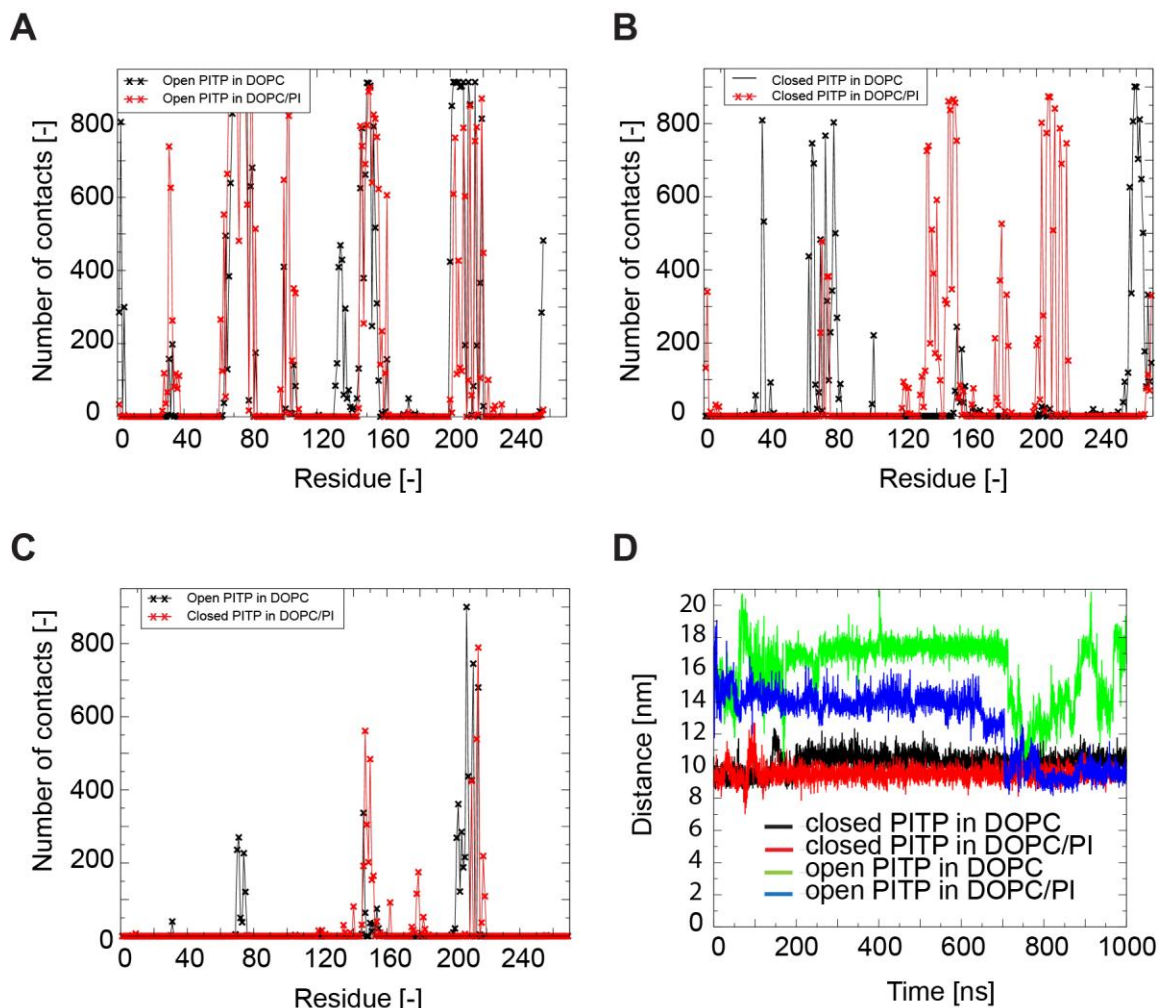
Figure 3.3. PITPα interacts with the membrane during simulations. Number of contacts between protein residues and lipids defined as the occurrence of the distance < 0.35 nm between any atom of protein residues and bilayer's lipids atoms in each frame of simulation (count as 1 contact) (**A, B, C**). Number of the protein – PtdCho contacts in the systems (as described in Table 3.1): 3 – black, 4 – red (**A**), 1 – black, 2 – red (**B**); and number of protein – PtdIns contacts in the systems: 2 – red, 4 – black (**C**). Distance between C-alpha atoms of Ser30-Glu41 residues in time in the systems 1 – black, 2 – blue, 3 – green, 4 – blue (**D**).

PITPα dynamics upon membrane association.

After membrane binding, the closed PITPα molecule remained relatively inert throughout the remainder of the simulation. No unloading of bound PtdCho or opening of the lid was observed. Specific conformational motions were observed upon membrane binding for the open conformer, however, and it is for this reason that focus is trained on the MD of open PITPα. As described above, residues 25-38 were implicated in membrane binding and exhibited enhanced mobility in the open form. Interestingly, using the inter-atomic distance between residues Ser_{30} and Glu_{41} as ruler for pocket closure, that distance decreased dramatically after 700 ns of simulation to the point that the inter-atomic Ser_{30}-Glu_{41} distance approached that observed in the closed conformer (Figure 3.4A, B; Figure 3.3D). The lipid exchange loop was also inserted into the cytoplasmic leaflet of the bilayer at this time where it underwent a transition from a turn to a 3_{10}-helix, and adopted a more extended conformation according to RMSF calculations (Figure 3.1B) and visual inspection (Figure 3.4A, B).

Most interestingly, bilayer insertion of the lipid exchange loop and the partial closure of the hydrophobic pocket initiated at 700 ns coincided with partial loading of a single DOPC molecule into the pocket opening (Figure 3.4C, D). We interpret the simulation data to conceptualize engagement of the lipid exchange loop with one DOPC molecule with the result that the engaged DOPC is extracted from the membrane bilayer and is moved towards the hydrophobic pocket/water interface. PITPα was unable to consolidate those movements into vectorial transfer of PL into the hydrophobic pocket, however. Rather, the partially extracted PLs either slid back into the bilayer or engaged in bobbing movements at the cavity opening/water interface. A rationale for this behavior is presented below.

The role of PITPα residues Trp_{203} and Trp_{204} in the lipid exchange cycle is unclear. Several studies conclude these residues are essential for lipid exchange by PITPα and closely-related PITPs (Tilley et al. 2004; Yadav et al. 2015), whereas other studies argue for

only minor roles for $Trp_{203}Trp_{204}$ in lipid-exchange (Phillips et al. 2006). The MD simulations reported no significant conformational transitions associated with this motif, and no obvious membrane insertion. These residues were the first to interact with the lipid bilayer, however, and the $Trp_{203}Trp_{204}$ motif maintained interactions with membrane lipids throughout the MD time course. The MD data suggest those Trp residues, and the residues that surround them, interact primarily with PtdIns (Figure 3.3C).
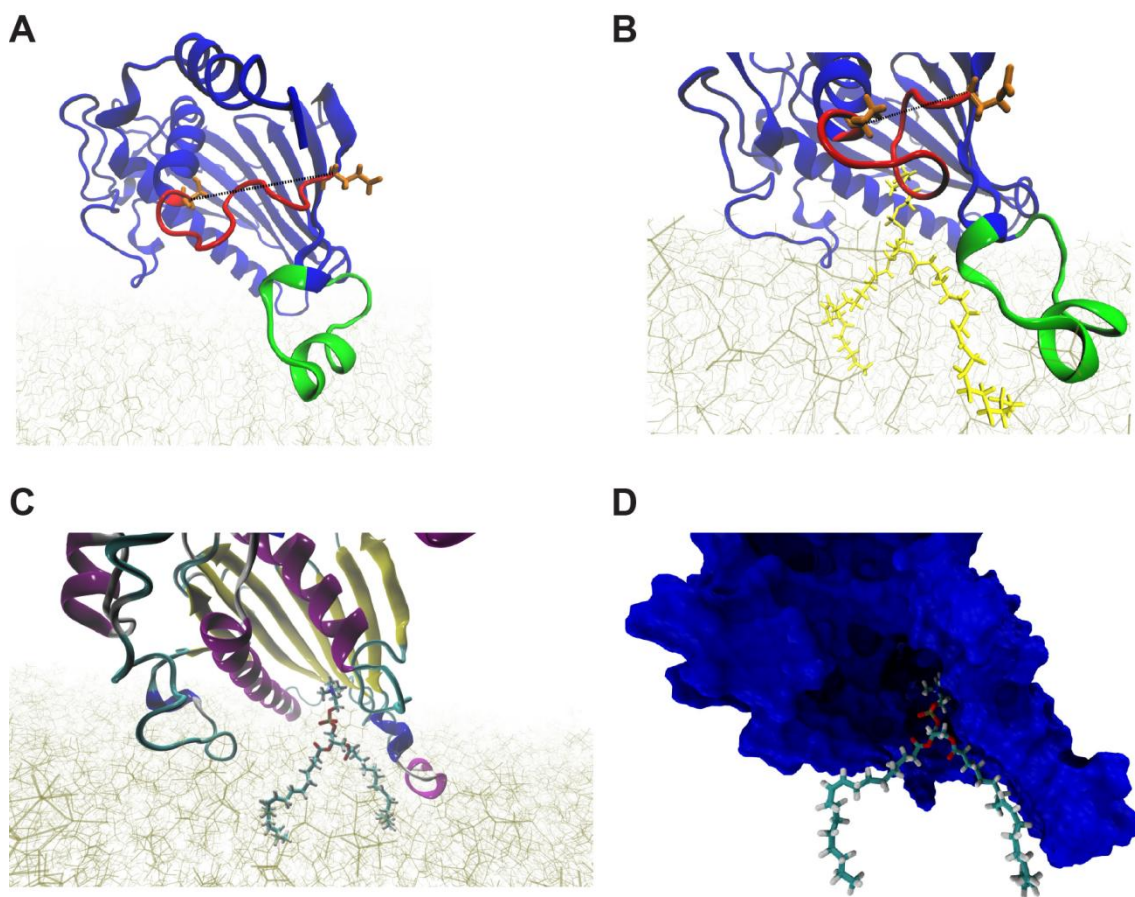
Figure 3.4. PITPα extracts lipids from the virtual membrane during simulations.

Snapshot of the open PITPα (blue and green new cartoon representation) from the

simulation 4 (Table 3.1) in the **(A)** initial (0 ns) and **(B)** final (1000 ns) step. Loop consisting

of residues 25-38 depicted in red, residues Ser_{30} and Glu_{41} depicted in orange licorice

representation, and the distance between their C-alpha atoms as a black dashed line, lipid

exchange loop colored in green, and DOPC lipid "grabbed" by the loop in yellow licorice

representation. Water molecules and ions not shown for clarity. Other lipids are depicted as

brown lines. **(C)** Snapshot from the simulation 4 (as described in Table 3.1) of the open

PITPα (new cartoon representation) and a PtdCho molecule (in licorice representation)

engaged by the lipid exchange loop in the final (1000 ns) step. Other lipids shown as brown

sticks, water molecules and ions not shown for clarity. **(D)** Snapshot of the open PITPα (blue

surface) from the simulation 4 (as described in Table 3.1) in the final (1000 ns) step. A single

PtdCho molecule (in licorice representation) is engaged by the lipid exchange loop which

aligns its molecular surface with the lipid acyl chain. Water molecules, ions and bilayer not

shown for clarity.

Free energies of PL loading/unloading by PITPα.

The 1 μs atomistic MD runs were of insufficient length to describe a complete PL loading/unloading half-cycle. Thus, suitable free-energy calculation methods were employed to study the energetics of PL loading/unloading by PITPα. A steered MD approach was used to obtain a pathway for positioning of DOPC and PtdIns within the PITPα binding pocket through a short pulling simulation (see Materials and Methods). Once this regime yielded a PL-loaded conformer, the pulling constraints imposed on PL position were released, and subsequent trajectories were used to extract the windows for umbrella sampling simulations. These umbrella sampling simulations were analyzed with by WHAM. Our selection of the force constant, together with the window spacing (see Materials and Methods), provided sufficient sampling of the configuration space along the reaction coordinate as indicated by the satisfactory overlap of the histograms in Figure 3.5A, B. Although each window was simulated for 40 ns, the obtained PMF stabilized within 10 ns of simulation – indicating the free energy profile converged to a stable value. We interpret this rapid convergence to reflect the fact that the starting structures for the umbrella sampling windows were extracted from unbiased trajectories. This interpretation follows previous demonstrations that the qualities of the starting structures for umbrella sampling have a significant impact on subsequent free energy profile quality (Paloncẏová et al. 2012).

Because the exchange cycle occurs efficiently with purified PITPα and pure liposomes, and without any ATP requirement, the activation energy for PL loading/unloading must be sufficiently low to be overcome by thermal fluctuations. Indeed, during the ensuing MD (150 and 240 ns for the systems with DOPC and PtdIns, respectively), bound PL was unloaded from the binding pocket and released into the bilayer (Figure 3.6). The PL unloading took place without any externally applied pulling forces. Taking advantage of these well-equilibrated starting configurations, umbrella sampling simulations were extracted from the unloading trajectories and the free energies related to PITPα interaction with DOPC and

PtdIns were calculated. The free energy profiles for both PLs as a function of the distance along the bilayer normal are presented in Figure 3.7A. Those profiles confirmed that PL loading into PITPα occurs within the realm of thermal fluctuation. The free energy of DOPC uptake by PITPα was ~ 20 kJ mol^{-1} (8 k$_B$T) -- as calculated from the bottom of the global minimum to the maximum peak at 3 nm (Figure 3.7A). In the absence of PITPα the values for DOPC and PtdIns desorption from the membrane bilayer were 90 kJ mol^{-1} and 120 kJ mol^{-1}, respectively (Table 3.4). The dramatic differences in the free energies of PL desorption in the presence vs absence of PITPα emphasize the remarkable role the protein plays in lowering the activation energy for that critical step.

For both DOPC and PtdIns, the free energy profiles identified two distinct minima. The first, at 1.5 nm, corresponded to the state where the PL was at equilibrium in the bilayer. The second was located in the membrane-distal region of the PL-binding cavity where the PL headgroups are coordinated by appropriate PITPα residues and the fatty acyl chains are incorporated into the most hydrophobic regions of the cavity. Unexpectedly, the free energies of loading for both PLs were similar – suggesting the affinity of PITPα for PtdIns in the initial loading stage(s) was not appreciably higher than PITPα's affinity for PtdCho. This was a surprising outcome given reports that PITPα has a 16-fold higher affinity for PtdIns than for PtdCho (Helmkamp et al. 1974; Wirtz et al. 1991). Another remarkable feature of the calculated free energy profiles was that the minima at ~3.5 nm were very shallow. This property accounts for why PL molecules that had partially loaded, or were otherwise steered, into the PITPα pocket were spontaneously and efficiently released into the bilayer via a reverse unloading reaction during simulation – the energy barrier for unloading of bound PL is low.
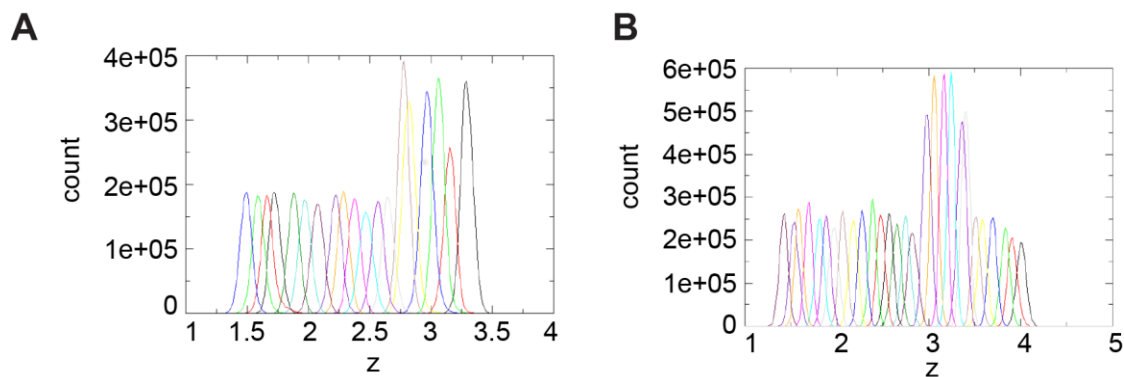
Figure 3.5. The simulations are stable. Overlap of the umbrella sampling histograms from the umbrella sampling simulations of the PtdCho (**A**) and PtdIns (**B**) release from the protein to the bilayer. Horizontal axis describes the distance along the membrane normal, where zero is the center of the lipid bilayer. The vertical axis shows the occurrence of given configuration, i.e. umbrella window (colored lines). The sampling of configurations was increased corresponding to 2.75-3.3 nm in the (**A**) and 3.0-3.4 nm in (**B**) to ensure sufficient overlap in those initially inadequately sampled regions of the free energy curve.
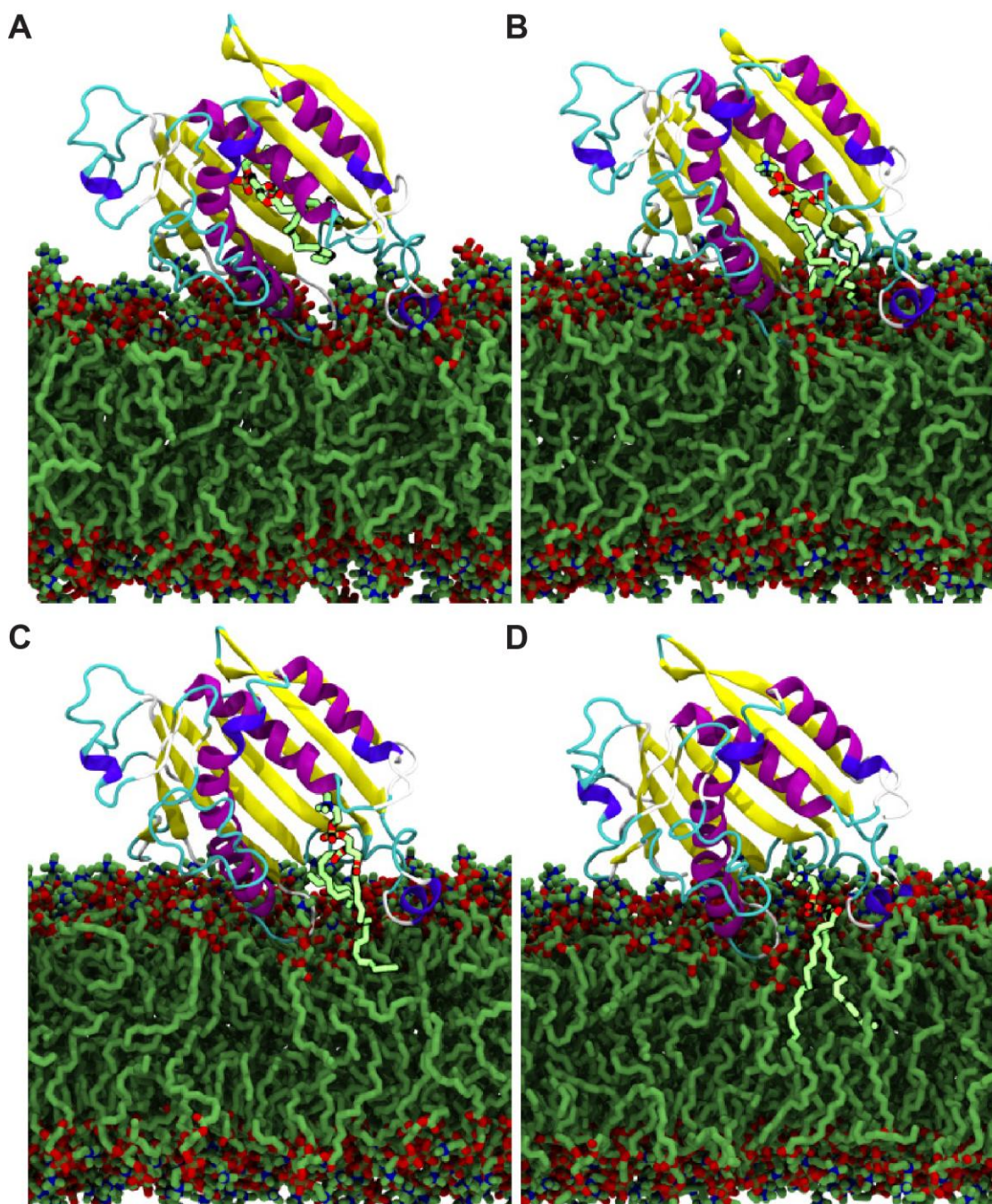
Figure 3.6. **Trajectory of lipids out of the PITP binding pocket.** Snapshots of the lipid unloading after the release of pulling force on the lipid (highlighted in bright green) in the steered MD simulation. Individual panels correspond to: ~0 ns **(A)**, ~75 ns **(B)**, ~100 ns **(C)**, and ~150 ns **(D)** after the release of pulling force. Lipids are shown in licorice and PITPα in new cartoon representation. Water molecules and ions not shown for clarity.
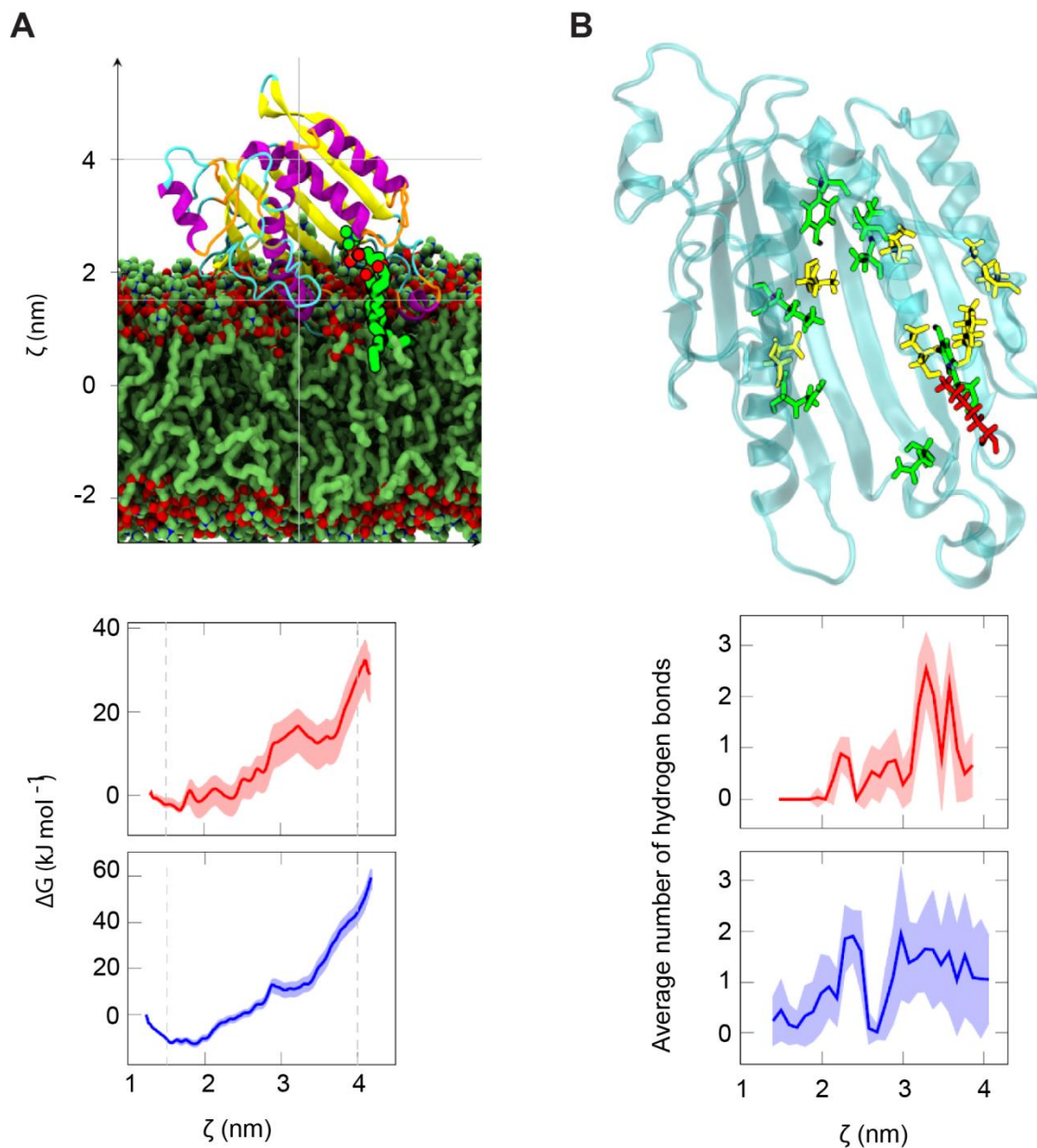
Figure 3.7. Hydrogen bonds stabilize the lipid during its trajectory through the PITP.

(A) Top: Snapshot from one of the umbrella sampling simulations windows showing PtdCho (green VdW spheres) being unloaded back into the membrane by PITPα (new cartoon representation). Vertical axis represents the reaction coordinate ζ (nm) where ζ = 0 nm corresponds to the midplane of the lipid bilayer, ζ = 2 nm and ζ = 4 nm correspond to the membrane-water interface and the upper part of the binding pocket, respectively. The

horizontal gray helplines define the borderlines for lipid movement. The same lines depicted

vertically on the bottom panel figure presents the free energy profiles for PtdCho (red) and

PtdIns (blue) uptake/unload. **(B)** Top: PITPα and amino acid residues that form H-bonds with

PtdCho and/or PtdIns. Residue projected to interact only with PtdCho is depicted in red

(Lys$_{68}$), only with PtdIns in yellow (Lys$_{61}$, Glu$_{86}$, Asn$_{90}$, Thr$_{114}$, Glu$_{218}$), and in green residues

that form H-bonds with both ligands (Tyr$_{18}$, Gln$_{22}$, Ser$_{25}$, Tyr$_{63}$, Asn$_{101}$, Lys$_{195}$, Gln$_{217}$). Bottom:

Average number of H-bonds interactions between PITPα and PtdCho (red) and PtdIns (blue),

as indicated, as a function of time. Profiles are calculated as a function of the umbrella

window which has been translated into the reaction coordinate ζ (nm).

Table 3.4. Free energies for the lipid desorption process.

Pulled lipid	PITP	DOPC	PI	Free energy
DOPC	-	192	0	90 kJ/mol
PI	-	191	1	120 kJ/mol
DOPC	1 (1KCM – open)	192	0	20 kJ/mol
PI	1 (1KCM – open)	191	1	25 kJ/mol

PITPα-PL interactions within the hydrophobic pocket.

Lipid-protein H-bond interactions within the PITPα hydrophobic pocket are likely

required for serial consolidation of the loading reaction so that vectoriality is imposed on this

process which culminates in a complete loading reaction (i.e. rather than a reversible and

futile partial loading reaction that we observed in the 1 μs MD). Indeed, both DOPC and

PtdIns engaged in H-bonding within the PITPα binding pocket, and the highest peaks in

average H-bond interaction coincided with minima in the free energy profiles (Figure 3.7A,

B). Those results argue that H-bond interactions make critical contributions to the free energy

landscapes of the DOPC and PtdIns loading/unloading reactions.

All pocket residues involved in H-bonding with DOPC and PtdIns are highlighted in Figure 3.7B. The unloading MD runs made the novel forecast that Lys_{68} interacts specifically with PtdCho, whereas Thr_{59}, Lys_{61}, Glu_{86}, Asn_{90}, Thr_{114}, and Glu_{218} interact specifically with PtdIns. Satisfyingly, the former four residues were known from previous studies to engage PtdIns specifically (Alb et al. 1995; Tilley et al. 2004), while the latter two interactions represent new insights. Tyr_{18}, Gln_{22}, Ser_{25}, Tyr_{63}, Asn_{101}, Lys_{195}, and Gln_{217} formed H-bonds with both DOPC and PtdIns, and these residues had not previously been implicated in the PL-exchange cycle. The strong single H-bond interaction of Lys_{68} with DOPC is particularly noteworthy as it was observed early in the loading reaction sequence (Figure 3.8A) – suggesting this previously unsuspected interaction plays a role in the extraction process. PtdIns did not interact with PITPα residue Lys_{68}. Rather, it formed two H-bonds with Glu_{218} -- another residue previously not suspected to play any role in lipid exchange (Figure 3.8B). The MD projected that interactions of DOPC and PtdIns with Lys_{68} and Glu_{218}, respectively, defined the major contribution to peaks in the average H-bond plot at ~2.3 nm (Figure 3.7B).
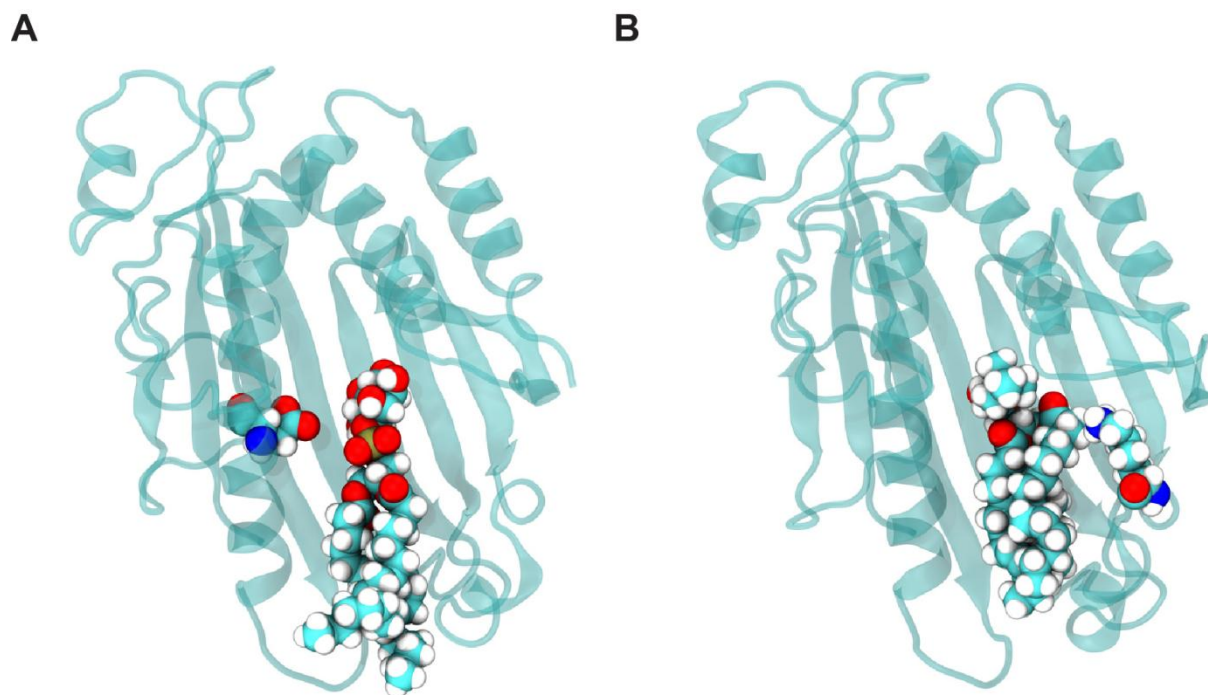
Figure 3.8. PITPα interacts specifically with PtdIns and PtdCho. Snapshots of PtdCho interacting with the residue Lys_{68} **(A)** and PtdIns interacting with the residue Glu_{218} **(B)** during the umbrella sampling simulation. Residues Lys_{68}, Glu_{218} and the respective phospholipids are shown as VdW spheres. PITPα is rendered in new cartoon representation.

Functional analyses of Ser$_{25}$ in PITPα activity.

A series of functional analyses were performed to test basic predictions of the MD data. Residues 25-38 define a conformationally flexible region predicted to be involved in membrane binding, and the boundary residue Ser$_{25}$ is projected to be involved in H-bonding to DOPC and PtdIns within the PITPα hydrophobic pocket. To assess the importance of Ser$_{25}$ to PITPα function, this residue was altered to Phe, Ala, Cys, Glu, Lys, and Thr. The mutant proteins were subsequently analyzed in *in vivo* and *in vitro* functional assays.

High-level expression of PITPα in yeast is sufficient to effect phenotypic rescue of the growth and membrane trafficking defects associated with temperature-sensitive mutations in the yeast *SEC14* gene (Skinner et al. 1993), and this system enables a general assessment of whether a mutant PITPα is functional or not. Expression of PITPα^{S25A}, PITPα^{S25C} and PITPα^{S25T} rescued *sec14-1^{ts}*-associated growth defects at the restrictive temperature of 37°C nearly as efficiently as observed for PITPα (Figure 3.9A). By contrast, PITPα^{S25E} was only partially functional in this assay whereas PITPα^{S25F} and PITPα^{S25K} scored as completely defective. Consistent with the *in vivo* results, purified recombinant PITPα^{S25F} and PITPα^{S25K} were also completely inactive for PtdIns and PtdCho-transfer *in vitro* in end-point assays using radiolabeled phospholipid substrates and a single clamped protein concentration (Figure 3.9B). Thus, while some substitutions are tolerated for Ser$_{25}$, these do not correlate with H-bonding capacity (e.g. S$_{25}$A scores as active). Rather, functionality correlated closely with the accessible surface area of the residue at that position. Residues compatible with efficient function (Ser, Ala, Cys and Thr) have small accessible surface areas (80Å^2, 67Å^2, 104Å^2, 102Å^2, respectively), those that support partial function have larger values (Glu, 138Å^2), and residues not tolerated at position 25 have the largest side chains (Phe and Lys – accessible surface areas of 175Å^2, 167Å^2, respectively).
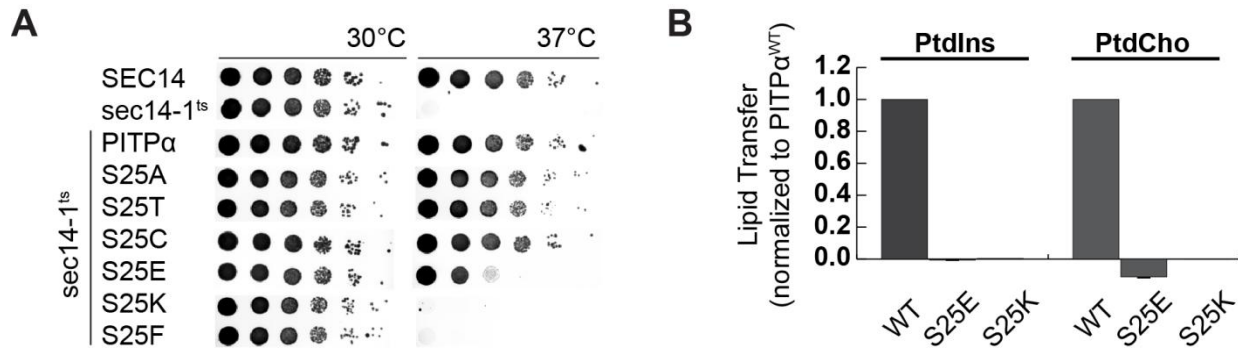
Figure 3.9. Functional consequences of missense substitutions for PITPα residue Ser$_{25}$. (A) Phenotypic rescue assays. Top panel: isogenic *SEC14* (CTY182) and *sec14-1ts* (CTY1-1A) strains served as positive and negative controls for PITP activity, respectively. The latter strain fails to grow at 37°C because activity of the major PITP is inactivated at that temperature (Bankaitis et al. 1989). Bottom panel: Isogenic *sec14-1ts* yeast strains carrying expression cassettes for *RnPITPNA*, or versions carrying the indicated substitutions for residue Ser$_{25}$, integrated at the *LEU2* locus, were spotted in 10-fold dilution series onto YPD agar plates and incubated at either permissive temperature of 30°C or restrictive temperature of 37°C for 48 hours. **(B)** Endpoint PtdIns and PtdCho transfer assays. Purified recombinant PITPα and indicated missense mutants (10μg protein per assay) were assayed for [^{3}H]-PtdIns and [^{14}C]-PtdCho transfer, as indicated. Transfer efficiencies of PITPα were set at 100% (n=3), and transfer of mutant PITPα proteins are normalized relative to PITPα activity values obtained from the same experiments. Assay efficiencies and backgrounds for these experiments are summarized in Table 3.5 and Table 3.6.

Table 3.5. Intrinsic PtdIns-transfer activities for mutant PITPα derivatives (cpm).

Mutant	% Transfer/Totals	Total Input [³H]PtdIns	Background
PITPα	7-18%	8600-17400	190-870
S25E	-0.18-0.006%	8600-9100	190-350
S25K	-0.12-0.22%	8600-9100	190-350
K68E	1.3-2.2%	8600-17400	190-870
K68Q	5.6-6.9%	9000-17400	400-870
E218A	8.8-14.4%	9000-14710	400-870
E248K	0.3%-0.56%	14700-17400	540-870
K248A	1.7-2.4%	11600-13290	570-780
E248T	0.88%-1.8%	8900-13300	400-570
M241T	33.2-57.8%	11600-13290	570-780

Table 3.6. Intrinsic PtdCho-transfer activities for mutant PITPα derivatives (cpm).

Mutant	% Transfer/Totals	Total Input [³H]PtdIns	Background
PITPα	9-30%	12550-19290	815-2600
S25E	-2.0-(-0.52)%	12550-19290	815-2460
S25K	0.01%	16500	815
K68E	5.7-9.8%	12550-14640	2460-2600
K68Q	16-21%	16500-19290	815-1120
E218A	12-22%	16500-19290	815-1140
E248K	11-18%	7060-12550	925-2460
E248A	17-30%	18140-18690	1140-1760
E248T	17-29%	7060-12650	925-2460
M241T	109-118%	12650-18140	1305-1760

Functional analyses of Lys$_{195}$ in PtdIns and PtdCho-transfer and binding.

Lys$_{195}$ was identified in the MDS as a major contributor to the hydrogen bond-mediated stabilization of either PtdIns or PtdCho with PITPα (Figure 3.7). Lys$_{195}$ occurs on the beta sheet that forms the lipid binding cavity of PITPα (Figure 3.10A), as such the residue is likely to interact with either lipid only once the lipid is fully extracted from the membrane. Analysis of the crystal structures of PtdIns or PtdCho bound PITPα reveals that the distance between Lys$_{195}$ and the phosphate moiety of PtdIns is 2.3Å, and 2.7Å for PtdCho. As the average length of a hydrogen bond is between 1.5-2.5Å, these distances are consistent with a role for Lys$_{195}$ with the stabilization of either lipid during binding within the PITP hydrophobic pocket. To test this prediction, we purified PITPα^{K195C} and used real-time de-quenching approaches to measure PtdCho- and PtdIns-transfer rates and efficiencies of PtdCho- and PtdIns-binding (Figure 3.10B, C). In these assays, transfer is recorded as enhanced fluorescence of pyrene-labeled phospholipid as it is mobilized from quencher-loaded donor vesicles to quencher-free acceptor vesicles, whereas binding is measured by shielding of pyrene-phospholipid from quencher by the PITP (see Materials and Methods). PITPα^{K195C} was unable to bind or transfer either PtdIns (Figure 3.10B) or PtdCho (Figure 3.10C). This data supports the MD prediction that Lys$_{159}$ stabilizes the binding of both ligands in the PITPα hydrophobic pocket through H-bond contributions.

Functional analyses of Lys$_{68}$ in PtdCho-transfer and binding.

Lys$_{68}$ is projected to engage in a significant H-bond interaction with DOPC early in the PITP loading reaction. Moreover, this is scored as a specific interaction as PtdIns is not projected to interact with Lys$_{68}$. Analysis of various substitutions at this position did not support an essential role for Lys$_{68}$ in PITPα activity, however. In the phenotypic rescue assay PITPα^{K68A}, PITPα^{K68C}, and PITPα^{K68Q} scored as functional. By contrast, PITPα^{K68E} and

PITPα^{K68R} expression supported only diminished efficiencies of phenotypic rescue of *sec14-1^{ts}*–associated growth defects (Figure 3.11A).

The biochemical properties of purified PITPα^{K68E} were further examined in the end-point PtdCho and PtdIns transfer assays and, as expected, PITPα^{K68E} showed diminished PL-transfer activity (Figure 3.11B). However, whereas PITPα^{K68E} showed a ~70% reduction in PtdCho-transfer activity, the mutant PITP was also strongly defective in PtdIns-transfer. In the real-time pyrene-label experimental systems, PITPα^{K68E} again showed significantly reduced initial rates of PtdCho- and PtdIns-transfer and binding (Figures 3.11C, D). These collective data reported that Lys$_{68}$ plays an important role in optimizing PtdCho- and the PtdIns-binding reactions.
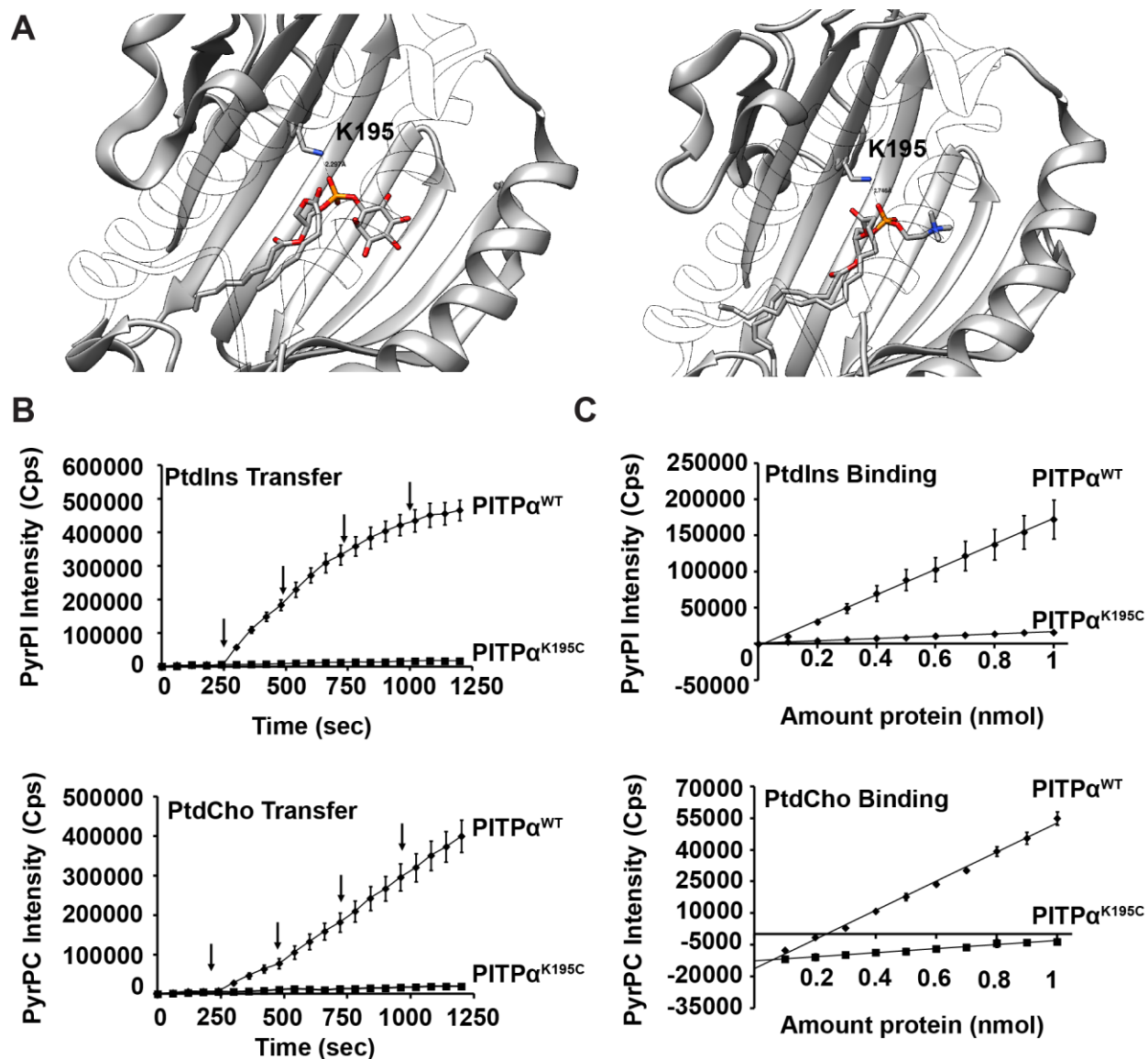
Figure 3.10. **Functional consequences of missense substitutions for PITPα residue**

Lys$_{195}$. **(A)** The lipid-binding pocket of PITPα bound to PtdIns (left panel, PDB1UW5) or PITPα

bound to PtdCho (right panel, PDB1T27) are shown with Lys$_{195}$ highlighted. **(B)** Kinetic analyses

of rates of PtdIns and PtdCho transfer. Purified recombinant PITPα and mutants were assayed

using PyrPtdIns or PyrPtdCho transfer activity as indicated. Fluorescence intensities of

PyrPtdIns or PyrPtdCho are plotted as a function of time. Black arrows mark addition of 1µg

increment of the indicated protein. Following protein addition, the observed increase in

fluorescence intensity was directly proportional to the relative transfer efficiency of the protein

being assayed. The initial slope after each addition was calculated to obtain relative transfer

efficiencies (Table 3.7). Error bars were calculated from two independent determinations. **(C)**

PtdIns and PtdCho binding assays. Recombinant PITPα and PITPα^{K195C} were assayed for

PyrPtdIns or PyrPtdCho binding as indicated. Fluorescence intensity of pyrene-PtdIns or

pyrene-PtdCho is plotted as a function of protein amount (nmol) and the slope value for each

protein was calculated to obtain relative binding efficiencies. Error bars were determined from

two independent determinations. PITPα^{K195C} was tested on a different fluorometer than the rest

of the mutants, as such the fluorescence intensities depicted in this figure cannot be compared

against mutants of other residues, but can be compared to the WT PITPα depicted within this

experimental set.

Table 3.7. Activity is expressed as % of WT PITPα.

Protein	PtdIns Binding		PtdIns Transfer		PtdCho Binding		PtdCho Transfer	
	Slope	Activity	Slope	Activity	Slope	Activity	Slope	Activity
PITPα^{K68E}	1430	13.76	0.895	8.59	619	22.55	1.299	36.48
PITPα^{E218A}	4741	45.62	6.149	59.04	1416	51.60	3.489	97.98
PITPα^{E248T}	601	5.79	1.753	16.84	884	32.22	2.817	79.11
PITPα^{E248A}	1193	11.48	1.036	9.94	2082	75.83	3.736	104.91
PITPα^{E248K}	828	7.96	0.496	4.76	1166	42.49	1.847	51.88
*PITPα^{K195C}	15854	9.01	13.02	2.05	9615	13.94	18.23	4.12

* PITPα^{K195C} was tested on a different fluorometer than the rest of the mutants, as such the

slope cannot be compared. The activity is normalized to WT PITPα tested during the same

experiment.
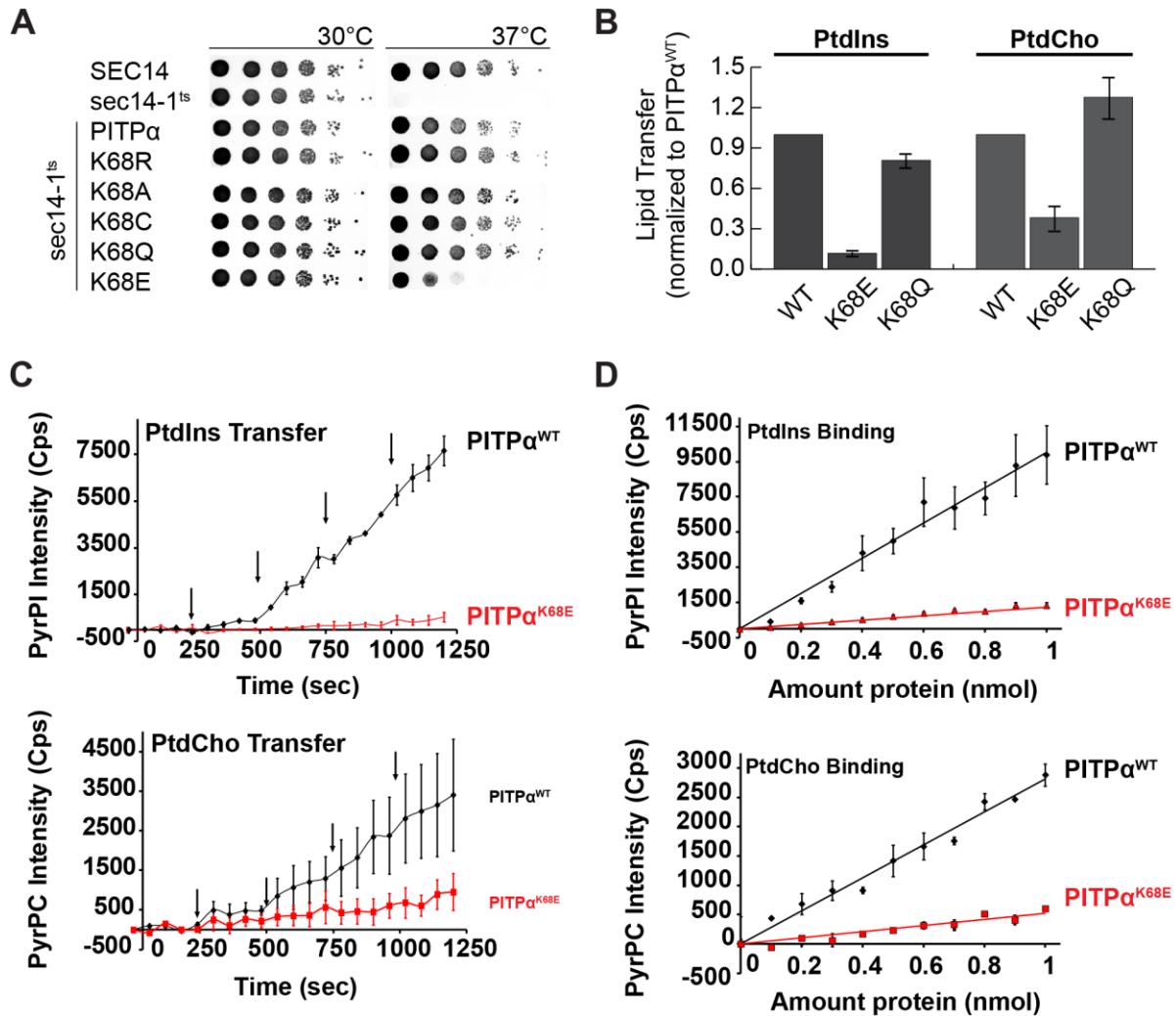
Figure 3.11. Functional consequences of missense substitutions for PITPα residue Lys$_{68}$. **(A)** Details of the phenotypic rescue assays for mutant PITPα versions carrying the indicated substitutions for Lys$_{68}$, and the organization of this Figure, are described in the legend to Figure 3.9A. **(B)** Endpoint PtdIns and PtdCho transfer assays of purified recombinant PITPα and indicated missense mutants. Experimental details and organization of the Figure are described in the legend to Figure 3.9B. Assay efficiencies and backgrounds for these experiments are summarized in Table 3.5 and Table 3.6. **(C)** Rates of PyrPtdIns and PyrPtdCho-transfer **(C)**, and efficiencies of PyrPtdIns and PyrPtdCho-binding **(D)** were

measured for the indicated PITPα^{K68E} protein. Experimental details and organization of Figures is as described in Figures 3.10C and 3.10D, respectively.

Functional analyses of Glu$_{218}$ in PtdIns-transfer and binding.

      The MD studies identify residues Thr$_{114}$ and Glu$_{218}$ as interacting specifically with PtdIns, and the Glu$_{218}$ is projected to be of particular significance given that it forms two H-bonds with PtdIns. Analyses of Thr$_{114}$ substitution mutants proved fruitless as the mutants were completely destabilized when expressed in yeast, and we were unable to recover recombinant mutant proteins from crude bacterial cytosol. In every case, the mutant proteins were quantitatively incorporated into inclusion bodies. Thus, our analyses focused on Glu$_{218}$. In the phenotypic rescue assay PITPα^{E218A}, PITPα^{E218D}, and PITPα^{E218K} scored as functional (Figure 3.11A). Both end-point and real-time PtdIns- and PtdCho-transfer de-quenching assays showed PITPα^{E218A} was not significantly compromised for either PtdIns- or PtdCho-transfer activity (Figures 3.12B, C). However, the mutant protein was defective in both PtdIns- and PtdCho-binding (Figure 3.12D).
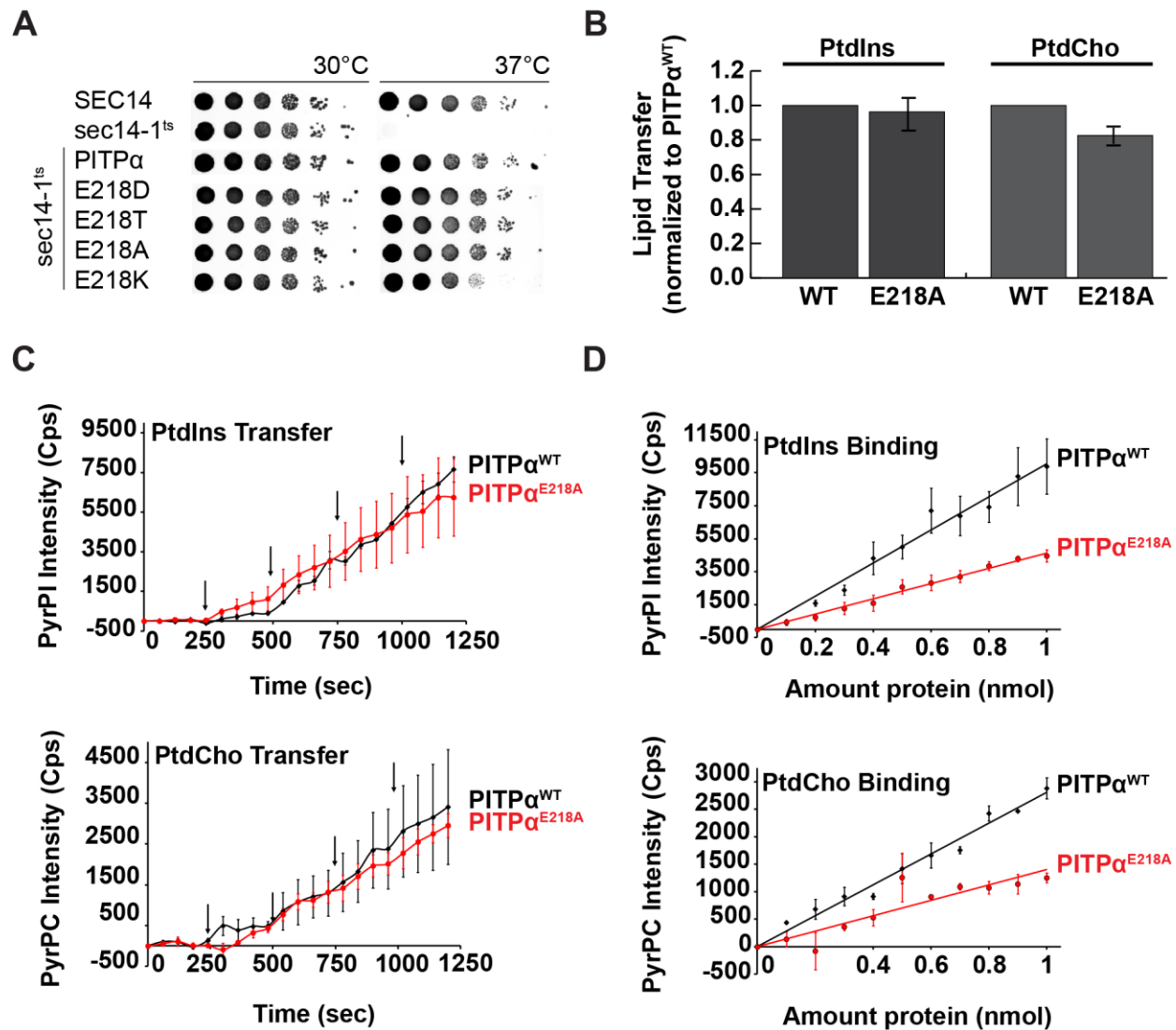
Figure 3.12. Functional consequences of missense substitutions for PITPα residue Glu$_{218}$. (A) Details of the phenotypic rescue assays for mutant PITPα versions carrying the indicated substitutions for Glu$_{218}$, and the organization of this Figure, are described in the legend to Figure 3.9A. **(B)** Endpoint PtdIns and PtdCho transfer assays of purified recombinant PITPα and indicated missense mutants. Experimental details and organization of the Figure are described in the legend to Figure 3.9B. Assay efficiencies and backgrounds for these experiments are summarized in Table 3.5 and Table 3.6. Rates of PyrPtdIns and PyrPtdCho-transfer **(C)**, and efficiencies of PyrPtdIns and PyrPtdCho-binding **(D)** were

measured for the indicated Glu_{218} substitution mutants. Experimental details and organization of Figures is as described in Figures 3.10C and 3.10D, respectively.

Glu_{248} executes specific functions in PtdIns-transfer and binding.

Although the MD simulations did not accurately predict Lys_{68} and Glu_{218} as residues that interact with PtdCho and PtdIns with absolute specificity, respectively, E_{248} was identified during the course of this study as a residue that showed strong selectivity for PtdIns-transfer and PtdIns-binding relative to PtdCho. In the phenotypic rescue assay, only PITPα^{E248D} showed activity while PITPα^{E248K}, PITPα^{E248A}, and PITPα^{E248T} all scored as strongly defective (Figure 3.13A). The defects from the rescue assay were recapitulated in end-point and real-time PtdIns-transfer assays – even though these mutant proteins retained the ability to transfer/bind PtdCho (Figures 3.13B, C). Congruent results were obtained from real-time binding assays where PITPα^{E248A} and PITPα^{E248K} showed no measurable PtdIns-binding activity in the time-course of the assay (Figure 3.13D). The binding defects were not as specific as the transfer defects. Both mutant proteins showed significant, albeit reduced, PtdCho-binding activity when compared to PITPα. Those data suggest that the binding reaction, at least as measured by the de-quenching assay, is not the rate-limiting step in PL-exchange.

It's unlikely that Glu_{248} interacts with PtdIns when the lipid is fully bound in the PITP hydrophobic cavity due to the large distance between the C-terminal helix and the bound lipid (Figure 3.14A). A simple model posits that Glu_{248} H-bonds with the PtdIns headgroup while the lipid is in transition in or out of the PITP cavity; however, the MD does not predict a hydrogen bonding role for Glu_{248} with PtdIns, or in fact, any of the C-terminal helix with either lipid. There are two alternative non-mutually exclusive explanations: (1) the contribution of placing PtdIns into the lipid binding pocket by Glu_{248} is repulsive rather than attractive, and/or (2) Glu_{248} cooperates with other residues to exert its effect on PtdIns binding. Repulsive

114

contributions are not scored by the MD, and a cumulitive effect coordinated by a network of

residues may be too complex to predict. Indeed, a polarity flip mutation of another residue on

the C-terminal helix, Met241Thr, also results in a PtdIns-specific transfer defect (Figure

3.14B). Like Glu_{248}, M_{241} also faces into the hydrophobic cavity (Figure 3.14A).
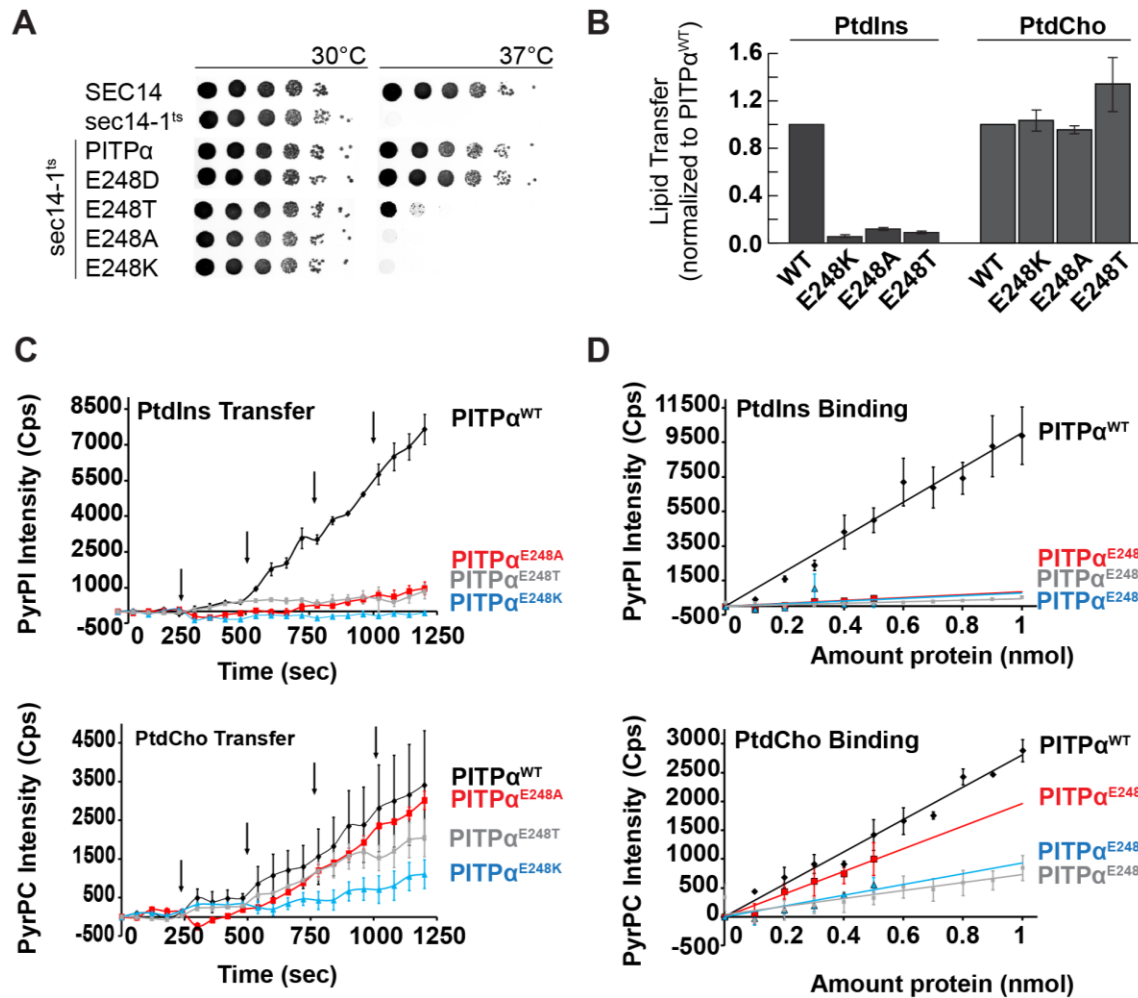
Figure 3.13. **PtdIns-selective defects associated with missense substitutions for PITPα residue Glu$_{248}$. (A)** Details of the phenotypic rescue assays for mutant PITPαs carrying the indicated substitutions for Glu$_{248}$, and the organization of this Figure, are described in the legend to Figure 3.9A. **(B)** Endpoint PtdIns and PtdCho transfer assays of purified recombinant PITPα and indicated missense mutants. Experimental details and organization of the Figure are described in the legend to Figure 3.9B. Assay efficiencies and backgrounds for these experiments are summarized in Table 3.5 and Table 3.6. Rates of PyrPtdIns and PyrPtdCho-transfer **(C)**, and efficiencies of PyrPtdIns and PyrPtdCho-binding **(D)** were measured for the indicated Glu$_{248}$ substitution mutants. Experimental details and organization of Figures are as described in Figures 3.10C and 3.10D, respectively.
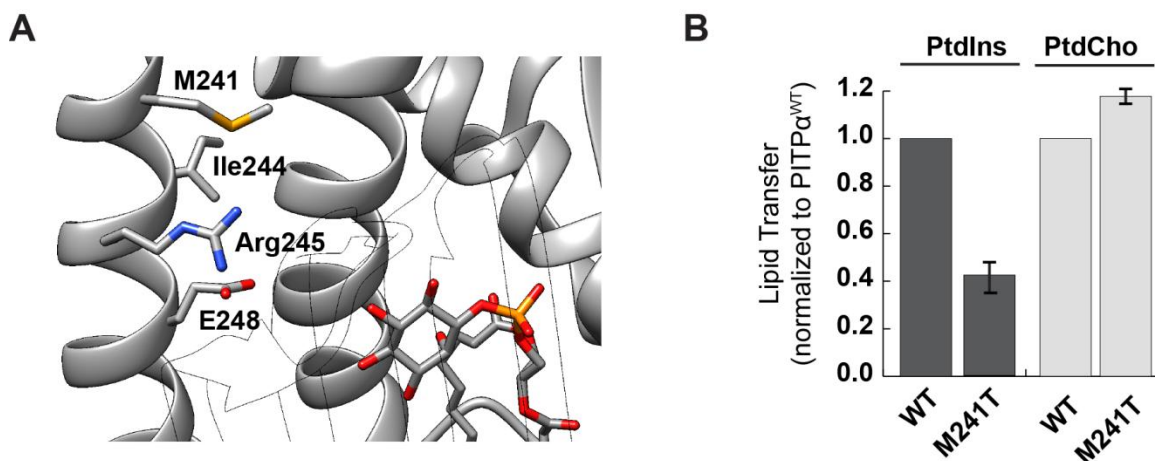
Figure 3.14. **PtdIns-selective defect associated with PITPα Met241Thr mutation. (A)** Close-up of the crystal structure of PtdIns-bound PITPα (PDB 1UW5) as viewed from behind the beta sheet floor, which has been made transparent. Four residues on the C-terminal helix are shown in molecular detail and labeled. **(B)** Endpoint PtdIns and PtdCho transfer assays of purified recombinant PITPα and PITPα^{M241T}. Experimental details and organization of the Figure are described in the legend to Figure 3.9B. Assay efficiencies and backgrounds for these experiments are summarized in Table 3.5 and Table 3.6.

Discussion

The PL-exchange cycles of PITPs are essential to their critical functions in stimulating the activities of PtdIns 4-OH kinases for biologically sufficient production of phosphoinositides (Bankaitis et al. 2010). The basic form of this cycle, however, is not at all understood for any PITP. Herein, we describe a series of unrestrained MD simulations of mammalian PITPα binding to membrane surfaces to model the ensuing protein and PL dynamics involved in the initial stages of PL-exchange by this PITP. As the MD simulations focused primarily on the results obtained using a starting structure that represents an 'open' conformer of PITPα, the data most likely model interfacial processes associated with the initial steps in the reloading of PITPα with PL after having ejected a previously bound PL molecule. Moreover, the MD supported the first calculations of the free energy landscape of PtdIns and PtdCho exchange by the mammalian PITPα. Taken together, these studies report new atomistic insights into the initial stages of PL-exchange by PITPα, describe specific H-bonding interactions between PL and protein within the PITPα hydrophobic pocket, and provide the first clues as to how PITPs lower the activation energy of PL desorption from the membrane bilayer.

PITPα binding to membrane surfaces.

Both the 'closed' and the 'open' PITPα conformers spontaneously bound membrane surfaces in equilibrium MD simulations, and the binding events were stable and occurred in the course of relatively short timescales (~200 ns). Membrane binding had three components. The first involved direct interactions of protein with lipid at the membrane surface as counted by the number of H-bonds established between protein and PL. This criterion identified two regions defined by residues Lys_{135}-Lys_{163} and Trp_{204}-Arg_{220} as membrane association domains. The second component was unique to the open PITPα conformer and involved a membrane insertion substructure (lipid exchange loop) that

118

penetrated deep into the bilayer and was defined by residues Lys_{68}-Ala_{81}. As described further below, this membrane penetration initialized the first steps of the PL-loading reaction of the PITP lipid exchange cycle.

The third component described PITPα conformational transitions that coincided with membrane binding/insertion events. One of these motions involved penetration of the lipid exchange loop (Lys_{68}-Ala_{81}) into the bilayer. The other involved increased conformational flexibility and membrane association of residues Ser_{25}-Glu_{41}. The importance of this region to PITPα biochemical and biological activity was confirmed by mutational analyses that showed Ser_{25} to be a functionally important residue where substitution with amino acids bearing large side-chains is incompatible with PITP activity. The mutational data are most consistent with Ser_{25} playing an important role in the conformational flexibility of this PITPα subdomain, and this flexibility being required for PL-exchange.

Initial steps of PL-loading into apo-PITPα

The MD predict that a consequence of lipid exchange loop insertion into a mixed bilayer is a partial loading of the open PITPα conformer with a single DOPC molecule at 700 ns in the simulation. This partial extraction of DOPC from bilayer into the PITPα hydrophobic pocket is accompanied by a shielding of the fatty acyl chains from bulk membrane by the lipid exchange loop, and a partial closure of the unit that gates accessibility to the lipid binding pocket. Functional assays indicated amino acid substitutions in this substructure (i.e. substitutions for Lys_{68}) compromise both PtdCho and PtdIns binding and exchange activities. Thus, the MD simulations provide the first mechanism for how the lipid exchange loop potentiates the early steps in the PL-exchange cycle. Indeed, it is both a reasonable and attractive proposition that the inserted lipid exchange loop is the first protein substructure to interact with a PL molecule and make it available to PITPα as a potential exchange ligand.

Under the simulation conditions employed, we failed to observe full incorporation of PL into the PITPα lipid binding pocket. Rather, the 'chosen' DOPC molecule ultimately slides back into the bilayer. Our interpretation of this behavior is that the partially loaded PL encounters a free energy well at this step, and that this barrier cannot be negotiated during 1000 ns simulation windows. Complete uptake of PL into the PITPα lipid binding pocket requires extending simulation timescales sufficiently to allow conformational transitions that direct the 'open' PITPα from a shallow breathing conformational dynamics regime to a trajectory converging onto a closed conformer. Such motions are expected to consolidate the PL-extraction process.

Free-energy landscape of PITPα interactions with lipid.

Previous electron spin resonance studies rationalized the ATP-independence of yeast Sec14-driven exchange cycle as a system where a PL molecule is engaged in a simple partitioning between two chemically similar microenvironments -- the bilayer and, in that case, the PITP PL-binding cavity (Smirnova et al. 2006; Smirnova et al. 2007). The PITPα studies reported herein extend that overly simplistic concept. Snapshots from non-biased MD simulations in non-equilibrium umbrella sampling molecular dynamics simulations provide fundamental new insights into the characteristics of PL incorporation into the PITPα lipid binding cavity. First, umbrella sampling free energy calculations demonstrated that, consistent with the established abilities of PITPα and other PITPs to execute ATP-independent lipid exchange reactions in the absence of any other co-factors, PITP dramatically lowers the free energy of PL desorption from the bilayer to within the realm of thermal fluctuation. This lowering of an otherwise very significant thermodynamic barrier is driven by specific H-bond interactions between PITPα residues and lipid headgroups. Second, free energy profiles for PtdIns and DOPC trajectories through the lipid binding pocket indicated that energy minima are shallow – thereby accounting for why PL molecules

that had partially loaded, or were otherwise steered, into the PITPα pocket were spontaneously and efficiently released into the bilayer via a reverse unloading reaction during simulation. This feature likely reflects the fact that no conformational transition of the protein from the open to the closed state was observed in the 1000 ns simulations. Such a conformational transition would dramatically impact the free energy landscapes and would also likely account for the 16-fold greater affinity of PITPα for PtdIns vs PtdCho. This experimentally determined difference in affinity was not at all apparent in our calculations that report the free energies of loading for both PLs to be similar.

PITP::PL interactions during the exchange cycle.

Umbrella sampling data of PL 'unloading' MD provided novel insights into which PITPα residues play direct roles in incorporation of PtdIns and PtdCho into the PITPα lipid binding pocket. These projected side-chain interactions were multiple and involved interactions both specific to PtdIns or PtdCho headgroups, and interactions common to both lipids. Of the set of identified specific interactions put to the functional test, the MD was not accurate in its description of headgroup-specific interactions. For example, the MD suggested a specific involvement of residue Lys_{68} in the interaction of the lipid exchange loop with DOPC, and not with PtdIns, while Glu_{218} was forecast to interact specifically with PtdIns and not PtdCho. In both cases, functional assays indicated amino acid substitutions at those respective positions affected both PtdCho and PtdIns binding and exchange activities. Nevertheless, the MD did accurately identify residues important for optimal lipid exchange activity whose functional involvement was invisible to analysis of PITPα crystal structures alone.

Superposition of the structural elements and residues identified in this study to play important roles in the PITPα PL-exchange cycle, with primary sequences of other members of the StART-like PITP family, lend further confidence in the veracity of the data. MD simulations project six residues of the PITPα lipid binding pocket interact with PtdIns

specifically (Thr$_{59}$, Lys$_{61}$, Glu$_{86}$, Asn$_{90}$, Thr$_{114}$, Glu$_{218}$) and, of those, all but Glu$_{218}$ are absolutely conserved in evolutionarily distant members of the StART-like PITP family (Figure 3.15). That one exception, Glu$_{218}$, is invariant among evolutionarily distant Class 1 StART-like PITPs. MD simulations also identified seven residues of the PITPα lipid binding pocket as engaging both PtdIns and PtdCho in H-bond interactions (Tyr$_{18}$, Gln$_{22}$, Ser$_{25}$, Tyr$_{63}$, Asn$_{101}$, Lys$_{195}$, Gln$_{217}$). Of those seven, three are absolutely invariant (Tyr$_{18}$, Asn$_{22}$, Lys$_{195}$), one is invariant with a single exception involving a conserved substitution at that position (Tyr$_{63}$), and two others are invariant from primates to flies among the Class 1 StART-like PITPs (Ser$_{25}$, Asn$_{101}$; Figure 3.10). We find this correspondence remarkable given MD simulations are agnostic to experiment and to primary sequence alignments.

Rationale for headgroup-specific involvement for Glu$_{248}$.

The power of the MD notwithstanding, the data also clearly highlight an important need for genetics-based structure-function analyses of PITPα activity. This is amply demonstrated by the fact that PITPα residue Glu$_{248}$, while not highlighted in the MD, plays an essential and specific role in PtdIns-exchange activity with no discernable involvement in PtdCho exchange. Moreover, that Glu$_{248}$ is an invariant residue amongst the StART-like PITPs (Figure 3.15), further emphasizes its essential and conserved involvement in the activities of this entire family of proteins. Given our results with PITPα, we project such involvement reflects a specific role in PtdIns-exchange by all StART-domain PITPs.

At this point we cannot distinguish whether the effect of Glu$_{248}$ mutations on PITPα PtdIns exchange activity reflect a conformational transition that occurs specifically during the PtdIns loading step, the unloading step, or at both steps. One interesting possibility is that directed motions of the Glu$_{248}$ side-chain provide a 'charge-push' that leverages the incompatability of PtdIns and Glu$_{248}$ electrostatics to propulsion of PtdIns into and/or out of the hydrophobic pocket. The observation that a mutation of another residue on the C-

terminal helix, Met$_{241}$, also exerts a PtdIns-specific defect suggests that Glu$_{248}$ cooperates with other residues on the helix toward a PtdIns-specific function, but whether that function is repulsive or attractive is unknown. Importantly, these data indicate that though PtdIns and PtdCho bind in nearly identical space in the PITP hydrophobic cavity, at some point during the transfer reaction their trajectories diverge.
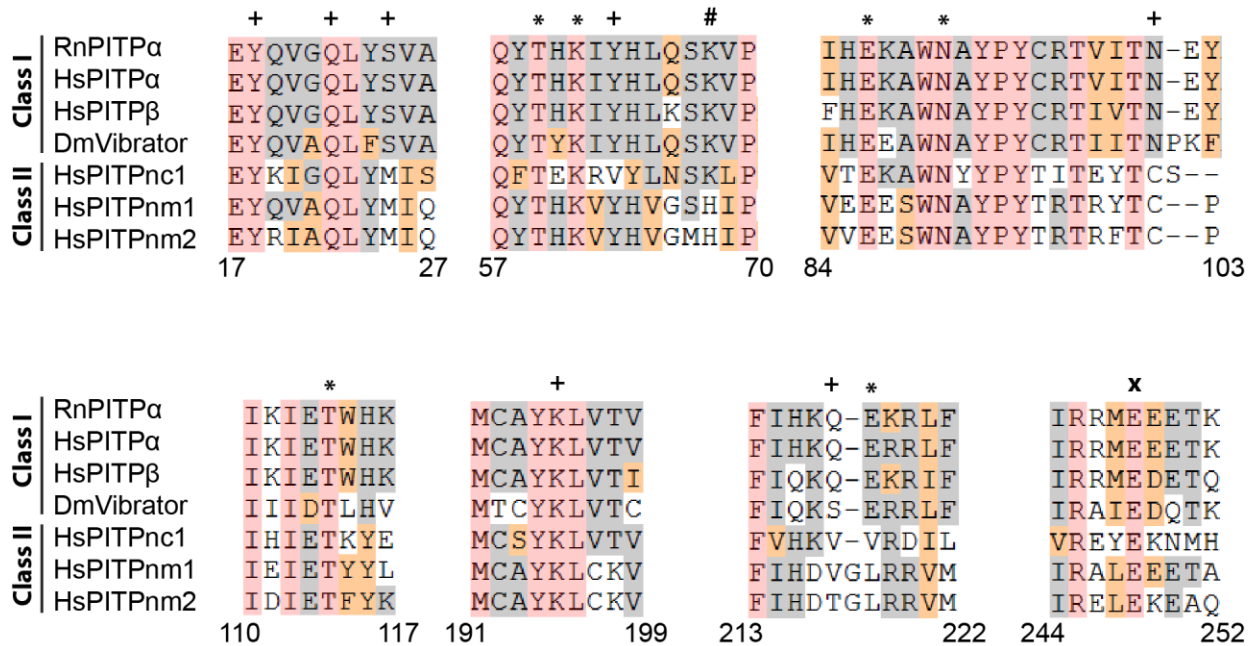
Figure 3.15. **Primary sequence alignments of selected regions of Class I and Class II StART-like PITPs.** Sequences for Class I PITP genes were extracted from the NCBI database using the following protein ascension numbers: *RnPITPNA* (NP_058927.1), *HsPITPNA* (NP_006125.1), *HsPITPNB* (NP_036531.1), Dm*Vibrator* (NP_524404). Sequences for Class II PITP genes were extracted from NCBI as follows: *HsPITPNC1* (NP_858057), *HsPITPNM1* (NP_004901.2), *HsPITPNM2* (NP_065896.1). For the multi-domain PITPs *HsPITPNM1* and *HPITPNM2*, only the PITP domain primary sequence is included in the alignment as guided by primary sequence homology to HsPITPα. Alignments were generated in VectorNTI using the

AlignX module set to default parameters. Indicated at bottom for purposes of reference are residue numbers according the RnPITPα primary sequence (initiator Met included). Color coding follows AlignX homology descriptors: identical residues (salmon), blocks of homology (grey), similar residues (orange), and nonsimilar residues (white). Residues predicted by MD to have PtdIns-specific interactions (*****), PtdCho-specific interactions (**#**), and interactions with both PtdIns and PtdCho (**+**) are indicated at top. The (**X**) at top identifies residue Glu_{248} which has PtdIns-specific interactions that were invisible to the MD.

Outstanding questions.

While the studies reported here describe the initial steps in a pathway of conformational transition from an apo-PITPα to a phospholipid-bound holo-PITPα, there remain outstanding considerations that will impact the details in important ways. First, the most productive MD involved a membrane-docked PITPα conformer. At this point, we do not precisely know how PL-unloading is spatially or temporally related to PL-loading. That is, are these concerted processes, or are these separable reactions that proceed through an apo-PITPα intermediate? While soluble probe accessibility experiments argue against the latter mode (our unpublished data), the MD data reported here do not explicitly consider concerted PL-loading/unloading exchange mechanisms. Whether the PL-loading and unloading reactions are perfectly symmetrical processes also remains to be determined, and such symmetry is unlikely if these are concerted reactions. Those open questions notwithstanding, the satisfying congruence of the MD data with the results of functional assays lend confidence that atomistic details of the PITPα PL-exchange reaction reported herein describe a reasonable approximation of the initial stages of this key biological reaction. Capitalizing on the membrane-docked apo- and holo-PITPα models described in this report as starting structures in more extended MD production runs now define promising approaches for extracting new and fundamental atomistic details of the PITP lipid-exchange cycle.

CHAPTER 4: START PITPS REGULATE SIGNALING FROM LATE SECRETORY MEMBRANES IN EUKARYOTES

Introduction

STuART PITPs were historically considered proteins of higher order eukaryotes as they are entirely absent from *S.cerevisae* and largely absent from plants (Phillips et al. 2006). With the genome sequencing of other ancient eukaryotes, such as members of Alveolata and Diplomonadi, it is now clear that START PITPs are far more ancient than previously believed. Furthermore, functional studies of *PITP* genes reveal the importance of these molecules in a range of developmental and cellular processes (Nile et al. 2010). A theme emerging from the study of Sec14 proteins is that PITPs regulate specific phosphoinositide pools, and at least in some cases do so a highly localized way, creating membrane signaling "pixels" (Schaaf et al. 2008; Bankaitis et al. 2010; Ghosh et al. 2015). In the first half of this chapter, we consider this concept in a review of START PITP signaling on secretory membranes. In the second half of the chapter, we will assess what we know about the *Toxoplasma* START PITP PIMP and its role in late secretory signaling from the dense granules.

Physiology of START PITPs

Loss of function studies of START PITPs from various eukaryotes reveal interesting roles for these proteins in development and physiology. The mammalian Class I PITPs are homologous to PITPα, and Class II PITPs are most similar to *Drosophila* RdgBα (Cockcroft and Garner 2011). An emerging theme, though not one without exception, is that when the physiology of START PITPs is queried in the context of a multi-cellular organism, often the

125

observed defects are associated with neuronal or sensory pathways. PITPα nullizygocity in mice results in spinocerebellar disease, in addition to intestinal and hepatic steatosis (Alb et al. 2003). The zebrafish PITPβ ortholog is not required for development, but knockdown of this PITP results in defective photoreceptor outer segment biogenesis and maintenance in double cone photoreceptor cells (Ile et al. 2010). The founding member of Class II PITPs, the Drosophila RdgBα (for *retinal degeneration B* mutant), is required for maintenance of photoreceptor cells in the fly retina (Harris and Stark 1977; Milligan et al. 1997). The *C.elegens* RdgBα ortholog, PITP-1 is required for chemoattraction mediated by sensory neurons (Iwata et al. 2011). Do these neuronal and sensory pathologies occur because PITPs are required to maintain the high PIP demand of these systems? Or are the defects subtler, reflecting a disorganization of signaling molecules in membranes that most require efficiency? We don't know, but the question is related to how we view PITP mechanism.

Mechanisms of START PITPs

PITPs transfer PtdIns between membranes *in vitro* in exchange for a second lipid ligand. How do we interpret this activity in cellular context? PITPs regulate specific PIP pools, and at least in some cases do so in a highly localized way, creating membrane signaling "pixels". We work within two conceptual models for PITP mechanism.

The transporter or supply model posits that the main function of PITPs is to maintain supply of specific lipids to signaling or metabolic membranes. This mechanism is often invoked in discussion of the $PtdIns(4,5)P_2$ cycle described in detail in Chapter 1 (Figure 1.2), which presents an important spatial problem (Michell 1975). Briefly, receptor signaling reactions at the plasma membrane activate PLC, which hydrolyzes $PtdIns(4,5)P_2$ to DAG and IP_3. In order to replenish these $PtdIns(4,5)P_2$ pools for future reactions, plasma membrane PtdIns 4-OH kinases must be supplied with PtdIns (Michell 1975). PtdIns is synthesized at the ER, and a mechanism must exist to transport it to the plasma membrane. PITPs are historically considered to fulfill this

role (Van Paridon et al. 1987). The opposing model, the nanoreactor or instructive regulation model, was first described for the yeast Sec14 (Schaaf et al. 2008; Ile et al. 2006). In this mechanism, the main function of a PITP is extraction of a lipid from a membrane, not transport. During extraction, the lipid becomes accessible to a PtdIns 4-OH kinase for phosphorylation. This lipid "presentation" activates the kinase. PITP-mediated instructive regulation of PtdIns kinases is discussed in more detail in Chapter 1.

The functions of START PITPs are often interpreted in the context of the supply model, though most of the available data are consistent with either mechanism. In this chapter, we will focus on the cellular functions of specific PITPs and how these can be interpreted in the context of the available functional models, and how this might contribute to the maintenance of PIP pools or their organization.

Determinants of biological specificity in START-like PITPs

With the high sequence identity between START PITPs within and between the two classes, and their common PtdIns-binding activity, what specifies the biological role of these proteins? And how would such characteristics feed into the models of PITP function? There are likely multiple factors, but we will focus on two major ones: (1) in all known cases, the PITP domain of START PITPs is on the N-terminus, and the C-termini may be diversified either by transcriptional regulation or by genetic coupling to additional domains; (2) while all PITPs bind and transfer PtdIns between membranes *in vitro*, the identities of the counter-ligand vary and contribute to cellular function. We will discuss these points in this section before reviewing how PITPs function in the late secretory pathway.

Diversity in C-termini

One of the most striking differences between PITP members is the length and composition of the C-terminus (Figure 1.5, Chapter 1). These regions are diversified either by

transcriptional regulation or by genetic coupling to other domains, and this contributes to cellular function. PITPβ is spliced into "canonical" and "alternative" splice variants that differ in their C-termini, a pattern recapitulated in the transcript processing of PITPγ: a PITPβ-like Class I PITP unique to Zebrafish (Ile et al. 2010). For these two genes, it's not clear what contribution splicing makes to regulation of the PITP. A direct role for regulation of protein function by splice variants has been shown for PITPnc1 (Garner et al. 2012). The C-terminus of PITPnc1 is spliced in two splice variants (Garner et al. 2012). This region contains a PEST (proline, glutamic acid, serine, threonine) sequence that promotes the turnover of the full-length protein. The PEST sequence is absent in the shorter splice variant of PITPnc1 (Garner et al. 2012). This is a good indication that transcriptional variants of PITPs are regulated differently. As such, future experiments must be careful to differentiate between the two isoforms.

The multi-domain Class II PITPs contain N-terminal PITP domains with ~40% homology to Class I PITPs (Chang et al. 1997; Lu et al. 1999, Fullwood et al. 1999 Garner et al. 2012). In addition, they contain several unique domains, including a hydrophobic region that associates with membranes (Elagin et al. 2000), a FFAT motif that anchors PITPnm1 to the ER (Kim et al. 2015), an LNS2 domain that binds PtdOH (Kim et al. 2013), and a DDHD domain of unknown function. The C-termini of Class II proteins also interact with the protein tyrosine kinase PYK2, a protein involved in signaling from cell surface receptors (Lev et al. 1999; Verma et al. 2015). As discussed in Chapter 2, the *Toxoplasma* PIMP links multiple domains associated with PtdIns4P signaling. Although the identity of the linked domains is novel, such a coupling strategy is commonly utilized by PITPs.

Indicative of the C-terminal domains' importance for at least some family members, the PITP domain of PITPnm1 is required for its role in Golgi trafficking, but it is not sufficient (Litvak et al. 2005). On the contrary, the PITP domain of *C.elegans* PITP-1 is both necessary and sufficient for performing the function of the full-length protein in chemosensory attraction and plasticity to extracellular cues (Iwata et al. 2011). These data suggest that the C-terminal

domains of PITPs may be important in some contexts but dispensable in others. Defects in human PITPNM3 (a homolog of PITPnm1 and PITPnm2 that lacks the entire PITP domain), result in an autosomal dominant retinal dystrophy called CORD5 wherein a cone photoreceptor dysfunction eventually leads to blindness in early adulthood (Reinis et al. 2012). This indicates that the non-PITP domains of PITPnm1 and PITPnm2 indeed have the capacity to participate in as-of-yet unidentified physiological contexts.

The very length of the multi-domain Class II PITPs may allow them to function at membrane contact sites. Indeed, such a mechanism is proposed for *Drosophila* RdgB and human PITPnm1 (Lev 2012; Yadav et al. 2015; Kim et al. 2015). A membrane-associated PITP can still fulfill the transport/supply function if it's part of a membrane contact site, and that is the mechanism postulated in these two cases. Because a key component of the nanoreactor mechanism is metabolic input that can then be translated to PtdIns presentation, multidomain PITPs are particularly suited to an instructive regulation model. We discuss the possibility of such a contact site role for *Toxoplasma* PIMP in the second half of this chapter.

Ligand Specificity and Binding

Class I PITPs use PtdCho as the counter-ligand to PtdIns. Class II PITPs are being increasingly recognized as PtdOH-transfer proteins, rather than PtdCho (Garner et al. 2012; Yadav et al. 2015; Kim et al. 2015). How does ligand specificity feed into the mechanistic models? The historical interpretation of PITPs as transporters dictates that PtdCho is simply an abundant lipid that acts as a placeholder while PITP transits back to the ER to pick up PtdIns. In this model, the cellular concentration of the counter-ligand is the critical consideration, rather than strictly the identity of the counter-ligand (Prinz 2010; Lev 2010). Why then should any PITP bind anything other than PtdCho? One explanation may be the second half of the PtdIns(4,5)P$_2$ cycle (Figure 1.2, Chapter 1). When PLC is activated by receptor stimulation, one product of PtdIns(4,5)P$_2$ hydrolysis is DAG, which is converted to PtdOH at the plasma membrane. PtdOH

is converted back to PtdIns at the ER. A PITP that binds PtdOH is conceptually suited to transport this lipid from the plasma membrane back to the ER. The nanoreactor model, on the other hand, posits that the counter-ligand is a critical regulator of PITP function and confers "metabolic sensor" status onto the PITP (Ile et al. 2006). For example, Sec14 binds PtdCho as a proxy for DAG, which allows coincidence detection for two factors critical in vesicle biogenesis, DAG and PtdIns4P (Bankaitis et al. 2010).

Though START PITPs and Sec14 PITPs share a common biochemical function, they belong to distinct structural families (Figure 4.1). The two families of PITPs have in common a globular structure with α-helices folded over a β-sheet floor (Figure 4.1A, C). Sec14 has distinct binding sites for the inositol or choline headgroup, wherein the PtdIns headgroup is exposed to solvent and the acyl chains are buried in the Sec14 cavity (Figure 4.1B, orange lipid). The kinetic trap model of Sec14 instructive regulation of PtdIns 4-OH kinase posits that slow egress of PtdCho from the Sec14 lipid binding pocket stalls PtdIns extraction from the membrane and allows PtdIns 4-OH kinase access to the headgroup (Schaaf et al. 2008; Bankaitis et al. 2010). In the START PITP structure, PtdIns and PtdCho bind in nearly identical conformations, such that the lipid headgroups are deep within the lipid-binding pocket (Figure 4.1D). If START PITPs do act in instructive regulation of PtdIns kinases, the mechanism of presentation would likely be unique compared to that of Sec14.
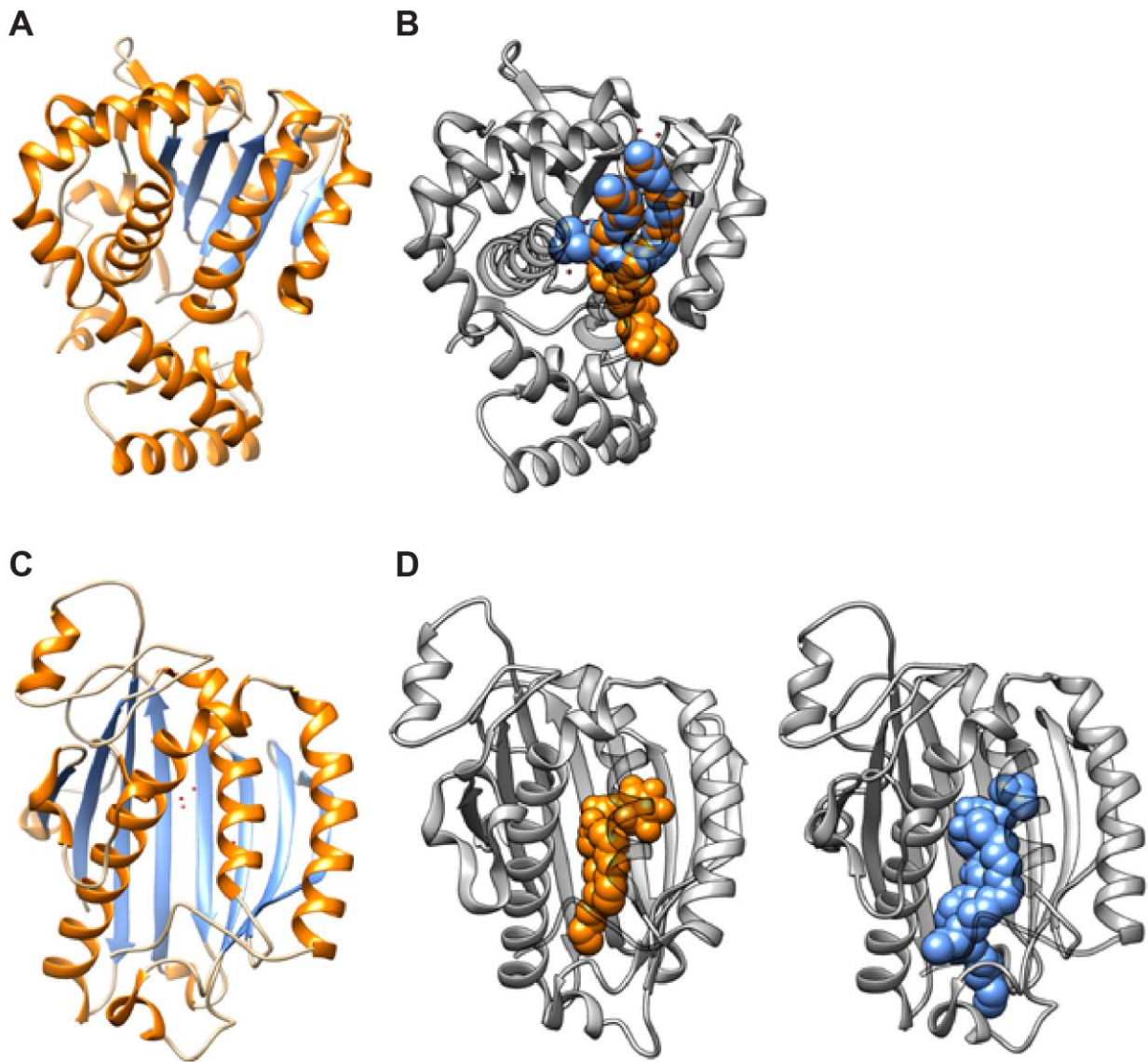
Figure 4.1. Comparison of the structures of Sec14 PITPs and START PITPs. (A, B) Crystal structures Sfh1 with (**B**) or without (**A**) bound lipids shown (PDB 3B7Z), and **(C, D)** PITPα (PDB 1T27 and 1UW5) with (**D**) or without (**C**) bound lipids shown. **(A, C)** Both structures feature a large B-sheet floor (blue) onto which the lipid binds and a-helices (orange) that define the closing mechanism. **(B, D)** PtdIns is shown in orange and PtdCho is shown in blue.

The Cellular Roles of START-Like PITPs in Membrane Signaling

PITPs as regulators of vesicular biogenesis

A number of studies have suggested roles for START PITPs in secretory trafficking. Reconstitution of vesicle budding from the *trans*-Golgi network, scission of coatomer-coated vesicles, and *cis*-to-medial intra-Golgi vesicular transport in a cell-free system are all PITP-dependent (Ohashi et al.1995; Jones et al.1998; Simon et al. 1998; Paul et al. 1998). PtdIns and PtdCho transfer activity of PITPβ is required for retrograde trafficking from the Golgi to the ER (Carvou et al. 2010). We will discuss one case of PITPs in vesicular biogenesis in particular: that of PITPnm1 as a regulator of DAG levels at the TGN.

PITPnm1 promotes membrane fission to allow vesicular biogenesis from the TGN (Litvak et al. 2005). Acute siRNA-mediated depletion of PITPnm1 in HeLa cells causes Golgi membranes to become dispersed and swollen, resulting in retention of secretory cargo in the *trans*-Golgi network and a subsequent delay of transport to the plasma membrane. Cargo retained in the TGN under the PITPnm1-deficient condition localizes to highly tubular membranes, and there is a marked decrease in intermediate carriers emerging from the Golgi.

These trafficking defects stem from a reduction of DAG pools at the TGN (Litvak et al. 2005). PITPnm1 is required for maintenance of the DAG pool used in the CDP-choline pathway for PtdCho biosynthesis, but is not involved in the sphingolipid biosynthesis pathway. The specificity for sensing the CDP-choline pathway is analogous to that of yeast Sec14, for which the PtdCho counter-ligand is derived from the CDP-choline pathway only (Bankaitis et al. 2010; Kearns et al. 1997; Ile and Schaaf 2006). PITPnm1 may be involved in such a coincidence detection mechanism for Golgi PtdIns4P and DAG, wherein in the absence of PITPnm1, Golgi membranes eliminate DAG by conversion to PtdCho to avoid initiation of vesicular biogenesis for which there is inadequate PtdIns4P co-signal. The authors excluded an effect of PITPnm1 depletion on Golgi PtdIns4P levels due to the insensitivity of a PtdIns4P reporter (the OSBP PH-domain) to PITPnm1 knockdown. Because there are multiple pools of PtdIns4P at the Golgi,

and PH domains are sensitive to these differences, analysis of a single biosensor does not exclude an effect of PITPnm1 depletion on Golgi PtdIns4P levels. Furthermore, PIP biosensors with high affinities for their substrates report only large changes in substrate concentration (Lemmon 2008). Decreases in PtdIns4P on Golgi membranes may be underestimated in these experiments.

Truncation studies show that the PITP domain of PITPnm1 is required, but not sufficient, to restore cargo trafficking from the TGN in the PITPnm1-silenced condition (Litvak et a. 2005). Though the full length PITPnm1 restores DAG pools at the TGN, the truncation mutants were not tested in this context, so it remains formally possible that the PITP domain is not responsible for maintenance of DAG pools – that, in fact, one of the other domains is responsible for this effect – and the PITP domain performs a distinct as-of-yet unidentified function that is critical to anterograde trafficking from the TGN, perhaps contribution to phosphoinositide pools (PtdIns4P or otherwise) not excluded by the OSBP-PH PtdIns4P biosensor. In such a model, PITPnm1 would be involved in instructive regulation of PtdIns4P synthesis in response to PtdOH as a proxy for DAG. This mechanism may be used to determine if TGN membranes in general are competent for trafficking, or in coincidence detection at specific sites where vesicular biogenesis machinery is accumulating.

START PITPs in non-cell autonomous physiology

Both PITPα and PITPnc1 have been found to promote secretion of specific soluble factors (Snoek et al. 1999; Kostenis 2004; Schenning et al. 2004; Bunte et al. 2006; Png et al. 2012). We will focus on PITPnc1 as example of this function. PITPNC1 is part of the miR-126 microRNA (miRNA) regulon involved in cancer cell metastasis (Guo et al. 2008; Feng et al. 2010; Png et al. 2012). Silencing of miR-126 in MDA-MB-231 human breast cancer cells promotes recruitment of endothelial cells in a non-cell autonomous fashion, and induction of angiogenesis that facilitates colonization of cancer cells in sites remote from the original tumor

(Png et al. 2012). PITPNC1 is one gene targeted for regulation by miR-126. Knockdown of

PITPNC1 from breast cancer cells decreases secretion of IGFBP2, insulin growth factor binding

protein 2, which is involved in endothelial recruitment, tumor colonization and angiogenesis

(Png et al. 2012). An extended analysis showed that PITPnc1 is involved in the secretion of

multiple factors that might contribute to metastasis, including metalloproteases and a pro-

angiogenic growth factor (Halberg et al. 2016). Liposome binding experiments identified

PITPnc1 as primarily a PtdIns4P binding protein, with negligible PtdIns and PtdOH binding

capacity, and mutation analysis argued that PtdIns4P binding occurs in the lipid binding pocket.

The proposed model posits that PITPnc1 binds PtdIns4P on Golgi membranes and, through an

unspecified mechanism that involves association with RAB1B, increases PtdIns4P levels and

promotes recruitment of GOLPH3, which tubulates Golgi membranes and promotes vesicular

biogenesis (Halberg et al. 2016). These conclusions stand in contention to previous reports that

define PtdIns and PtdOH as the primary ligands for PITPnc1 (Garner et al. 2012; Cockcroft et

al. 2016). Furthermore, it's unlikely that a phosphorylated inositol headgroup could be

accommodated by the known structures of START PITPs (Figure 4.1B). Until a Class II PITP is

crystalized, however, we can't exclude the possibility that the lipid binding pocket of PITPnc1

presents a more sterically favorable environment than that of the Class I proteins. The ability of

a PITP to directly sense PdtIns4P is reminiscent of that ability in the PIMP PH domain. It's not

clear however, how the PITPnc1 PITP domain can itself both sense and upregulate PtdIns4P

levels at the Golgi. The transporter model would postulate that PITPnc1 transfers PtdIns4P to

the Golgi from another membrane.

START PITPs in PtdIns(4,5)P$_2$ signaling

   START PITPs have been proposed to function on both sides of the PtdIns(4,5)P$_2$ cycle:

as transporters of PtdIns required to supply plasma membrane PtdIns(4,5)P$_2$ pool for PLC

substrate, and as transporters of PtdOH required to remove the downstream product of PLC

activation from the plasma membrane (Figure 1.2, Chapter 1). PITPα has been reported to function in the forward supply of PtdIns to the plasma membrane for Epidermal Growth Factor Receptor (EGFR) and for netrin receptor signaling (Kauffmann-Zeh et al. 1995; Xie et al. 2005). PITPnm1 has recently been described in the reverse cycle, where it functions at ER-plasma membrane contact sites to remove PtdOH following PLC activation by angiotensin receptor (Kim et al. 2015). We will review this case, as well as that of the worm PITP-1.

PITPnm1 has been identified as a component of ER-PM contact sites in human cells (Kim et al. 2015). The cellular system used in these experiments were HEK293T cells stably over-expressing angiotensin receptor (HEF293T-AT1 cells), in which the plasma membrane $PtdIns(4,5)P_2$ cycle was stimulated by addition of angiotensin II (AngII). Unstimulated HEK293T-AT1 cells knocked down for PITPnm1 have a lower basal level of $PtdIns(4,5)P_2$, PtdIns, and PtdIns4P, suggesting that PITPnm1 plays a role in maintaining signaling lipid pools at basal conditions (Kim et al. 2015). When cells are stimulated, PITPnm1 is required for sustained signaling through PLC as measured by intracellular calcium as well as FRET-based biosensors of DAG and PtdOH. Depletion of PITPnm1 with siRNA leads to the accumulation of PtdOH, and these cells are unable to convert PtdOH to CDP-DAG and PtdIns.

At steady-state, PITPnm1 localizes to the cytoplasm and the ER. Following stimulation of cells with AngII, PITPnm1 translocated to ER-plasma membrane contact sites, as reported by the contact site marker STIM1. The C-terminal regions of PITPnm1 are important for plasma membrane association, while the PITP domain is inhibitory (Kim et al. 2016). Considering that the LNS2 domain of PITPnm1 binds PtdOH (Kim et al. 2013), it's possible that this domain mediates the plasma membrane interaction of full length PITPnm1 following PLC activation in these cells. This does not preclude the model wherein the PtdOH-transfer activity of the PITPnm1 PITP domain is responsible for propagation of the $PtdIns(4,5)P_2$ cycle.

135

PITP-1, a protein orthologous to Class II START-like PITPs, was identified in a genetic screen for *C. elegans* mutants that are defective in plasticity at the ASER gustatory neuron (Iwata et al. 2011). ASER is a sensory neuron responsible for sensing salt under attraction and avoidance conditions. *C. elegans* chemotaxis is dependent on prior experience, e.g. worms normally exhibit attractive behavior to NaCl but convert to avoidance behavior by prior-exposure to NaCl in a starvation environment (Saeki et al. 2001). This conditioning is reversible and dependent on two opposing phosphoinositide signaling cascades: (1) DAG/PKC signaling for attractive cues, such that high DAG levels are associated with attraction and low levels with avoidance, and (2) PtdIns(3,4,5)P_3/PI3K signaling for plasticity and repulsive chemotaxis. Genetic or pharmacological activation of DAG signaling pathways results in constitutive attraction to salt, and mutations of the PI3K pathway eliminate plasticity (Adachi et al. 2010; Tomioka et al. 2006).

The *PITP-1* mutant identified in this screen, called pitp-1(pe1209), exhibits overall reduced attraction to NaCl and ablated plasticity in response to starvation conditioning (Iwata et al. 2011). PITP-1 localizes to RAB-3 positive synaptic vesicles in the axon of presynaptic regions in ASER, and is also localized presynaptically in AIB interneurons. Unlike with the *rdgB* mutant in Drosophila, which results in light-induced degeneration of photoreceptor cells, *pitp-1* mutations in worms did not result in degeneration of ASER when exposed to stimulatory cues (Harris and Stark 1977; Iwata et al. 2011). The PITP-1 PITP domain was necessary and sufficient to rescue the chemoattraction defects. Whether PITP-1 is capable of PtdIns transfer has not been tested experimentally, as such it is formally possible that PITP-1 modulates chemotactic signaling though some other mechanism.

Mutations in DAG kinase suppress attraction defects in pitp-1(pe1209) worms but not plasticity defects (Iwata et al. 2011), suggesting that PITP-1 mediates the interface between two separate signaling pathways that determine attractive or repulsive responses to a specific cue: (1) a DAG-dependent pathway, possibly due to regulation of PtdIns(4,5)P_2 pools, and (2) a

136

pathway insensitive to DAG pools (at least those subject to regulation by DAG kinase), possibly through PtdIns(3,4,5)P$_3$ signals that mediate starvation responses in worms. These data suggest conservation of the ability of RdgBs to promote DAG signaling. Though the data were interpreted from the perspective that the role of PITP-1 is to provide PtdIns substrate from the ER to the synaptic membrane during signaling reactions, we suggest that this work fits more closely with the nanoreactor model. PITP-1, perhaps START-like PITPs in general, may shift phosphoinositide signaling between opposing pools of phosphoinositide-modifying enzymes that compete for substrate, such as between PLC and PI3K. Such a mechanism requires PITP-1 to choose a specific phosphoinositide pool to activate through direct interface with PI4K, thereby activating distinct membrane pixels (Figure 4.2).

Summary

The functions of START PITPs on the cellular and multicellular levels are being elucidated with increasing interest. Often these roles are interpreted in light of the supply model of PITP function, though none of the data distinguish between this mechanism and that postulated by the nanoreactor model. There are several key questions that will provide insight. First, further molecular dynamics simulations that build on the initial steps of extraction we've described in Chapter 3 will address whether the START PITP transfer process is conducive to instructive regulation, i.e., is there a spatial and temporal chance for a kinase to interact with the PtdIns headgroup as it is being extracted from the membrane? Secondly, can we demonstrate a physical interaction between a PITP and a kinase? The lack of such an interaction does not exclude instructive regulation, but its presence argues strongly against a supply model. Finally, can we distinguish contributions of PITPs to specific PIP pools? This is a necessary prediction of instructive regulation.
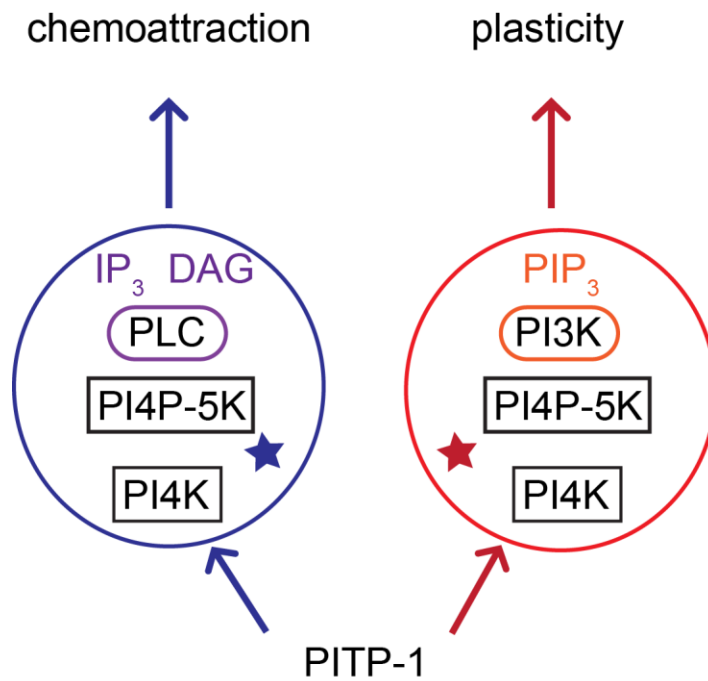
Figure 4.2. Model of how PITP-1 might specify PIP pixels in worms. Distinct membrane pixels are depicted in blue or red. Both include PtdIns 4-OH kinase and PtdIns4P 5-OH kinase, but they are distinguished by the presence of either PLC or PtdIns(4,5)P_2 3-OH kinase (PI3K). PITP-I chooses which PtdIns 4-OH kinase to stimulate by associating with a specific effector protein (blue or red star). The effect is to activate the entire pixel, which results in production of IP$_3$ and DAG (PLC activation, blue) or of PtdIns(3,4,5)P_3 (PIP$_3$) (PI3K activation, red), resulting in distinct neuronal program: chemoattraction or plasticity, respectively.

Cellular Role of PIMP in *Toxoplasma*

The linkage of PITP and OSBP modules in PIMP, and the ability of the full length protein to recognize, and associate with, distinct PtdIns4P pools on specific secretory membranes, suggests that PIMP may modulate these pools to affect trafficking of dense granules. Is this really the case? What role does PIMP play in the *Toxoplasma* secretory pathway, and how does that contribute to parasite biology? These are outstanding questions we are currently addressing experimentally. In the following section, we discuss our insights so far.

Regulation of PIMP signaling by coupling of the PITP and OSBP domains

There are multiple avenues through which PIMP might receive cellular information and integrate it into a PIP signaling circuit. As discussed in Chapter 2, the presence of HT/PEXEL sequences N-terminal to the OSBP domain suggest that the linkage between the PITP and OSBP domains may itself be subject to regulation. Of the Apicomplexa with reliably sequenced genomes, *Toxoplasma*, *Hammondia, Neospora* and *Eimeria PIMP* orthologs encode an ORF where the PITP domain is coupled to an OSBP domain. In *Plasmodium* and *Babesia* it is not (Figure 4.3). All three organisms belong to the Class Conoidasida, while *Plasmodium* and *Babesia* belong to the Class Aconoidasida. The key distinction is the ability of these parasites to form spores: all three members of the Conoidasida belong to the Coccidia subclass, which form spores, while *Plasmodium* and *Babesia* are vector-borne parasites (Lau 2009). It's possible that PIMP mediates a biological process related to the specific differentiation or infection cycle of these parasites, and that the coupling of the PITP and OSBP domains is an important component of this regulation. Furthermore, this pattern correlates to that seen with the unique insertion loops found in the PIMP PITP domain and PITP domains of PIMP orthologs in other Coccidia.

The coupling and de-coupling of antagonistic domains in PIMP and its orthologs is reminiscent of the transcriptional regulation of a *Lotus* Sec14 homology gene. LjPLP-IV is the

Lotus ortholog of *Arabidopsis* AtSfh1 (Vincent et al. 2005; Ghosh et al. 2015). In plants, Sec14-domain containing proteins are coupled to nodulin domains. Nodulins are expressed in leguminous plants during a developmental program that establishes a symbiotic relationship with N_2-fixing rhizobia bacteria in the plant root hairs (Long 2001; Brewin 2002; Desbrosses et al. 2011; Suzaki et al. 2014). In *Arabidopsis*, the Sec14-homology PITP, AtSfh1, controls polarized membrane morphogenesis in the context of root hair development by organizing PtdIns(4,5)P_2 patterns (Vincent et al. 2005; Ghosh et al. 2015). AtSfh1 is expressed in root hairs, and localizes most strongly to the root hair tip as well as discrete plasma membrane domains (Vincent et al. 2005). Genetic ablation of AtSfh1 results in disorganization of root hair PIP polarity that disrupts the cytoskeleton, vesicle trafficking, and calcium responses (Vincent et al. 2005).

AtSfh1 has an N-terminal PITP domain and a C-terminal nodulin domain (Vincent et al. 2005). The PITP domain supports synthesis of PtdIns4P. The nodulin domain, when expressed by itself, is a potent PtdIns(4,5)P_2 sink (Vincent et al. 2005; Ghosh et al. 2015). Nodulin domain binding to PtdIns(4,5)P_2 is required for the biological activity of AtSfh1 in the context of the full length protein (Ghosh et al. 2015). Thus, AtSfh1 can promote PIP synthesis via its PITP domain and then use the nodulin domain to arrange the PIP pools into relevant foci. Together with specific effector proteins, this process generates a signaling pixel that can polarize the root hair at specific sites of the plasma membrane and initiate membrane morphogenesis (Ghosh et al. 2015).

During nodulation, the cell polarity required for root hair development is turned off in favor of creating a nodule in which symbiotic bacteria can fix nitrogen. In this context, the transcription of the Sec14 domain of AtSfh1 is potently blocked, whereas the nodulin domain continues to be made (Gage 2004; Kapranov et al. 2001). In this case the nodulin domain would act as a PtdIns(4,5)P_2 sink to depolarize the root hair (Ghosh et al. 2015). This regulated coupling of antagonistic domains is a good example of how a multidomain PITP can regulate

140

PIP-based membrane pixels or specific developmental needs. It's possible that decoupling of

the PITP and OSBP domains in PIMP differentially organizes the dense granule PtdIns4P pools

during specific points of the *Toxoplasma* life cycle to regulate secretion of effector proteins.
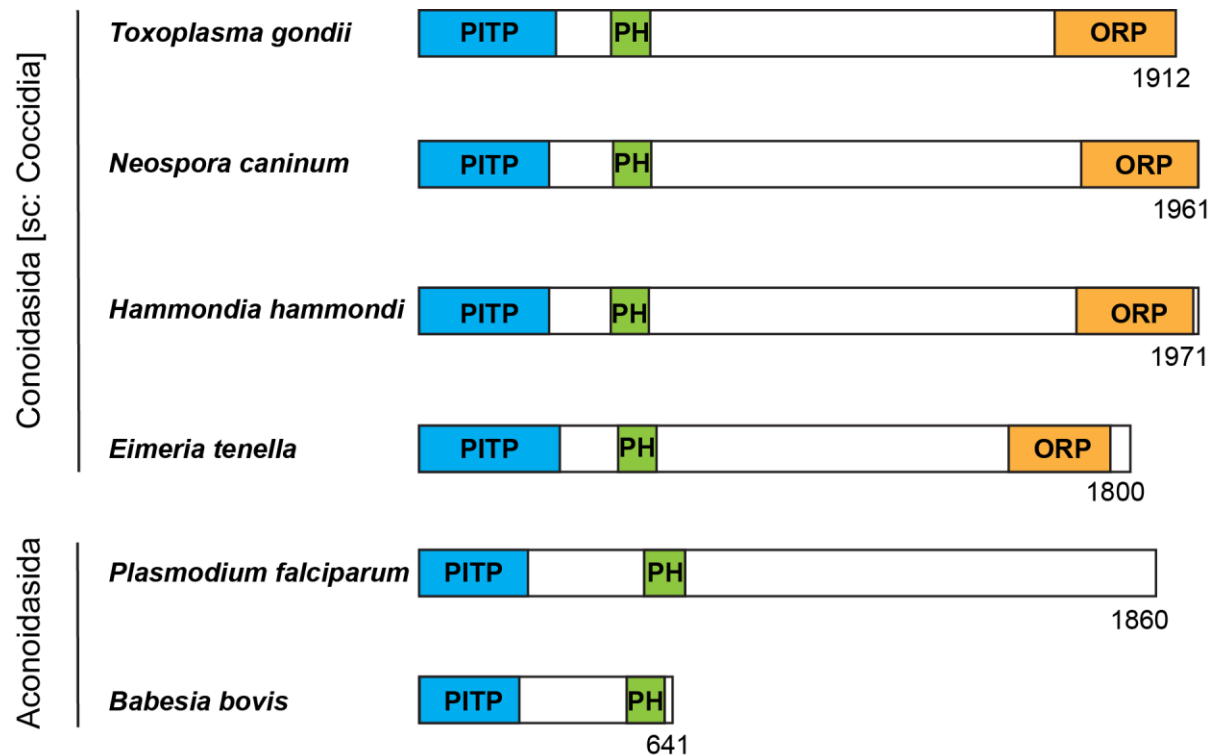
Figure 4.3. Domain structure of PIMP orthologs among Apicomplexa. The proteins are grouped according to phylogenetic Class: Conoidasdia or Aconoidasida. The protein denoted as *Toxoplama gondii* is PIMP, and the others were derived from BLAST homology searches (http://www.ncbi.nlm.nih.gov/BLAST) against full length PIMP. The sequences used are as follows: *Neospora caninum* (XP_003881140.1); *Hammondia hammondi* (XP_008889127.1); *Eimeria tenella* (CDJ42839.1); *Plasmodium falciparum* (XP_001350223.2); *Babesia bovis* (XP_001609056.1). Identification of domains as PITP (blue), PH (green), or ORP (orange) was derived directly from NCBI annotations.

PIMP at the membrane interface

Dense granules must interact with at least one other membrane, the plasma membrane, in order to affect exocytosis. Dense granule secretion is complicated by the fact that the cytoplasmic leaflet of the Apicomplexan plasma membrane is nearly covered by a distinct membrane-cytoskeleton scaffold called the inner membrane complex (IMC). It's likely that exocytosis of dense granules occurs in breaks in the IMC called micropores, though the mechanics of targeting and membrane-dense granule interaction are not well understood (Joiner and Roos 2002; Mercier et al. 2005). What is the biochemical composition of the plasma membrane adjacent to a micropore? Is the entire plasma membrane competent for dense granule exocytosis, or only the micropore-adjacent plasma membrane? These questions raise the possibility of highly localized membrane signaling suited to pixel-type regulation.

It's possible that PIMP functions at such sites, wherein the PITP domain samples one membrane and the OSBP another. Hydrophobicity prediction software scored four potential transmembrane helices in the center of the full length protein (data not shown, Figure 2.1). We have no evidence that PIMP is an integral membrane protein, and these hydrophobic regions may represent the interior of the folded full-length PIMP or of an as-of-yet unidentified domain. Nonetheless, it's possible that PIMP domains integrate signals from membranes other than just the dense granules.

Genetic analysis of PIMP

In order to understand the role of PIMP in *Toxoplsama* biology, we have attempted several loss-of-function studies. *Toxoplasma* have a limited siRNA processing pathway that has some demonstrated functionality but cannot be reliably exploited to silence endogenous transcripts (Kolev et al. 2011). Direct gene editing approaches are the primary strategy for loss of function studies in *Toxoplasma.* Though wild-type *Toxoplasma* normally repair DNA damage through Non-Homologous End Joining (NHEJ) pathways, these cells can be engineered to favor

homologous recombination (HR) by deletion of the *ku80* gene involved in NHEJ (Fox et al. 2009). Parasites replicating as tachyzoites in tissue culture are haploid, so knock-out of a gene requires only a single homologous recombination event, and this is efficient for non-essential genes (Fox et al. 2009). We attempted to replace a portion of the *PIMP* ORF with a dihydrofolate reductase (DHFR) cassette (confers resistance to pyrimethamine) by homologous recombination, but we could not recover resistant parasites. Technical explanations include the possibility that our construct design or the region of the genome that encodes *PIMP* are not optimal for homologous recombination.

CRISPR associated protein 9 (Cas9) is a DNA endonuclease targeted to a specific site of eukaryotic genomes by a guide RNA sequence. Double-stranded DNA cleavage by Cas9 edits the genome, and this technique has been successfully adapted to *Toxoplasma* (Shen et al. 2014; Sidik et al. 2014). This strategy does not depend on HR (Shen et al. 2014). We designed guide RNA constructs against the *PIMP* exon 1 and exon 5. Though both of these target the region coding for the PITP domain, the editing event is predicted to disrupt the entire ORF. We co-transfected these with Cas9 and a linear DHFR cassette amplicon. In both cases, all resistant clones were modified at a non-specific site.

One possible explanation for the failures of these approaches is that *PIMP* is an essential gene, or its presence confers a significant competitive advantage to parasites growing *in vitro*. To this end, we have modified a promoter insertion cassette for conditional transcription of the *PIMP* gene. This cassette includes the *Toxoplasma SAG* gene promoter under the control of a TET-repressible element, the DHFR gene for clonal selection. These are flanked by homologous regions to the *PIMP* 5'UTR and exon 1 to appropriately orient the insertion cassette. We have generated guide RNA to target Cas9 to the *PIMP* promoter to facilitate gene editing and promoter replacement. We anticipate that this approach will allow us to test the functional contribution of PIMP to dense granule trafficking.

PIMP loss-of-function studies

We will assay the effect of PIMP knockdown on PtdIns4P pools in *Toxoplasma* as well as on dense granule structure and function. One strategy will be to query PH^{FAPP1} and SidM-P4M localization in the PIMP knockdown condition. A problem with the biosensors in such an experiment is that their high affinity for PtdIns4P may mask moderate deficits of PIP pools in the PIMP knockdown condition (Lemmon 2008). As such, it's fortunate that PH^{PIMP} is fairly sensitive to PtdIns4P derangements (Figure 2.5. Chapter 2), so we can use this domain itself as a PtdIns4P sensor. We can assume that the threshold of PtdIns4P that PH^{PIMP} senses is functionally relevant to the one we predict PIMP maintains, though we would not be able to resolve whether PH^{PIMP} localization defects stem from a PtdIns4P or PtdIns(4,5)P$_2$ deficit. Dense granules have not been isolated with high purity, so a biochemical analysis of PIPs on these membranes is not ideal.

We might expect PIMP-deficient parasites to phenocopy defects associated with TgArf1 dominant negative expression (discussed in Chapter 2), namely inefficient loading of proteins into dense granules, and subsequent defects in dense granule exocytosis (Liendo et al. 2001). Significant defects in dense granule secretion would be manifested by derangements in the vacuole in which the parasites reside during intracellular replication. We do not expect defects in infection of, or egress from, host cells, as these processes are mostly mediated by microneme and rhopty secretion pathways (Mercier et al. 2005). It's possible that cellular defects may be masked in the relatively non-competitive *in vitro* environment in which these parasites are cultured. It will be productive to test whether PIMP knockdown affects the efficiency of *Toxoplasma* to infect rodents.

Our inability to generate a full knockout of the *PIMP* gene suggests it may be essential. The absence of the OSBP domain from PIMP orthologs among the Aconoidasida, however, implies that the coupling of these domains cannot be necessary for basic cellular functions. It's possible that the PITP domain of these proteins is essential, but that the OSBP domain is not.

The PIMP conditional expression system will allow us to test this idea, to assay the general function of the PIMP OSBP domain, and to query the concept that the PITP and OSBP domains are antagonistic.

Summary

Our identification of PtdIns4P pools on distinct late secretory membranes in *Toxoplasma* contributes to the understanding of signaling events that regulate secretion of Apicomplexan effector proteins during the parasite infection cycle. As yeast PtdIns4P signaling and TGN/endosomal secretion can be potently and specifically interrupted by targeting Sec14 (Nile et al. 2014; Tripathi et al. 2014), our identification of a cognate signaling system adapted to the unique secretory requirements of *Toxoplasma* opens novel avenues of therapy for parasitic infections. Dense granules are specialized organelles found only in Apicomplexa; as such, PITPs that regulate dense granule secretory signaling are promising targets of drug and immune intervention.

REFERENCES

ADACHI, T., KUNITOMO, H., TOMIOKA, M., OHNO, H., OKOCHI, Y., MORI, I. & IINO, Y. 2010. Reversal of salt preference is directed by the insulin/PI3K and Gq/PKC signaling in Caenorhabditis elegans. Genetics, 186, 1309-19.

AITKEN, J. F., VAN HEUSDEN, G. P., TEMKIN, M. & DOWHAN, W. 1990. The gene encoding the phosphatidylinositol transfer protein is essential for cell growth. J Biol Chem, 265, 4711-7.

ALB, J. G., JR., CORTESE, J. D., PHILLIPS, S. E., ALBIN, R. L., NAGY, T. R., HAMILTON, B. A. & BANKAITIS, V. A. 2003. Mice lacking phosphatidylinositol transfer protein-alpha exhibit spinocerebellar degeneration, intestinal and hepatic steatosis, and hypoglycemia. J Biol Chem, 278, 33501-18.

ALB, J. G., JR., GEDVILAITE, A., CARTEE, R. T., SKINNER, H. B. & BANKAITIS, V. A. 1995. Mutant rat phosphatidylinositol/phosphatidylcholine transfer proteins specifically defective in phosphatidylinositol transfer: implications for the regulation of phospholipid transfer activity. Proc Natl Acad Sci U S A, 92, 8826-30.

ALB, J. G., JR., PHILLIPS, S. E., ROSTAND, K., CUI, X., PINXTEREN, J., COTLIN, L., MANNING, T., GUO, S., YORK, J. D., SONTHEIMER, H., COLLAWN, J. F. & BANKAITIS, V. A. 2002. Genetic ablation of phosphatidylinositol transfer protein function in murine embryonic stem cells. Mol Biol Cell, 13, 739-54.

ALB, J. G., JR., PHILLIPS, S. E., WILFLEY, L. R., PHILPOT, B. D. & BANKAITIS, V. A. 2007. The pathologies associated with functional titration of phosphatidylinositol transfer protein alpha activity in mice. J Lipid Res, 48, 1857-72.

ALCAZAR-ROMAN, A. R., TRAN, E. J., GUO, S. & WENTE, S. R. 2006. Inositol hexakisphosphate and Gle1 activate the DEAD-box protein Dbp5 for nuclear mRNA export. Nat Cell Biol, 8, 711-6.

BAIRD, D., STEFAN, C., AUDHYA, A., WEYS, S. & EMR, S. D. 2008. Assembly of the PtdIns 4-kinase Stt4 complex at the plasma membrane requires Ypp1 and Efr3. J Cell Biol, 183, 1061-74.

BALLA, T. 2013. Phosphoinositides: tiny lipids with giant impact on cell regulation. Physiol Rev, 93, 1019-137.

BANKAITIS, V. A., AITKEN, J. R., CLEVES, A. E. & DOWHAN, W. 1990. An essential role for a phospholipid transfer protein in yeast Golgi function. Nature, 347, 561-2.

BANKAITIS, V. A., MALEHORN, D. E., EMR, S. D. & GREENE, R. 1989. The Saccharomyces cerevisiae SEC14 gene encodes a cytosolic factor that is required for transport of secretory proteins from the yeast Golgi complex. J Cell Biol, 108, 1271-81.

BANKAITIS, V. A., MOUSLEY, C. J. & SCHAAF, G. 2010. The Sec14 superfamily and mechanisms for crosstalk between lipid metabolism and lipid signaling. Trends Biochem Sci, 35, 150-60.

BERRIDGE, M. J. & IRVINE, R. F. 1984. Inositol trisphosphate, a novel second messenger in cellular signal transduction. Nature, 312, 315-21.

BHATTACHARJEE, S., VAN OOIJ, C., BALU, B., ADAMS, J. H. & HALDAR, K. 2008. Maurer's clefts of Plasmodium falciparum are secretory organelles that concentrate virulence protein reporters for delivery to the host erythrocyte. Blood, 111, 2418-26.

BOOTHROYD, J. C. & GRIGG, M. E. 2002. Population biology of Toxoplasma gondii and its relevance to human infection: do different strains cause different disease? Curr Opin Microbiol, 5, 438-42.

BREWIN, N. J. 2002. Pods and Nods: a new look at symbiotic nitrogen fixing bacteria. Biologist (London), 49, 113-7.

BUSSI, G., DONADIO, D. & PARRINELLO, M. 2007. Canonical sampling through velocity rescaling. J Chem Phys, 126, 014101.

CARLISLE, F. A., PEARSON, S., STEEL, K. P. & LEWIS, M. A. 2013. Pitpnm1 is expressed in hair cells during development but is not required for hearing. Neuroscience, 248C, 620-625.

CARVOU, N., HOLIC, R., LI, M., FUTTER, C., SKIPPEN, A. & COCKCROFT, S. 2010. Phosphatidylinositol- and phosphatidylcholine-transfer activity of PITPbeta is essential for COPI-mediated retrograde transport from the Golgi to the endoplasmic reticulum. J Cell Sci, 123, 1262-73.

CHARRON, A. J. & SIBLEY, L. D. 2002. Host cells: mobilizable lipid resources for the intracellular parasite Toxoplasma gondii. J Cell Sci, 115, 3049-59.

CLEVES, A., MCGEE, T. & BANKAITIS, V. 1991. Phospholipid transfer proteins: a biological debut. Trends Cell Biol, 1, 30-4.

CLEVES, A. E., MCGEE, T. P., WHITTERS, E. A., CHAMPION, K. M., AITKEN, J. R., DOWHAN, W., GOEBL, M. & BANKAITIS, V. A. 1991. Mutations in the CDP-choline pathway for phospholipid biosynthesis bypass the requirement for an essential phospholipid transfer protein. Cell, 64, 789-800.

CLEVES, A. E., NOVICK, P. J. & BANKAITIS, V. A. 1989. Mutations in the SAC1 gene suppress defects in yeast Golgi and yeast actin function. J Cell Biol, 109, 2939-50.

COCKCROFT, S. 2007. Special issue: Lipid transporters in cell biology. BBA Mol Cell Biol, 1771, 641 - 643.

COCKCROFT, S. & CARVOU, N. 2007. Biochemical and biological functions of class I phosphatidylinositol transfer proteins. Biochim Biophys Acta, 1771, 677-91.

COCKCROFT, S. & GARNER, K. 2011. Function of the phosphatidylinositol transfer protein gene family: is phosphatidylinositol transfer the mechanism of action? Crit Rev Biochem Mol Biol, 46, 89-117.

COCKCROFT, S., GARNER, K., YADAV, S., GOMEZ-ESPINOZA, E. & RAGHU, P. 2016. RdgBalpha reciprocally transfers PA and PI at ER-PM contact sites to maintain PI(4,5)P2 homoeostasis during phospholipase C signalling in Drosophila photoreceptors. Biochem Soc Trans, 44, 286-92.

COPPENS, I., SINAI, A. P. & JOINER, K. A. 2000. Toxoplasma gondii exploits host low-density lipoprotein receptor-mediated endocytosis for cholesterol acquisition. J Cell Biol, 149, 167-80.

CUNNINGHAM, E., TAN, S. K., SWIGART, P., HSUAN, J., BANKAITIS, V. & COCKCROFT, S. 1996. The yeast and mammalian isoforms of phosphatidylinositol transfer protein can all restore phospholipase C-mediated inositol lipid signaling in cytosol-depleted RBL-2H3 and HL-60 cells. Proc Natl Acad Sci, 93, 6589-6593.

CZECH, M. P. 2000. PIP2 and PIP3: complex roles at the cell surface. Cell, 100, 603-6.

DAHER, W., MORLON-GUYOT, J., SHEINER, L., LENTINI, G., BERRY, L., TAWK, L., DUBREMETZ, J. F., WENGELNIK, K., STRIEPEN, B. & LEBRUN, M. 2015. Lipid kinases are essential for apicoplast homeostasis in Toxoplasma gondii. Cell Microbiol, 17, 559-78.

DE SAINT-JEAN, M., DELFOSSE, V., DOUGUET, D., CHICANNE, G., PAYRASTRE, B., BOURGUET, W., ANTONNY, B. & DRIN, G. 2011. Osh4p exchanges sterols for phosphatidylinositol 4-phosphate between lipid bilayers. J Cell Biol, 195, 965-78.

DESBROSSES, G. J. & STOUGAARD, J. 2011. Root nodulation: a paradigm for how plant-microbe symbiosis influences host developmental pathways. Cell Host Microbe, 10, 348-58.

DESFOUGERES, T., FERREIRA, T., BERGES, T. & REGNACQ, M. 2008. SFH2 regulates fatty acid synthase activity in the yeast Saccharomyces cerevisiae and is critical to prevent saturated fatty acid accumulation in response to haem and oleic acid depletion. Biochem J, 409, 299-309.

DI PAOLO, G. & DE CAMILLI, P. 2006. Phosphoinositides in cell regulation and membrane dynamics. Nature, 443, 651-7.

DIPPOLD, H. C., NG, M. M., FARBER-KATZ, S. E., LEE, S. K., KERR, M. L., PETERMAN, M. C., SIM, R., WIHARTO, P. A., GALBRAITH, K. A., MADHAVARAPU, S., FUCHS, G. J., MEERLOO, T., FARQUHAR, M. G., ZHOU, H. & FIELD, S. J. 2009. GOLPH3 bridges phosphatidylinositol-4- phosphate and actomyosin to stretch and shape the Golgi to promote budding. Cell, 139, 337-51.

DONAHOE, S. L., SLAPETA, J., KNOWLES, G., OBENDORF, D., PECK, S. & PHALEN, D. N. 2015. Clinical and pathological features of toxoplasmosis in free-ranging common wombats (Vombatus ursinus) with multilocus genotyping of Toxoplasma gondii type II-like strains. Parasitol Int, 64, 148-53.

DOWLER, S., CURRIE, R. A., CAMPBELL, D. G., DEAK, M., KULAR, G., DOWNES, C. P. & ALESSI, D. R. 2000. Identification of pleckstrin-homology-domain-containing proteins with novel phosphoinositide-binding specificities. Biochem J, 351, 19-31.

EL HAJJ, H., LEBRUN, M., FOURMAUX, M. N., VIAL, H. & DUBREMETZ, J. F. 2007. Inverted topology of the Toxoplasma gondii ROP5 rhoptry protein provides new insights into the association of the ROP2 protein family with the parasitophorous vacuole membrane. Cell Microbiol, 9, 54-64.

ESSMANN, U., PERERA, L., BERKOWITZ, M. L., DARDEN, T., LEE, H. & PEDERSEN, L. G. 1995. A smooth particle mesh Ewald method. J Chem Phys, 103, 8577-8593.

FAIRN, G. D., CURWIN, A. J., STEFAN, C. J. & MCMASTER, C. R. 2007. The oxysterol binding protein Kes1p regulates Golgi apparatus phosphatidylinositol-4-phosphate function. Proc Natl Acad Sci U S A, 104, 15352-7.

FANG, M., KEARNS, B. G., GEDVILAITE, A., KAGIWADA, S., KEARNS, M., FUNG, M. K. & BANKAITIS, V. A. 1996. Kes1p shares homology with human oxysterol binding protein and participates in a novel regulatory pathway for yeast Golgi-derived transport vesicle biogenesis. EMBO J, 15, 6447-59.

FENG, R., CHEN, X., YU, Y., SU, L., YU, B., LI, J., CAI, Q., YAN, M., LIU, B. & ZHU, Z. 2010. miR-126 functions as a tumour suppressor in human gastric cancer. Cancer Lett, 298, 50-63.

FOX, B. A., RISTUCCIA, J. G., GIGLEY, J. P. & BZIK, D. J. 2009. Efficient gene replacements in Toxoplsma gondii strains deficient for nonhomologous end joining. Eukaryot Cell, 8, 520-9.

FRUMAN, D. A., MEYERS, R. E. & CANTLEY, L. C. 1998. Phosphoinositide kinases. Annu Rev Biochem, 67, 481-507.

GAGE, D. J. 2004. Infection and invasion of roots by symbiotic, nitrogen-fixing rhizobia during nodulation of temperate legumes. Microbiol Mol Biol Rev, 68, 280-300.

GARCIA, P., GUPTA, R., SHAH, S., MORRIS, A. J., RUDGE, S. A., SCARLATA, S., PETROVA, V., MCLAUGHLIN, S. & REBECCHI, M. J. 1995. The pleckstrin homology domain of phospholipase C-delta 1 binds with high affinity to phosphatidylinositol 4,5-bisphosphate in bilayer membranes. Biochemistry, 34, 16228-34.

GARCIA-REGUET, N., LEBRUN, M., FOURMAUX, M. N., MERCEREAU-PUIJALON, O., MANN, T., BECKERS, C. J., SAMYN, B., VAN BEEUMEN, J., BOUT, D. & DUBREMETZ, J. F. 2000. The microneme protein MIC3 of Toxoplasma gondii is a secretory adhesin that binds to both the surface of the host cells and the surface of the parasite. Cell Microbiol, 2, 353-64.

GARNER, K., HUNT, A. N., KOSTER, G., SOMERHARJU, P., GROVES, E., LI, M., RAGHU, P., HOLIC, R. & COCKCROFT, S. 2012. Phosphatidylinositol transfer protein, cytoplasmic 1 (PITPNC1) binds and transfers phosphatidic acid. J Biol Chem, 287, 32263-76.

GARNER, K., LI, M., UGWUANYA, N. & COCKCROFT, S. 2011. The phosphatidylinositol transfer protein RdgBbeta binds 14-3-3 via its unstructured C-terminus, whereas its lipid-binding domain interacts with the integral membrane protein ATRAP (angiotensin II type I receptor-associated protein). Biochem J, 439, 97-111.

GHOSH, R., DE CAMPOS, M. K., HUANG, J., HUH, S. K., ORLOWSKI, A., YANG, Y., TRIPATHI, A., NILE, A., LEE, H. C., DYNOWSKI, M., SCHAFER, H., ROG, T., LETE, M. G., AHYAYAUCH, H., ALONSO, A., VATTULAINEN, I., IGUMENOVA, T. I., SCHAAF, G. & BANKAITIS, V. A. 2015. Sec14-nodulin proteins and the patterning of phosphoinositide landmarks for developmental control of membrane morphogenesis. Mol Biol Cell, 26, 1764-81.

GIANSANTI, M. G., BONACCORSI, S., KUREK, R., FARKAS, R. M., DIMITRI, P., FULLER, M. T. & GATTI, M. 2006. The class I PITP giotto is required for Drosophila cytokinesis. Curr Biol, 16, 195-201.

GIETZ, R. D. & WOODS, R. A. 2002. Transformation of yeast by lithium acetate/single-stranded carrier DNA/polyethylene glycol method. Methods Enzymol, 350, 87-96.

GORDESKY, S. E. & MARINETTI, G. V. 1973. The asymetric arrangement of phospholipids in the human erythrocyte membrane. Biochem Biophys Res Commun, 50, 1027-31.

GRABON, A., KHAN, D. & BANKAITIS, V. A. 2015. Phosphatidylinositol transfer proteins and instructive regulation of lipid kinase biology. Biochim Biophys Acta, 1851, 724-35.

GUO, C., SAH, J. F., BEARD, L., WILLSON, J. K., MARKOWITZ, S. D. & GUDA, K. 2008. The noncoding RNA, miR-126, suppresses the growth of neoplastic cells by targeting phosphatidylinositol 3-kinase signaling and is frequently lost in colon cancers. Genes Chromosomes Cancer, 47, 939-46.

GUO, S., STOLZ, L. E., LEMROW, S. M. & YORK, J. D. 1999. SAC1-like domains of yeast SAC1, INP52, and INP53 and of human synaptojanin encode polyphosphoinositide phosphatases. J Biol Chem, 274, 12990-5.

GUPTA, C. M., RADHAKRISHNAN, R. & KHORANA, H. G. 1977. Glycerophospholipid synthesis: improved general method and new analogs containing photoactivable groups. Proc Natl Acad Sci U S A, 74, 4315-9.

HAASE, S., CABRERA, A., LANGER, C., TREECK, M., STRUCK, N., HERRMANN, S., JANSEN, P. W., BRUCHHAUS, I., BACHMANN, A., DIAS, S., COWMAN, A. F., STUNNENBERG, H. G., SPIELMANN, T. & GILBERGER, T. W. 2008. Characterization of a conserved rhoptry-associated leucine zipper-like protein in the malaria parasite Plasmodium falciparum. Infect Immun, 76, 879-87.

HALBERG, N., SENGELAUB, C. A., NAVRAZHINA, K., MOLINA, H., URYU, K. & TAVAZOIE, S. F. 2016. PITPNC1 Recruits RAB1B to the Golgi Network to Drive Malignant Secretion. Cancer Cell, 29, 339-53.

HAMILTON, B. A., SMITH, D. J., MUELLER, K. L., KERREBROCK, A. W., BRONSON, R. T., VAN BERKEL, V., DALY, M. J., KRUGLYAK, L., REEVE, M. P., NEMHAUSER, J. L., HAWKINS, T. L., RUBIN, E. M. & LANDER, E. S. 1997. The vibrator mutation causes

neurodegeneration via reduced expression of PITP alpha: positional complementation cloning and extragenic suppression. Neuron, 18, 711-22.

HAMMOND, G. R., MACHNER, M. P. & BALLA, T. 2014. A novel probe for phosphatidylinositol 4-phosphate reveals multiple pools beyond the Golgi. J Cell Biol, 205, 113-26.

HARRIS, W. A. & STARK, W. S. 1977. Hereditary retinal degeneration in Drosophila melanogaster. A mutant defect associated with the phototransduction process. J Gen Physiol, 69, 261-91.

HAY, J. C. & MARTIN, T. F. 1993. Phosphatidylinositol transfer protein required for ATP-dependent priming of Ca(2+)-activated secretion. Nature, 366, 572-5.

HE, J., HANEY, R. M., VORA, M., VERKHUSHA, V. V., STAHELIN, R. V. & KUTATELADZE, T. G. 2008. Molecular mechanism of membrane targeting by the GRP1 PH domain. J Lipid Res, 49, 1807-15.

HE, J., SCOTT, J. L., HEROUX, A., ROY, S., LENOIR, M., OVERDUIN, M., STAHELIN, R. V. & KUTATELADZE, T. G. 2011. Molecular basis of phosphatidylinositol 4-phosphate and ARF1 GTPase recognition by the FAPP1 pleckstrin homology (PH) domain. J Biol Chem, 286, 18650-7.

HE, X., LOBSIGER, J. & STOCKER, A. 2009. Bothnia dystrophy is caused by domino-like rearrangements in cellular retinaldehyde-binding protein mutant R234W. Proc Natl Acad Sci U S A, 106, 18545-50.

HESS, B. 2008. P-LINCS: A Parallel Linear Constraint Solver for Molecular Simulation. J Chem Theory Comput, 4, 116-22.

HESS, B., BEKKER, H., BERENDSEN, H. J. C. & FRAAIJE, J. G. E. M. 1997. LINCS: A linear constraint solver for molecular simulations. J Computational Chem, 18, 1463-1472.

HESS, B., KUTZNER, C., VAN DER SPOEL, D. & LINDAHL, E. 2008. GROMACS 4: Algorithms for Highly Efficient, Load-Balanced, and Scalable Molecular Simulation. J Chem Theory Comput, 4, 435-47.

HILGEMANN, D. W., FENG, S. & NASUHOGLU, C. 2001. The complex and intriguing lives of PIP2 with ion channels and transporters. Sci STKE, 2001, re19.

HILLER, N. L., BHATTACHARJEE, S., VAN OOIJ, C., LIOLIOS, K., HARRISON, T., LOPEZ-ESTRANO, C. & HALDAR, K. 2004. A host-targeting signal in virulence proteins reveals a secretome in malarial infection. Science, 306, 1934-7.

HOLIC, R., SIMOVA, Z., ASHLIN, T., PEVALA, V., POLONCOVA, K., TAHOTNA, D., KUTEJOVA, E., COCKCROFT, S. & GRIAC, P. 2014. Phosphatidylinositol binding of Saccharomyces cerevisiae Pdr16p represents an essential feature of this lipid transfer protein to provide protection against azole antifungals. Biochim Biophys Acta, 1842, 1483-90.

HOLTHUIS, J. C. & LEVINE, T. P. 2005. Lipid traffic: floppy drives and a superhighway. Nat Rev Mol Cell Biol, 6, 209-20.

HORROCKS, P. & MUHIA, D. 2005. Pexel/VTS: a protein-export motif in erythrocytes infected with malaria parasites. Trends Parasitol, 21, 396-9.

HSIAO, C. H., LUISA HILLER, N., HALDAR, K. & KNOLL, L. J. 2013. A HT/PEXEL motif in Toxoplasma dense granule proteins is a signal for protein cleavage but not export into the host cell. Traffic, 14, 519-31.

HUANG, J., KIM, C. M., XUAN, Y. H., PARK, S. J., PIAO, H. L., JE, B. I., LIU, J., KIM, T. H., KIM, B. K. & HAN, C. D. 2013. OsSNDP1, a Sec14-nodulin domain-containing protein, plays a critical role in root hair elongation in rice. Plant Mol Biol, 82, 39-50.

HUMPHREY, W., DALKE, A. & SCHULTEN, K. 1996. VMD: visual molecular dynamics. J Mol Graph, 14, 33-8, 27-8.

ILE, K. E., KASSEN, S., CAO, C., VIHTEHLIC, T., SHAH, S. D., MOUSLEY, C. J., ALB, J. G., JR., HUIJBREGTS, R. P., STEARNS, G. W., BROCKERHOFF, S. E., HYDE, D. R. & BANKAITIS, V. A. 2010. Zebrafish class 1 phosphatidylinositol transfer proteins: PITPbeta and double cone cell outer segment integrity in retina. Traffic, 11, 1151-67.

ILE, K. E., SCHAAF, G. & BANKAITIS, V. A. 2006. Phosphatidylinositol transfer proteins and cellular nanoreactors for lipid signaling. Nat Chem Biol, 2, 576-83.

IM, Y. J., RAYCHAUDHURI, S., PRINZ, W. A. & HURLEY, J. H. 2005. Structural mechanism for sterol sensing and transport by OSBP-related proteins. Nature, 437, 154-8.

ITO, H., FUKUDA, Y., MURATA, K. & KIMURA, A. 1983. Transformation of intact yeast cells treated with alkali cations. J Bacteriol, 153, 163-8.

IWATA, R., ODA, S., KUNITOMO, H., LINO, Y. 2011. Roles for class IIA phosphatidylinositol transfer protein in neurotransmission and behavioral plasticity at the sensory neuron synapses of Caenorhabditis elegans. Proc Natl Acad Sci U S A, 108, 7589-94.

JOINER, K. A. & ROOS, D. S. 2002. Secretory traffic in the eukaryotic parasite Toxoplasma gondii: less is more. J Cell Biol, 157, 557-63.

JONES, S. M., ALB, J. G., JR., PHILLIPS, S. E., BANKAITIS, V. A. & HOWELL, K. E. 1998. A phosphatidylinositol 3-kinase and phosphatidylinositol transfer protein act synergistically in formation of constitutive transport vesicles from the trans-Golgi network. J Biol Chem, 273, 10349-54.

JORGENSEN, W. L., CHANDRASEKHAR, J., MADURA, J. D., IMPEY, R. W. & KLEIN, M. L. 1983. Comparison of Simple Potential Functions for Simulating Liquid Water. J Chem Phys, 79.

JORGENSEN, W. L. & TIRADO-RIVES, J. 1988. The OPLS [optimized potentials for liquid simulations] potential functions for proteins, energy minimizations for crystals of cyclic peptides and crambin. J Am Chem Soc, 110, 1657–1666.

KAISER, H. J., ORLOWSKI, A., ROG, T., NYHOLM, T. K., CHAI, W., FEIZI, T., LINGWOOD, D., VATTULAINEN, I. & SIMONS, K. 2011. Lateral sorting in model membranes by cholesterol-mediated hydrophobic matching. Proc Natl Acad Sci U S A, 108, 16628-33.

KAMPMANN, M., BASSIK, M. C. & WEISSMAN, J. S. 2013. Integrated platform for genome-wide screening and construction of high-density genetic interaction maps in mammalian cells. Proc Natl Acad Sci U S A, 110, E2317-26.

KAPLAN, M. R. & SIMONI, R. D. 1985. Intracellular transport of phosphatidylcholine to the plasma membrane. J Cell Biol, 101, 441-5.

KAPRANOV, P., ROUTT, S. M., BANKAITIS, V. A., DE BRUIJN, F. J. & SZCZYGLOWSKI, K. 2001. Nodule-specific regulation of phosphatidylinositol transfer protein expression in Lotus japonicus. Plant Cell, 13, 1369-82.

KÄSTNER, J. 2011. Umbrella sampling. Wiley Interdisciplinary Reviews: Computational Molecular Science, 1, 932-942.

KAUFFMANN-ZEH, A., THOMAS, G. M., BALL, A., PROSSER, S., CUNNINGHAM, E., COCKCROFT, S. & HSUAN, J. J. 1995. Requirement for phosphatidylinositol transfer protein in epidermal growth factor signaling. Science, 268, 1188-90.

KEARNS, B. G., MCGEE, T. P., MAYINGER, P., GEDVILAITE, A., PHILLIPS, S. E., KAGIWADA, S. & BANKAITIS, V. A. 1997. Essential role for diacylglycerol in protein transport from the yeast Golgi complex. Nature, 387, 101-5.

KIM, S., KEDAN, A., MAROM, M., GAVERT, N., KEINAN, O., SELITRENNIK, M., LAUFMAN, O. & LEV, S. 2013. The phosphatidylinositol-transfer protein Nir2 binds phosphatidic acid and positively regulates phosphoinositide signalling. EMBO Rep, 14, 891-9.

KIM, Y. J., GUZMAN-HERNANDEZ, M. L. & BALLA, T. 2011. A highly dynamic ER-derived phosphatidylinositol-synthesizing organelle supplies phosphoinositides to cellular membranes. Dev Cell, 21, 813-24.

KIM, Y. J., GUZMAN-HERNANDEZ, M. L., WISNIEWSKI, E. & BALLA, T. 2015. Phosphatidylinositol-Phosphatidic Acid Exchange by Nir2 at ER-PM Contact Sites Maintains Phosphoinositide Signaling Competence. Dev Cell, 33, 549-61.

KOLEV, N. G., TSCHUDI, C. & ULLU, E. 2011. RNA interference in protozoan parasites: achievements and challenges. Eukaryot Cell, 10, 1156-63.

KONO, N., OHTO, U., HIRAMATSU, T., URABE, M., UCHIDA, Y., SATOW, Y. & ARAI, H. 2013. Impaired alpha-TTP-PIPs interaction underlies familial vitamin E deficiency. Science, 340, 1106-10.

KOSTENKO, E. V., MAHON, G. M., CHENG, L. & WHITEHEAD, I. P. 2005. The Sec14 homology domain regulates the cellular distribution and transforming activity of the Rho-specific guanine nucleotide exchange factor Dbs. J Biol Chem, 280, 2807-17.

KULIG, W., CWIKLIK, L., JURKIEWICZ, P., ROG, T. & VATTULAINEN, I. 2016. Cholesterol oxidation products and their biological importance. Chem Phys Lipids.

KULIG, W., PASENKIEWICZ-GIERULA, M. & ROG, T. 2015. Topologies, structures and parameter files for lipid simulations in GROMACS with the OPLS-aa force field: DPPC, POPC, DOPC, PEPC, and cholesterol. Data Brief, 5, 333-6.

KULIG, W., PASENKIEWICZ-GIERULA, M. & ROG, T. 2016. Cis and trans unsaturated phosphatidylcholine bilayers: A molecular dynamics simulation study. Chem Phys Lipids, 195, 12-20.

KUMAR, S., ROSENBERG, J. M., BOUZIDA, D., SWENDEN, R. H. & KOLLMAN, P. A. 1992. The weighted histogram analysis method for free-energy calculations on biomolecules. I. The method. J Computational Chem, 13, 1011-1021.

LARIJANI, B., ALLEN-BAUME, V., MORGAN, C. P., LI, M. & COCKCROFT, S. 2003. EGF regulation of PITP dynamics is blocked by inhibitors of phospholipase C and of the Ras-MAP kinase pathway. Curr Biol, 13, 78-84.

LAU, A. O. 2009. An overview of the Babesia, Plasmodium and Theileria genomes: a comparative perspective. Mol Biochem Parasitol, 164, 1-8.

LECUIT, T. & PILOT, F. 2003. Developmental control of cell morphogenesis: a focus on membrane growth. Nat Cell Biol, 5, 103-8.

LEE, A. Y., ST ONGE, R. P., PROCTOR, M. J., WALLACE, I. M., NILE, A. H., SPAGNUOLO, P. A., JITKOVA, Y., GRONDA, M., WU, Y., KIM, M. K., CHEUNG-ONG, K., TORRES, N. P., SPEAR, E. D., HAN, M. K., SCHLECHT, U., SURESH, S., DUBY, G., HEISLER, L. E., SURENDRA, A., FUNG, E., URBANUS, M. L., GEBBIA, M., LISSINA, E., MIRANDA, M., CHIANG, J. H., APARICIO, A. M., ZEGHOUF, M., DAVIS, R. W., CHERFILS, J., BOUTRY, M., KAISER, C. A., CUMMINS, C. L., TRIMBLE, W. S., BROWN, G. W., SCHIMMER, A. D., BANKAITIS, V. A., NISLOW, C., BADER, G. D. & GIAEVER, G. 2014. Mapping the cellular response to small molecules using chemogenomic fitness signatures. Science, 344, 208-11.

LEE, Y. S., MULUGU, S., YORK, J. D. & O'SHEA, E. K. 2007. Regulation of a cyclin-CDK-CDK inhibitor complex by inositol pyrophosphates. Science, 316, 109-12.

LEMMON, M. A. 2008. Membrane recognition by phospholipid-binding domains. Nat Rev Mol Cell Biol, 9, 99-111.

LEMMON, M. A., FERGUSON, K. M., O'BRIEN, R., SIGLER, P. B. & SCHLESSINGER, J. 1995. Specific and high-affinity binding of inositol phosphates to an isolated pleckstrin homology domain. Proc Natl Acad Sci U S A, 92, 10472-6.

LEV, S., HERNANDEZ, J., MARTINEZ, R., CHEN, A., PLOWMAN, G., & SCHLESSINGER, J. 1999. Identification of a novel family of targets of PYK2 related to Drosophila retinal degeneration B (rdgB) protein. Molecular and Cellular Biology, 19(3), 2278

LEV, S. 2010. Non-vesicular lipid transport by lipid-transfer proteins and beyond. Nat Rev Mol Cell Biol, 11, 739-50.

LEV, S. 2012. Nonvesicular lipid transfer from the endoplasmic reticulum. Cold Spring Harb Perspect Biol, 4.

LEVINE, N. D. 1970. Protozoan parasites of nonhuman primates as zoonotic agents. Lab Anim Care, 20, 377-82.

LI, X., RIVAS, M.P., FANG, M., MARCHENA, J., MEHROTRA, B., CHAUDHARY, A., FENG, L., PRESTWICH, G.D., BANKAITIS, V.A. 2002. Analysis of oxysterol binding protein homologue Kes1p function in regulation of Sec14p-dependent protein transport from the yeast Golgi complex. J Cell Biol, 157, 63-77.

LI, X., ROUTT, S. M., XIE, Z., CUI, X., FANG, M., KEARNS, M. A., BARD, M., KIRSCH, D. R. & BANKAITIS, V. A. 2000. Identification of a novel family of nonclassic yeast phosphatidylinositol transfer proteins whose function modulates phospholipase D activity and Sec14p-independent cell growth. Mol Biol Cell, 11, 1989-2005.

LIENDO, A. & JOINER, K. A. 2000. Toxoplasma gondii: conserved protein machinery in an unusual secretory pathway? Microbes Infect, 2, 137-44.

LIENDO, A., STEDMAN, T. T., NGO, H. M., CHATURVEDI, S., HOPPE, H. C. & JOINER, K. A. 2001. Toxoplasma gondii ADP-ribosylation factor 1 mediates enhanced release of constitutively secreted dense granule proteins. J Biol Chem, 276, 18272-81.

LITVAK, V., DAHAN, N., RAMACHANDRAN, S., SABANAY, H. & LEV, S. 2005. Maintenance of the diacylglycerol level in the Golgi apparatus by the Nir2 protein is critical for Golgi secretory function. Nat Cell Biol, 7, 225-34.

LONG, S. R. 2001. Genes and signals in the rhizobium-legume symbiosis. Plant Physiol, 125, 69-72.

LU, C., PENG, Y. W., SHANG, J., PAWLYK, B. S., YU, F. & LI, T. 2001. The mammalian retinal degeneration B2 gene is not required for photoreceptor function and survival. Neuroscience, 107, 35-41.

MACBETH, M. R., SCHUBERT, H. L., VANDEMARK, A. P., LINGAM, A. T., HILL, C. P. & BASS, B. L. 2005. Inositol hexakisphosphate is bound in the ADAR2 core and required for RNA editing. Science, 309, 1534-9

MACIEJEWSKI, A., PASENKIEWICZ-GIERULA, M., CRAMARIUC, O., VATTULAINEN, I. & ROG, T. 2014. Refined OPLS all-atom force field for saturated phosphatidylcholine bilayers at full hydration. J Phys Chem B, 118, 4571-81.

MARTI, M., GOOD, R. T., RUG, M., KNUEPFER, E. & COWMAN, A. F. 2004. Targeting malaria virulence and remodeling proteins to the host erythrocyte. Science, 306, 1930-3.

MCGEE, T. P., SKINNER, H. B., WHITTERS, E. A., HENRY, S. A. & BANKAITIS, V. A. 1994. A phosphatidylinositol transfer protein controls the phosphatidylcholine content of yeast Golgi membranes. J Cell Biol, 124, 273-87.

MCNAMARA, C. W., LEE, M. C., LIM, C. S., LIM, S. H., ROLAND, J., NAGLE, A., SIMON, O., YEUNG, B. K., CHATTERJEE, A. K., MCCORMACK, S. L., MANARY, M. J., ZEEMAN,

A. M., DECHERING, K. J., KUMAR, T. R., HENRICH, P. P., GAGARING, K., IBANEZ, M., KATO, N., KUHEN, K. L., FISCHLI, C., ROTTMANN, M., PLOUFFE, D. M., BURSULAYA, B., MEISTER, S., RAMEH, L., TRAPPE, J., HAASEN, D., TIMMERMAN, M., SAUERWEIN, R. W., SUWANARUSK, R., RUSSELL, B., RENIA, L., NOSTEN, F., TULLY, D. C., KOCKEN, C. H., GLYNNE, R. J., BODENREIDER, C., FIDOCK, D. A., DIAGANA, T. T. & WINZELER, E. A. 2013. Targeting Plasmodium PI(4)K to eliminate malaria. Nature, 504, 248-53.

MERCIER, C., ADJOGBLE, K. D., DAUBENER, W. & DELAUW, M. F. 2005. Dense granules: are they key organelles to help understand the parasitophorous vacuole of all apicomplexa parasites? Int J Parasitol, 35, 829-49.

MESMIN, B., BIGAY, J., MOSER VON FILSECK, J., LACAS-GERVAIS, S., DRIN, G. & ANTONNY, B. 2013. A four-step cycle driven by PI(4)P hydrolysis directs sterol/PI(4)P exchange by the ER-Golgi tether OSBP. Cell, 155, 830-43.

MICHELL, R. H. 1975. Inositol phospholipids and cell surface receptor function. Biochim Biophys Acta, 415, 81-47.

MICHELL, R. H. 2008. Inositol derivatives: evolution and functions. Nat Rev Mol Cell Biol, 9, 151-61.

MILLIGAN, S. C., ALB, J. G., JR., ELAGINA, R. B., BANKAITIS, V. A. & HYDE, D. R. 1997. The phosphatidylinositol transfer protein domain of Drosophila retinal degeneration B protein is essential for photoreceptor cell survival and recovery from light stimulation. J Cell Biol, 139, 351-63.

MOUSLEY, C. J., TYERYAR, K., ILE, K. E., SCHAAF, G., BROST, R. L., BOONE, C., GUAN, X., WENK, M. R. & BANKAITIS, V. A. 2008. Trans-Golgi network and endosome dynamics connect ceramide homeostasis with regulation of the unfolded protein response and TOR signaling in yeast. Mol Biol Cell, 19, 4785-803.

MOUSLEY, C. J., YUAN, P., GAUR, N. A., TRETTIN, K. D., NILE, A. H., DEMINOFF, S. J., DEWAR, B. J., WOLPERT, M., MACDONALD, J. M., HERMAN, P. K., HINNEBUSCH, A. G. & BANKAITIS, V. A. 2012. A sterol-binding protein integrates endosomal lipid metabolism with TOR signaling and nitrogen sensing. Cell, 148, 702-15.

NAGAMUNE, K., XIONG, L., CHINI, E. & SIBLEY, L. D. 2008. Plants, endosymbionts and parasites: Abscisic acid and calcium signaling. Commun Integr Biol, 1, 62-5.

NILE, A. H., BANKAITIS, V. A. & GRABON, A. 2010. Mammalian diseases of phosphatidylinositol transfer proteins and their homologs. Clin Lipidol, 5, 867-897.

NILE, A. H., TRIPATHI, A., YUAN, P., MOUSLEY, C. J., SURESH, S., WALLACE, I. M., SHAH, S. D., POHLHAUS, D. T., TEMPLE, B., NISLOW, C., GIAEVER, G., TROPSHA, A., DAVIS, R. W., ST ONGE, R. P. & BANKAITIS, V. A. 2014. PITPs as targets for selectively interfering with phosphoinositide signaling in cells. Nat Chem Biol, 10, 76-84.

ODOM, A. R., STAHLBERG, A., WENTE, S. R. & YORK, J. D. 2000. A role for nuclear inositol 1,4,5-trisphosphate kinase in transcriptional control. Science, 287, 2026-9.

OHASHI, M., JAN DE VRIES, K., FRANK, R., SNOEK, G., BANKAITIS, V., WIRTZ, K. & HUTTNER, W. B. 1995. A role for phosphatidylinositol transfer protein in secretory vesicle formation. Nature, 377, 544-7.

ORLOWSKI, A., ST-PIERRE, J. F., MAGARKAR, A., BUNKER, A., PASENKIEWICZ-GIERULA, M., VATTULAINEN, I. & ROG, T. 2011. Properties of the membrane binding component of catechol-O-methyltransferase revealed by atomistic molecular dynamics simulations. J Phys Chem B, 115, 13541-50.

PALONCYOVA, M., BERKA, K. & OTYEPKA, M. 2012. Convergence of Free Energy Profile of Coumarin in Lipid Bilayer. J Chem Theory Comput, 8, 1200-1211.

PARRINELLO, M. & RAHMAN, A. 1981. Polymorphic transitions in single crystals: A new molecular dynamics method. J Applied Physics, 52, 7182-7190.

PATTON, G. M., FASULO, J. M. & ROBINS, S. J. 1982. Separation of phospholipids and individual molecular species of phospholipids by high-performance liquid chromatography. J Lipid Res, 23, 190-6.

PHILLIPS, S. E., ILE, K. E., BOUKHELIFA, M., HUIJBREGTS, R. P. & BANKAITIS, V. A. 2006. Specific and nonspecific membrane-binding determinants cooperate in targeting phosphatidylinositol transfer protein beta-isoform to the mammalian trans-Golgi network. Mol Biol Cell, 17, 2498-512.

PHILLIPS, S. E., SHA, B., TOPALOF, L., XIE, Z., ALB, J. G., KLENCHIN, V. A., SWIGART, P., COCKCROFT, S., MARTIN, T. F., LUO, M. & BANKAITIS, V. A. 1999. Yeast Sec14p deficient in phosphatidylinositol transfer activity is functional in vivo. Mol Cell, 4, 187-97.

PHILLIPS, S. E., VINCENT, P., RIZZIERI, K. E., SCHAAF, G., BANKAITIS, V. A. & GAUCHER, E. A. 2006. The diverse biological functions of phosphatidylinositol transfer proteins in eukaryotes. Crit Rev Biochem Mol Biol, 41, 21-49.

PIEPERHOFF, M. S., SCHMITT, M., FERGUSON, D. J. & MEISSNER, M. 2013. The role of clathrin in post-Golgi trafficking in Toxoplasma gondii. PLoS One, 8, e77620.

PINXTEREN, J. A., GOMPERTS, B. D., ROGERS, D., PHILLIPS, S. E., TATHAM, P. E. & THOMAS, G. M. 2001. Phosphatidylinositol transfer proteins and protein kinase C make separate but non-interacting contributions to the phosphorylation state necessary for secretory competence in rat mast cells. Biochem J, 356, 287-96.

PNG, K. J., HALBERG, N., YOSHIDA, M. & TAVAZOIE, S. F. 2012. A microRNA regulon that mediates endothelial recruitment and metastasis by cancer cells. Nature, 481, 190-4.

PRINZ, W. A. 2010. Lipid trafficking sans vesicles: where, why, how? Cell, 143, 870-4.

PRINZ, W. A. 2014. Bridging the gap: membrane contact sites in signaling, metabolism, and organelle dynamics. J Cell Biol, 205, 759-69.

PRONK, S., PALL, S., SCHULZ, R., LARSSON, P., BJELKMAR, P., APOSTOLOV, R., SHIRTS, M. R., SMITH, J. C., KASSON, P. M., VAN DER SPOEL, D., HESS, B. & LINDAHL, E.

2013. GROMACS 4.5: a high-throughput and highly parallel open source molecular simulation toolkit. Bioinformatics, 29, 845-54.

REN, J., PEI-CHEN LIN, C., PATHAK, M. C., TEMPLE, B. R., NILE, A. H., MOUSLEY, C. J., DUNCAN, M. C., ECKERT, D. M., LEIKER, T. J., IVANOVA, P. T., MYERS, D. S., MURPHY, R. C., BROWN, H. A., VERDAASDONK, J., BLOOM, K. S., ORTLUND, E. A., NEIMAN, A. M. & BANKAITIS, V. A. 2014. A phosphatidylinositol transfer protein integrates phosphoinositide signaling with lipid droplet metabolism to regulate a developmental program of nutrient stress-induced membrane biogenesis. Mol Biol Cell, 25, 712-27.

RENTSCH, D., LALOI, M., ROUHARA, I., SCHMELZER, E., DELROT, S. & FROMMER, W. B. 1995. NTR1 encodes a high affinity oligopeptide transporter in Arabidopsis. FEBS Lett, 370, 264-8.

RHEE, S. G. 2001. Regulation of phosphoinositide-specific phospholipase C. Annu Rev Biochem, 70, 281-312.

RIEKHOF, W. R., WU, W. I., JONES, J. L., NIKRAD, M., CHAN, M. M., LOEWEN, C. J. & VOELKER, D. R. 2014. An assembly of proteins and lipid domains regulates transport of phosphatidylserine to phosphatidylserine decarboxylase 2 in Saccharomyces cerevisiae. J Biol Chem, 289, 5809-19.

RIVAS, M. P., KEARNS, B. G., XIE, Z., GUO, S., SEKAR, M. C., HOSAKA, K., KAGIWADA, S., YORK, J. D. & BANKAITIS, V. A. 1999. Pleiotropic alterations in lipid metabolism in yeast sac1 mutants: relationship to "bypass Sec14p" and inositol auxotrophy. Mol Biol Cell, 10, 2235-50.

ROTHSTEIN, R. J. 1983. One-step gene disruption in yeast. Methods Enzymol, 101, 202-11.

ROUSER, G., FKEISCHER, S. & YAMAMOTO, A. 1970. Two dimensional then layer chromatographic separation of polar lipids and determination of phospholipids by phosphorus analysis of spots. Lipids, 5, 494-6.

ROUTT, S. M., RYAN, M. M., TYERYAR, K., RIZZIERI, K. E., MOUSLEY, C., ROUMANIE, O., BRENNWALD, P. J. & BANKAITIS, V. A. 2005. Nonclassical PITPs activate PLD via the Stt4p PtdIns-4-kinase and modulate function of late stages of exocytosis in vegetative yeast. Traffic, 6, 1157-72.

ROY, A. & LEVINE, T. P. 2004. Multiple pools of phosphatidylinositol 4-phosphate detected using the pleckstrin homology domain of Osh2p. J Biol Chem, 279, 44683-9.

RYAN, M. M., TEMPLE, B. R., PHILLIPS, S. E. & BANKAITIS, V. A. 2007. Conformational dynamics of the major yeast phosphatidylinositol transfer protein sec14p: insight into the mechanisms of phospholipid exchange and diseases of sec14p-like protein deficiencies. Mol Biol Cell, 18, 1928-42.

SAEKI, S., YAMAMOTO, M. & IINO, Y. 2001. Plasticity of chemotaxis revealed by paired presentation of a chemoattractant and starvation in the nematode Caenorhabditis elegans. J Exp Biol, 204, 1757-64.

SAITO, K., TAUTZ, L. & MUSTELIN, T. 2007. The lipid-binding SEC14 domain. Biochim Biophys Acta, 1771, 719-26.

SCHAAF, G., DYNOWSKI, M., MOUSLEY, C. J., SHAH, S. D., YUAN, P., WINKLBAUER, E. M., DE CAMPOS, M. K., TRETTIN, K., QUINONES, M. C., SMIRNOVA, T. I., YANAGISAWA, L. L., ORTLUND, E. A. & BANKAITIS, V. A. 2011. Resurrection of a functional phosphatidylinositol transfer protein from a pseudo-Sec14 scaffold by directed evolution. Mol Biol Cell, 22, 892-905.

SCHAAF, G., ORTLUND, E. A., TYERYAR, K. R., MOUSLEY, C. J., ILE, K. E., GARRETT, T. A., REN, J., WOOLLS, M. J., RAETZ, C. R., REDINBO, M. R. & BANKAITIS, V. A. 2008. Functional anatomy of phospholipid binding and regulation of phosphoinositide homeostasis by proteins of the sec14 superfamily. Mol Cell, 29, 191-206.

SCHOUTEN, A., AGIANIAN, B., WESTERMAN, J., KROON, J., WIRTZ, K. W. & GROS, P. 2002. Structure of apo-phosphatidylinositol transfer protein alpha provides insight into membrane association. EMBO J, 21, 2117-21.

SCHWAB, J. C., BECKERS, C. J. & JOINER, K. A. 1994. The parasitophorous vacuole membrane surrounding intracellular Toxoplasma gondii functions as a molecular sieve. Proc Natl Acad Sci U S A, 91, 509-13.

SELINGER, Z. & LAPIDOT, Y. 1966. Synthesis of fatty acid anhydrides by reaction with dicyclohexylcarbodiimide. J Lipid Res, 7, 174-175.

SERON, K., DZIERSZINSKI, F. & TOMAVO, S. 2000. Molecular cloning, functional complementation in Saccharomyces cerevisiae and enzymatic properties of phosphatidylinositol synthase from the protozoan parasite Toxoplasma gondii. Eur J Biochem, 267, 6571-9.

SHA, B., PHILLIPS, S. E., BANKAITIS, V. A. & LUO, M. 1998. Crystal structure of the Saccharomyces cerevisiae phosphatidylinositol-transfer protein. Nature, 391, 506-10.

SHADAN, S., HOLIC, R., CARVOU, N., EE, P., LI, M., MURRAY-RUST, J. & COCKCROFT, S. 2008. Dynamics of lipid transfer by phosphatidylinositol transfer proteins in cells. Traffic, 9, 1743-56.

SHEN, B. & SIBLEY, L. D. 2012. The moving junction, a key portal to host cell invasion by apicomplexan parasites. Curr Opin Microbiol, 15, 449-55.

SHERMAN, F., FINK, G. R. & HICKS, J. B. 1983. Methods in Yeast Genetics. Cold Spring Harbor Laboratory, 1-113.

SIDIK, S. M., HACKETT, C. G., TRAN, F., WESTWOOD, N. J. & LOURIDO, S. 2014. Efficient genome engineering of Toxoplasma gondii using CRISPR/Cas9. PLoS One, 9, e100450.

SIMON, J. P., MORIMOTO, T., BANKAITIS, V. A., GOTTLIEB, T. A., IVANOV, I. E., ADESNIK, M. & SABATINI, D. D. 1998. An essential role for the phosphatidylinositol transfer protein in the scission of coatomer-coated vesicles from the trans-Golgi network. Proc Natl Acad Sci U S A, 95, 11181-6.

SKINNER, H. B., ALB, J. G., JR., WHITTERS, E. A., HELMKAMP, G. M., JR. & BANKAITIS, V. A. 1993. Phospholipid transfer activity is relevant to but not sufficient for the essential function of the yeast SEC14 gene product. EMBO J, 12, 4775-84.

SLEIGHT, R. G. & PAGANO, R. E. 1983. Rapid appearance of newly synthesized phosphatidylethanolamine at the plasma membrane. J Biol Chem, 258, 9050-8.

SLOVES, P. J., DELHAYE, S., MOUVEAUX, T., WERKMEISTER, E., SLOMIANNY, C., HOVASSE, A., DILEZITOKO ALAYI, T., CALLEBAUT, I., GAJI, R. Y., SCHAEFFER-REISS, C., VAN DORSSELEAR, A., CARRUTHERS, V. B. & TOMAVO, S. 2012. Toxoplasma sortilin-like receptor regulates protein transport and is essential for apical secretory organelle biogenesis and host infection. Cell Host Microbe, 11, 515-27.

SMIRNOVA, T. I., CHADWICK, T. G., MACARTHUR, R., POLUEKTOV, O., SONG, L., RYAN, M. M., SCHAAF, G. & BANKAITIS, V. A. 2006. The chemistry of phospholipid binding by the Saccharomyces cerevisiae phosphatidylinositol transfer protein Sec14p as determined by EPR spectroscopy. J Biol Chem, 281, 34897-908.

SMIRNOVA, T. I., CHADWICK, T. G., VOINOV, M. A., POLUEKTOV, O., VAN TOL, J., OZAROWSKI, A., SCHAAF, G., RYAN, M. M. & BANKAITIS, V. A. 2007. Local polarity and hydrogen bonding inside the Sec14p phospholipid-binding cavity: high-field multi-frequency electron paramagnetic resonance studies. Biophys J, 92, 3686-95.

SOLDATI, D. & BOOTHROYD, J. C. 1993. Transient transfection and expression in the obligate intracellular parasite Toxoplasma gondii. Science, 260, 349-52.

SOMERHARJU, P. & WIRTZ, K. W. A. 1982. Semisynthesis and properties of a fluorescent phosphatidylinositol analogue containing a cis-parinaoyl moiety. Chem Phys Lipids, 30, 81-91.

SOMERHARJU, P. J., VAN LOON, D. & WIRTZ, K. W. 1987. Determination of the acyl chain specificity of the bovine liver phosphatidylcholine transfer protein. Application of pyrene-labeled phosphatidylcholine species. Biochemistry, 26, 7193-9.

STEFAN, C. J., MANFORD, A. G., BAIRD, D., YAMADA-HANFF, J., MAO, Y. & EMR, S. D. 2011. Osh proteins regulate phosphoinositide metabolism at ER-plasma membrane contact sites. Cell, 144, 389-401.

SUH, P. G., PARK, J. I., MANZOLI, L., COCCO, L., PEAK, J. C., KATAN, M., FUKAMI, K., KATAOKA, T., YUN, S. & RYU, S. H. 2008. Multiple roles of phosphoinositide-specific phospholipase C isozymes. BMB Rep, 41, 415-34.

SUZAKI, T. & KAWAGUCHI, M. 2014. Root nodulation: a developmental program involving cell fate conversion triggered by symbiotic bacterial infection. Curr Opin Plant Biol, 21, 16-22.

TAN, X., CALDERON-VILLALOBOS, L. I., SHARON, M., ZHENG, C., ROBINSON, C. V., ESTELLE, M. & ZHENG, N. 2007. Mechanism of auxin perception by the TIR1 ubiquitin ligase. Nature, 446, 640-5.

TAVAZOIE, S. F., ALARCON, C., OSKARSSON, T., PADUA, D., WANG, Q., BOS, P. D., GERALD, W. L. & MASSAGUE, J. 2008. Endogenous human microRNAs that suppress breast cancer metastasis. Nature, 451, 147-52.

TAWK, L., DUBREMETZ, J. F., MONTCOURRIER, P., CHICANNE, G., MEREZEGUE, F., RICHARD, V., PAYRASTRE, B., MEISSNER, M., VIAL, H. J., ROY, C., WENGELNIK, K. & LEBRUN, M. 2011. Phosphatidylinositol 3-monophosphate is involved in toxoplasma apicoplast biogenesis. PLoS Pathog, 7, e1001286.

THOMAS, C. C., DOWLER, S., DEAK, M., ALESSI, D. R. & VAN AALTEN, D. M. 2001. Crystal structure of the phosphatidylinositol 3,4-bisphosphate-binding pleckstrin homology (PH) domain of tandem PH-domain-containing protein 1 (TAPP1): molecular basis of lipid specificity. Biochem J, 358, 287-94.

TILLEY, S. J., SKIPPEN, A., MURRAY-RUST, J., SWIGART, P. M., STEWART, A., MORGAN, C. P., COCKCROFT, S. & MCDONALD, N. Q. 2004. Structure-function analysis of human [corrected] phosphatidylinositol transfer protein alpha bound to phosphatidylinositol. Structure, 12, 317-26.

TOMAVO, S. 2014. Evolutionary repurposing of endosomal systems for apical organelle biogenesis in Toxoplasma gondii. Int J Parasitol, 44, 133-8.

TOMIOKA, M., ADACHI, T., SUZUKI, H., KUNITOMO, H., SCHAFER, W. R. & IINO, Y. 2006. The insulin/PI 3-kinase pathway regulates salt chemotaxis learning in Caenorhabditis elegans. Neuron, 51, 613-25.

VAN PARIDON, P. A., GADELLA, T. W., JR., SOMERHARJU, P. J. & WIRTZ, K. W. 1987. On the relationship between the dual specificity of the bovine brain phosphatidylinositol transfer protein and membrane phosphatidylinositol levels. Biochim Biophys Acta, 903, 68-77.

VANCE, J. E., AASMAN, E. J. & SZARKA, R. 1991. Brefeldin A does not inhibit the movement of phosphatidylethanolamine from its sites for synthesis to the cell surface. J Biol Chem, 266, 8241-7.

VERMA, N., KEINAN, O., SELITRENNIK, M., KARN, T., FILIPITS, M., & LEV, S. 2015. PYK2 sustains endosomal-derived receptor signalling and enhances epithelial-to-mesenchymal transition. Nature communications, 6.

VIDA, T. A. & EMR, S. D. 1995. A new vital stain for visualizing vacuolar membrane dynamics and endocytosis in yeast. J Cell Biol, 128, 779-92.

VIHTELIC, T. S., HYDE, D. R. & O'TOUSA, J. E. 1991. Isolation and characterization of the Drosophila retinal degeneration B (rdgB) gene. Genetics, 127, 761-8.

VINCENT, P., CHUA, M., NOGUE, F., FAIRBROTHER, A., MEKEEL, H., XU, Y., ALLEN, N., BIBIKOVA, T. N., GILROY, S. & BANKAITIS, V. A. 2005. A Sec14p-nodulin domain phosphatidylinositol transfer protein polarizes membrane growth of Arabidopsis thaliana root hairs. J Cell Biol, 168, 801-12.

WALCH-SOLIMENA, C. & NOVICK, P. 1999. The yeast phosphatidylinositol-4-OH kinase pik1 regulates secretion at the Golgi. Nat Cell Biol, 1, 523-5.

WIRTZ, K. W. 1991. Phospholipid transfer proteins. Annu Rev Biochem, 60, 73-99.

WIRTZ, K. W. 2006. Phospholipid transfer proteins in perspective. FEBS Lett, 580, 5436-41.

WOOD, C. S., SCHMITZ, K. R., BESSMAN, N. J., SETTY, T. G., FERGUSON, K. M. & BURD, C. G. 2009. PtdIns4P recognition by Vps74/GOLPH3 links PtdIns 4-kinase signaling to retrograde Golgi trafficking. J Cell Biol, 187, 967-75.

WU, W. I., ROUTT, S., BANKAITIS, V. A. & VOELKER, D. R. 2000. A new gene involved in the transport-dependent metabolism of phosphatidylserine, PSTB2/PDR17, shares sequence similarity with the gene encoding the phosphatidylinositol/phosphatidylcholine transfer protein, SEC14. J Biol Chem, 275, 14446-56.

XIE, Y., DING, Y. Q., HONG, Y., FENG, Z., NAVARRE, S., XI, C. X., ZHU, X. J., WANG, C. L., ACKERMAN, S. L., KOZLOWSKI, D., MEI, L. & XIONG, W. C. 2005. Phosphatidylinositol transfer protein-alpha in netrin-1-induced PLC signalling and neurite outgrowth. Nat Cell Biol, 7, 1124-32.

YADAV, S., GARNER, K., GEORGIEV, P., LI, M., GOMEZ-ESPINOSA, E., PANDA, A., MATHRE, S., OKKENHAUG, H., COCKCROFT, S. & RAGHU, P. 2015. RDGBalpha, a PtdIns-PtdOH transfer protein, regulates G-protein-coupled PtdIns(4,5)P2 signalling during Drosophila phototransduction. J Cell Sci, 128, 3330-44.

YANAGISAWA, L. L., MARCHENA, J., XIE, Z., LI, X., POON, P. P., SINGER, R. A., JOHNSTON, G. C., RANDAZZO, P. A. & BANKAITIS, V. A. 2002. Activity of specific lipid-regulated ADP ribosylation factor-GTPase-activating proteins is required for Sec14p-dependent Golgi secretory function in yeast. Mol Biol Cell, 13, 2193-206.

YODER, M.D., THOMAS, L.M., TREMBLAY, J.M., OLIVER, R.L., YARBROUGH, L.R., HELMKAMP, G.M. 2001. Structure of a multifunctional protein. Mammalian phosphatidylinositol transfer protein complexed with phosphatidylcholine. J Biol Chem, 276, 9246-52.